Faculty of Graduate Studies
University of Jordan

Performance Simulation of Serpentine Type Metallic and Non-metallic Solar Collectors

by
Abul-Qasim A.M.Al-Sageer

Supervisor
Prof. Mohammed Al-Saad

Submitted in partial fulfillment of the requirement
for the degree of Masterof Since in
Mechanical Engineering

Faculty of Graduate Studies
University of Jordan

April, 1996

COMMITTEE DECISION

This thesis was defended successfully on 20, April, 1996

COMMITTEE MEMBERS	SIGNATURE
Prof. Mohammed Al-Saad	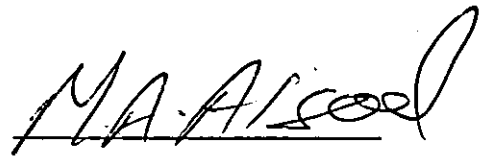
Prof. Mohammed A. Hamdan	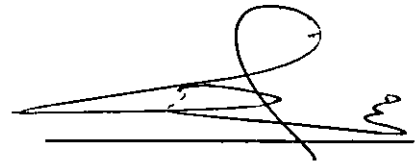
Dr. Mahmoud Hammad	

To my Parents and Wife

ACKNOWLEDGEMENTS

I am grateful to Prof. Mohammad Al-Saad for his support and precious effort in helping, and guiding me through the preparation of this work.

Finally, I would like to thank all my friends who helped me during my work especially Eng. Rami Al-Tarawnah.

Contents

List Of Figures

List Of Tables

NOMENCLATURE

A_c	Collector area, (m^2).
C_p	Water specific heat, (kJ/kg.°C).
D_i	Inside tube diameter, (m).
D_o	Outside tube diameter, (m).
F_r	Collector heat removal factor, (dimensionless).
h_w	Wind convective transfer coefficient, (W/m^2.°C).
I	Incident solar radiation on tilted surface, (Wh/m^2).
K	Thermal conductivity, (W/m.°C).
m	mass flow rate of water, (kg/s).
$(mc)_e$	Effective heat capacity of the collector, (kJ/°C).
N	Number of glass covers.
Nu	Nusselt number.
Q_u	Useful heat gain, (kJ).
Q_l	Lost energy, (kJ).
Q_s	Stored energy, (kJ).
Re	Renold number.
S	Incident solar radiation on tilted surface, (kJ).
T_a	Ambient temperature, (°C).

T_g Glass cover temperature, (°C).

T_i Inlet temperature, (°C).

T_o Outlet temperature, (°C).

T_p Plate temperature, (°C).

T_s Sky temperature, (°C).

U_l Overall heat loss coefficient from the collector, ($W/m^{2o}C$).

V_s Storage tank volume, (Liter).

W Distance between tubes, (m).

Greek symbols

α	Absorbance; (dimensionless).
β	Collector tilt angle, (degree).
γ	Collector azimuth angle, (degree).
η_d	Collector daily efficiency, (dimensionless).
η_I	Collector instantaneous efficiency, (dimensionless).
θ	Latitude angle, (degree).
τ	Transmissivity, (dimensionless).
$(\tau\alpha)_e$	Effective transmittance-Absorbance product, (dimensionless).

ABSTRACT

Performance Simulation of Serpentine Type Metallic and Non-metallic Solar Collectors

by

Abul_Qasim .a. M. Al_Sageer

Supervisor

Prof. Mohammed Al-Saad.

This thesis presents a theoretical investigation of metallic and non-metallic solar water collector models for evaluating its performance parameters. The determined parameters include heat removal factor, overall heat loss coefficients, heat gain, daily and hourly efficiencies.

The present study reports that, under forced circulation test, the non-metallic collector has an inferior performance parameters when compared to that of the metallic one. It was also revealed that the overall heat loss coefficients of both collectors show weak dependence on the flow rate variations. It was also noticed that the heat removal factor for both models is more sensitive to the flow rate variations when small storage tank capacities are used.

The stored energy in the non-metallic serpentine solar collector model constitutes a significant part of the useful energy, even after the diminishing of the solar intensity.

Finally, a comparison of performance parameters of the theoretical and experimental studies showed good agreements for most hours of the day, except the results obtained at the early morning and late after noon hours.

Chapter One

INTRODUCTION AND LITERATURE REVIEW

1.1 INTRODUCTION:

Solar energy is by far our most plentiful energy souree. It has man interesting properties, such as it is clean, non-depletable and reliable, which makes it a vast field of research and investigation. On the other hand, it is very dilute and of variable nature, which dictates the use of large surface area collectors to collect and concentrate the incoming insolation.

The flat plate collector is the simplest and the most widely used means for converting the incoming insolation into useful heat. Different configurations and types of solar collectors are now commercially available in Jordan. Such types of collectors can be designed for applications requiring energy delivery at moderate temperatures, up to perhaps 100°C above ambient [1]. They use both beam and diffuse solar radiation component, and do not require tracking of the sun, and they require little maintenance. They are mechanically simpler than concentrating collectors. The major applications of these units are in solar water heating and building heating, whereas potential uses include domestic hot water, space air conditioning and industrial process heating.

In the mid. 1970, many new collector designs appeared on the commercial market, and each one of these collectors has its own

performance, characteristics, advantages and disadvantages. Serpentine flat plate solar collector is one of these designs.

1.2 Types of Solar Collectors:

Solar collectors can be categorized into four basic classes [2]:

1. Flat plate collectors which collect but do not concentrate sun's radiant energy. Figure (1.1) shows number of different liquid flat plate solar collector designs of this type.
2. Vacuum tube collectors, where the space around the absorber surface is evacuated, so the convective heat losses are eliminated or minimized.
3. Medium performance focusing collectors which utilize a curved surface to focus the sun's rays on a heat exchanger, such as a collecting pipe or plate-pipe collector. Such collectors are adopted for slightly higher temperature than that of the flat plate type.
4. Concentrating collectors which utilize large curved surfaces composed of multiple mirrors. Such collectors can attain high temperature ranges for use in operating steam generators, turbines and the like.

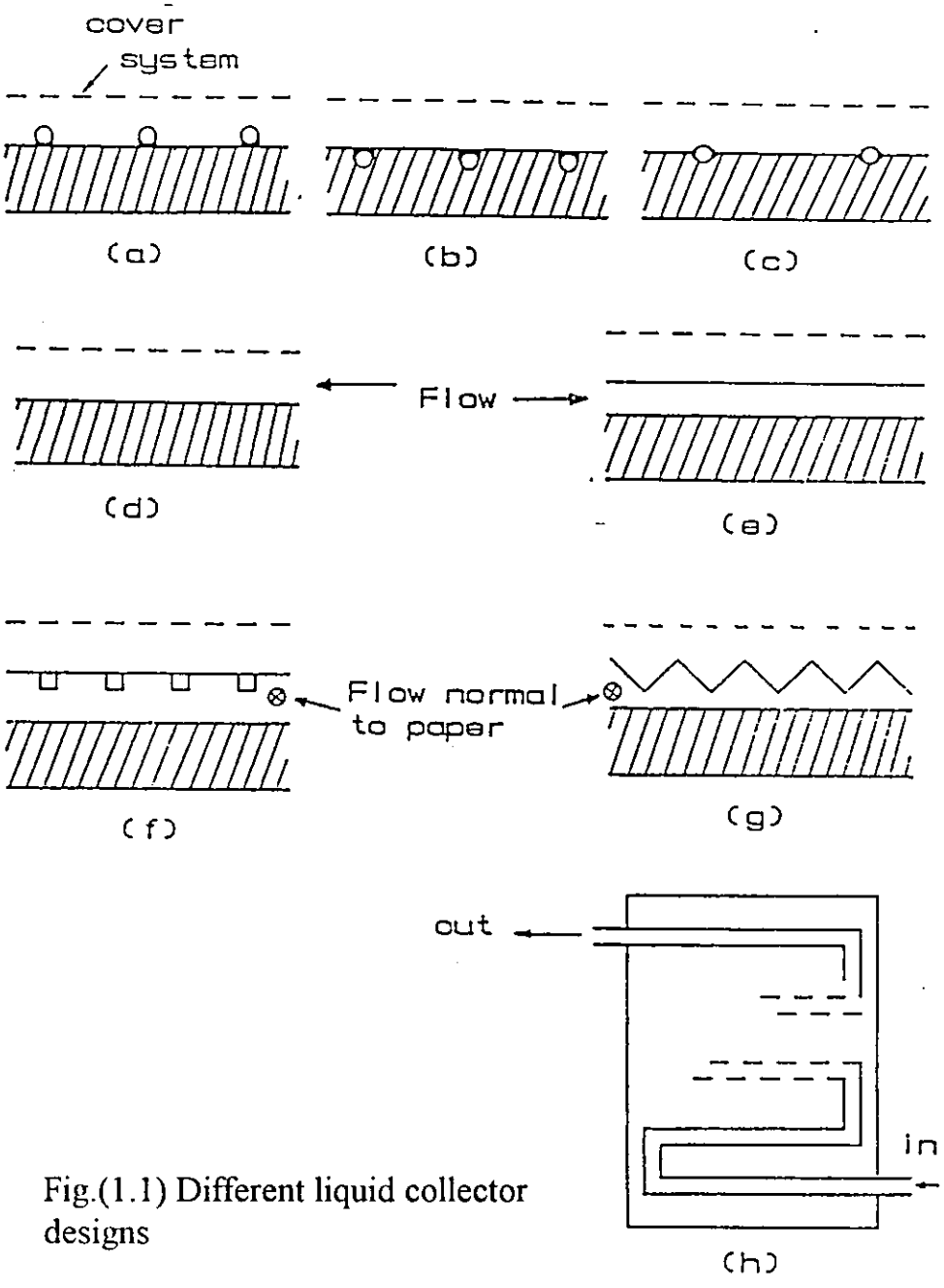

Fig.(1.1) Different liquid collector designs

1.3 SERPENTINE AND PARALLEL TYPES SOLAR COLLECTORS:

In the parallel type flat plate solar collector the flow occurs in parallel risers connected between inlet and outlet headers. While in the serpentine type the tube is fixed to the absorber plate in a serpentine fashion, therefore, the flow passages can be constructed from a single integral length of tubing.

The manufacturing process of a serpentine solar collector is easier than that of the parallel tube type, since it consists of a single tube. This means saving in time and money, because welding is no longer needed to join the pipes together as for the case of the parallel tube type where risers should be joined with headers by welding.

In the serpentine type the flow is forced to travel into one passage. Thus any deposit formed on the internal surface of the tube will represent an obstruction to the flow. The case in the parallel type is different, since there are at least seven risers where the flow can travel through. Consequentiy, it is obvious that the life cycle of the serpentine type is lower than that of the parallel type.

The pressure drop in the serpentine type is higher than that of the parallel type. This is due to the accumulation of pressure drops in the bends and straight runs. Thus the driving force in the case of the serpentine type is less than that of the parallel type when natural circulation is used.

1.4 Literature Survey:

Performance of parallel tubes flat plate solar collectors have received a lot of investigations, while the performance of the serpentine collectors has received a little attention. This survey is divided into three parts. Literature dealt with parallel tube solar collectors, literature dealt with metallic serpentine flat plate solar collectors, and finally, literature dealt with non-metallic serpentine flat plate solar collectors.

The first study of the performance of the parallel type solar collector was introduced by Hottel and Woertz [3]. The study was based on energy balance measurements of an array of collectors on an experimental solar heated building. The performance calculations were based on mean plate temperature. A correlation for thermal losses was reported.

Moore et al. [4] made extensive comparisons of the performance of a flat plate liquid heating collector with results predicted by use of the Hottel and Woertz method. The operating conditions were similar to those of Hottel and Woertz and good agreement was reported. Spencer and Strud [5] had conducted research on an integration of solar collectors into building elements. Frank and Mcgowan [6] reported that the performance of non-metallic collectors is equal or better than that of conventional collectors in applications where high temperatures are not required. They also found that the Hottel-Whillier-Bliss model can be used to predict the performance of the non-metallic solar collector if some alterations are incorporate in it, such as the effects of long wave transmittance, variable plate forced convection coefficients, and finite absorber plate thermal conductivity. Finally they showed that the thermal conductivity of the top plate absorber configurations

with thin absorber plates is not critical beyond about 0.1 *W/m°C*. Turner [7] presented a simplified mathematical model for predicting the useful solar heat gain by water in tubes placed under concrete surface, but no experimental data were reported. Russel and Guven [8] reported that high stagnation temperature presents serious problems for most plastics. But this problem can be minimized by venting the passage between the absorber plate and the cover. Also they reported that the overall performance of all plastics flat plate collectors is reasonably high for low and medium temperature collector operation. Such collectors have some potential for possible cost reduction of solar systems.

Madsen and Goss [9] provided a report on non-metallic solar collectors which indicates that the use of plastics in flat plate solar collectors is rapidly growing and this is leading to reduced costs. The use of lower molecular weight plastics in flat plate collectors is easier to handle and less expensive to install. Wilhelm [10] reported on the low cost solar collectors using plastic absorber and glazers. His approach was to select materials suitable for higher temperature applications, but less expensive materials for outer covers such as polyethylene, polycarbonate, glass reinforced polyester and acrylic. He also proposed to reduce stagnation effects by mounting the collector with a tilt angle calculated for solar conditions. Currin [11] investigated that the polysulfone or glass reinforced-silicone are suitable for stagnation temperatures up to 150-170°*C*.

Abu Faris [12] had conducted an experimental research on three non-metallic parallel tube solar collectors under Jordanian climatic conditions. Three models of flat plate solar collectors were constructed of concrete, each had a gross area of $1m^2$. The only difference between these models was the flow passage material. These passages were made from locally

manufactured PVC (Polyvinyl Chloride), thermo-pipe, and Galvanized steel pipes. These collectors were tested according to ASHRAE standard 93-77 (1977) [13].

Upon comparing the performance of each concrete collector with that of a locally manufactured metallic solar collector, the instantaneous efficiency of all tested models was higher than that of the selected metallic solar collector.

Abdel-Khalik [14] obtained an analytical solution for heat removal factor, F_r, for metallic serpentine absorber plate of a signal bend (two segments). He solved the problem numerically for large values of segments. He concluded that the dependence of the heat removal factor on the number of segments is slight. Zhang and Lavan [15] analyzed the thermal performance of a serpentine type. They obtained analytical solutions for three and four segments. They showed that, what was concluded by Abdel-Khalik was in error for a certain range.

Akgun [16] presented two analytical solutions resulting from two assumptions which uncouple the governing matrix differential equation. He concluded that, the dependence of the heat removal factor on the number of segments is slight, which is the same conclusion reached by Adel-Khalik.

Brode et al. [17] tested the parallel and the serpentine collector types under identical conditions. They found experimentally that the thermal efficiency was higher for parallel type than that for serpentine type.

Chiou and Perera [18] reported analysis and experimental study of a metallic serpentine collector. Their results showed a higher performance of the parallel type during mid-day, but conversely, higher performance for the

serpentine type during early morning when compared to prior experiments with serpentine type [19] and parallel type [20].

Abu Yahia [21] conducted an experimental study that aimed to compare the performance of a metallic serpentine type collector, with that of a parallel type, under Jordan climatic conditions. The results revealed that under forced circulation conditions, the serpentine type has superior performance when compared to the parallel type, for all the investigated flow rates and time intervals. Zhang [22] developed mathematical relations to predict the performance of the non-metallic serpentine collectors, based on the non-dimensional mass flow rate and some other non-dimensional parameters. He stated that the thermal performance of collectors (parallel or serpentine types) made out of metallic or non-metallic materials can be readily obtained.

Adas [23] performed an experimental investigation to predict a relative performance for two serpentine concrete collectors. He concluded that under no load conditions, the performance parameters for both collectors are improved as the storage tank capacity is increased from 50 litter to 150 litter. On the other hand, the performance parameters for the concrete collector with galvanized steel tubes are better than that of thermo-pipe tubes.

1.5 Objectives of the Present Work:

Thermal performance of two solar serpentine (Metallic and Non-Metallic) tube collector arrangements are theoretically predicted under Jordan's climatic conditions.

This work is performed as follows:

1. The mathematical model is developed and formulated .
2. A computer program that simulates the two models is developed and written.
3. The various performance parameters of interest are computed under different operating conditions.
4. The obtained theoretical results are compared with that of available experimental ones.

The thermal performance parameters of each type are studied and analyzed theoretically.

The following parameters are evaluated:

1. The collector overall heat loss coefficient.
2. The heat removal factor.
3. Hourly and daily heat collected per unit area of the collector.
4. Instantaneous and daily efficiencies.
5. Hourly heat stored per unit area of the collector (for non-metallic one).

1.6 Layout of the Thesis:

The thesis is divided into five chapters of which this introduction and literature review is the first chapter. Chapter two descries the performance of the serpentine solar collector models for metallic and non-metallic flat plat collectors. Chapter three presents the results and discussion of the models suggested in this thesis. Chapter Four shows a comparison between the suggested models in this thesis and some of the previous experimental studies. Finally, Chapter Five lists the general conclusions and recommendations reached by the present study.

Chapter Two

PERFORMANCE OF METALLIC AND NON-METALLIC SERPENTINE TUBE SOLAR COLLECTORS

2.1 Introduction:

The main objective of the present study is to evaluate the theoretical performance of the metallic and non-metallic serpentine solar collector under Jordanian climatic conditions. In this chapter the theoretical analysis and the basic mathematical equations used to evaluate the performance parameters of the considered collectors are outlined.

2.2 Assumptions:

The following assumptions were adopted:

1. Steady flow.
2. Dust, dirt, and shading effects are negligible.
3. One dimensional heat flow through glass cover and back insulation.
4. Properties of working fluid are independent of temperature.

2.3 Parameters effecting the performance of flat plate solar collectors:

The performance of a solar collector is influenced by a large number of operational and design parameters. The useful energy gain of the collector can be readily evaluated upon knowledge of its three governing parameters, which are the heat removal factor F_r, the heat loss coefficient U_l, and the effective transmittance-absorptance product of the cover system $(\tau\alpha)_e$.

2.3.1 The heat removal factor :

The heat removal factor for the serpentine type is given by [1].

$$F_r/F_1 = B\left[1-\exp\left[(F_2-1)/B\right]\right] \quad \text{..... (2-1)}$$

where

$$F_1 = \frac{NK_1L}{F_2A_cU_1C} \quad \text{..... (2-2)}$$

$$B = \frac{mC_p}{F_1A_cU_1} \quad \text{..... (2-3)}$$

$$F_2 = \frac{1}{\left[K_1R(1+\gamma)^2 - 1 - \gamma - K_1R\right]} \quad \text{..... (2-4)}$$

$$C = \left[K_1R(1+\gamma)-1\right]^2 - (K_1R)^2 \quad \text{..... (2-5)}$$

$$K_1 = \frac{k\delta n}{(W - D_o)\sinh n} \quad \text{..... (2-6)}$$

$$n^2 = (W - D_o)^2\left(\frac{U_l}{K\delta}\right) \quad \text{..... (2-7)}$$

$$\gamma = -2\cosh n - \left(\frac{D_o U_l}{K_1}\right) \quad \text{..... (2-8)}$$

$$R = \frac{1}{C_b} + \frac{1}{\pi D_i h_{f,i}} \quad \text{..... (2-9)}$$

The notations appearing in equations (2.1) -(2.9) are defined as follows:

m- The mass flow rate.

C_p- The specific heat of the flowing fluid (4.186 Kj/Kg. C°) water 20C°

W- Is the distance between tubes.

D_o- Is the outside diameter.

D_i- Is the inside diameter.

C_b- The bond conductance which equal $K_b b/t$

K_b- Is the bond thermal conductivity.

B- Is the collector capacitance.

N- The number of the tube segments of the serpentine type.

L- The length of the tube segments of the serpentine.

R- Thermal resistance between the plate and flowing fluid.

$h_{f,i}$- Heat transfer coefficient inside tubes.

To calculate the value of the $h_{f,i}$ the R_e must be calculated, where's

$$R_e = \frac{4m}{\pi D_o \mu} \quad \text{..... (2-10)}$$

If R_e, turned to turbulent flow the value of, $h_{f,i}$,can be obtain from the equation [1].

$$h_{f,i} = \frac{\left(\frac{f}{8}\right) R_e P_r}{1.07 + 12.7\left(P_r^{\frac{2}{3}} - 1\right)\sqrt{\frac{f}{8}}} x \frac{D_o}{K} \quad \text{..... (2-11)}$$

The Darcy Fraction factor f for smooth pipes defined as:

$$f = \left(0.79 \text{Ln} R_e - 1.64\right)^{-2} \quad \text{..... (2-12)}$$

The Prandtl number,P_r ,is given by [1].

$$P_r = \frac{\nu}{\alpha} \quad \text{..... (2-13)}$$

α- Thermal Diffusivity.

ν- Kinematic Viscosity.

K- Thermal conductivity of water.

D_o- Outside diameter.

2.3.2 Overall heat transfer coefficient:

The top heat lost coefficient, U_t, is required during the performance estimation of flat-plate solar collectors. This parameter can be found from the governing equations of heat balance. However, the governing equations are non-linear and require an iterative solution. Muhaddin et al. [24] suggested a large number of iterative solutions for calculating both U_t and glass temperature, T_g, at different sky temperatures, T_s. The results for glass temperature were then correlated in the form of an equation. This resulted in a slightly extended proposal for the top loss coefficient. It can be stated as:

$$U_t = \left[\left\{ \frac{12.75\left((T_p - T_g)\cos\beta\right)^{0.264}}{(T_p + T_g)^{0.46} L^{0.21}} + \frac{\sigma\left(T_p^2 + T_g^2\right)(T_p + T_g)}{1/\epsilon_p + 1/\epsilon_g - 1} \right\}^{-1} + \left\{ h_w + \frac{\epsilon_g \left(T_g^4 - T_{sc}^4\right)}{(T_g - T_a)} \right\} \right]^{-1} \quad \text{..... (2-14)}$$

where

$$T_g = C\frac{h_w^{0.38}}{430}\left[240\,\epsilon_p - 170 + T_p\right]\left[T_p - T_a\right] + T_a \quad \text{..... (2-15)}$$

$$C = 1 - \exp\left[\left(-0.01(T_p - T_a)\right)\right] / (T_a - T_{sc} + 1) \quad \text{..... (2-16)}$$

$$T_{sc} = 0.0552 T_a^{1.5} \quad \text{..... (2-17)}$$

The wind convection coefficient, h_w, is estimated as [1].

$$h_w = \frac{8.6V^{0.6}}{L^{0.4}} \quad \text{(2-18)}$$

where

V- Wind speed (m/s).

L- characteristics length (m).

The bottom loss coefficient, U_b , is equal

$$U_b = K_i/L_b \quad \text{(2-19)}$$

where

K_i- Insulation thermal conductivity.

L_b- Back-insulation thickness.

Edge loss coefficient, U_e , can be expressed as

$$U_e = \frac{(UA)_{edge}}{A_c} \quad \text{(2-20)}$$

where

$(UA)_{edge}$- The edge loss coefficient-area product.

A_c - The collector area.

The overall heat loss coefficient, U_L, is the sum of the top, bottom, and edge loss coefficients:

$$U_L = U_t + U_b + U_e \quad \text{(2-21)}$$

2.3.3 Transmittance-Absorbtance Product:

The value of the transmittance absorbtance product, $(\tau\alpha)_e$, is nearly equal to 1.02 times the product of τ and α [1]. Then

$$(\tau\alpha)_e \approx 1.02\tau\alpha \quad \text{..... (2-22)}$$

2.4. Performance of the metallic serpentine solar collector:

In terms of the heat removal factor, F_r, overall heat loss coefficient, U_L, and the effective transmittance-absorptance product of the cover system, $(\tau\alpha)_e$, the instantaneous useful energy gain of the collector per unit time Q_u is given by [1]:

$$Q_u = A_c F_r\left[I(\tau\alpha)_e - U_L(T_i - T_a)\right] \quad \text{..... (2-23)}$$

where

A_c- is the collector area.

I - is the incident solar flux on the collector.

T_i- is the inlet fluid temperature.

T_a- is the ambient air temperature.

$I(\tau\alpha)_e$- is the absorbed solar energy per unit area of the collector.

The useful heat gain is also given by [1]:

$$Q_u = mC_p(T_o - T_i).\tau_t \quad \text{..... (2-24)}$$

where

T_o- is the collector outlet fluid temperature.

τ_t- is the time in seconds of the test interval.

The instantaneous efficiency, (η_i), can be expressed as:

$$\eta_i = \frac{Q_u}{A_c I} * 100\% \quad \text{..... (2-25)}$$

Using Eq. (2.23), and Eq. (2.24), then efficiency can be expressed as:

$$\eta_i = \left[F_r(\tau\alpha)_e - F_r U_L \frac{(T_i - T_a)}{I} \right] * 100\% \quad \text{..... (2-26)}$$

and

$$\eta_i = \frac{\dot{m} C_p (T_o - T_i)}{A_c I} * 100\% \quad \text{..... (2-27)}$$

If the governing parameters F_r, U_l, $(\tau\alpha)_e$, were all constants, then the plot of η_i versus $(T_i - T_a)/I$ would be a straight line with intercept $F_r(\tau\alpha)_e$ and slope $-F_r U_L$.

The daily efficiency of the solar collector is the ratio of the useful energy gain obtained during the test day to the total radiation incident on the collector area during the complete day, thus,

$$\eta_d = \frac{Q_{ut}}{A_c I} * 100\% \quad \text{..... (2-28)}$$

2.5 Performance of the non- metallic serpentine solar collector:

An energy balance can be employed to describe the performance of the serpentine non-metallic solar collectors. This energy balance shows that the incident solar flux is divided into three portions; useful energy gain, lost energy to the surrounding and stored energy.

Considering the control volume around the water tubes, the energy balance for the concrete collector becomes:

$$SA_c = Q_u + Q_l + Q_s \quad \text{..... (2-29)}$$

where:

S- is the absorber solar radiation given by:

$$S = I_T(\tau\alpha)_e A_c * 3600 \quad \text{..... (2-30)}$$

$(\tau\alpha)_e$ -is the effective transmittance absorptance product;(dimensionless).

I_T- is the incident solar radiation on the tilted surface.

A_c- is the aperture area of the collector.

Q_u- is the useful energy gain to the working fluid, expressed as:

$$Q_u = \dot{m}C_p(T_o - T_i).\tau_t \quad \text{..... (2-31)}$$

The stored energy, Q_s, in the collector, is positive in the morning and negative in the afternoon and can be evaluated as:

$$Q_s = (mc)_e (T_{p2} - T_{p1}) \quad \text{(2-32)}$$

where

$(mc)_e$-is the effective heat capacity of the non-metallic collector [23].

T_p-is the plate mean temperature which can be calculated from

$$F_r = \frac{S - U_l (T_p - T_a) - Q_s}{S - U_l (T_i - T_a) - Q_s} \quad \text{(2-33)}$$

using Eq. (2-32) for Q_s and solving for T_{p2}, then the resulting equation is:

$$T_{p2} = \frac{T_{p1} \times (Mc)_e \times (F_R - 1) + T_a \times U_l \times (F_R - 1) - T_i \times F_R \times U_l + s \times (F_R - 1)}{F_R \times (Mc)_e - U_l - (Mc)_e} \quad \text{(2-34)}$$

where T_{p1} is the initial plate temperature.

The energy stored in the concrete slab can constitute a significant portion of the total incident energy, because the collector have a large thermal effective mass.

The instantaneous efficiency for the non metallic collector is given by:

$$\eta_i = \frac{Q_u}{A_c I_T - Q_s} * 100\% \quad \text{(2-35)}$$

Using Eq. (2-31), η_i, can be expressed as:

$$\eta_i = \frac{mC_p (T_o - T_i).\tau_t}{A_c I_T - Q_s} * 100\% \quad \text{(2-36)}$$

If Eq. (2-29) is used then η_i, can be expressed as

$$\eta_i = \frac{S.A_c - Q_l - Q_s}{A_c.I_t - Q_s} \quad \text{..... (2-37)}$$

Which can be shown to:

$$\eta_i = \frac{(\tau\alpha)_e.I_T.A_c}{A_c.I_T - Q_s} - \frac{F_R.U_l(T_i - T_a)}{A_c.I_T - Q_s} - \frac{Q_s}{A_c.I_T - Q_s} \quad \text{..... (2-38)}$$

The daily efficiency of the solar collector is the ratio of the useful energy gain obtained during the test day to the total radiation incident on the collector area during the complete day, thus,

$$\eta_d = \frac{Q_{ut}}{A_c I} * 100\% \quad \text{..... (2-39)}$$

2.6 Estimation of Solar Energy:

Solar radiation measurements are made mainly by the Meteorological Department and the Royal Scientific Society, Jordan. A first attempt to put total radiation measurements into empirical formulas using the modified Angstrom linear regression formula was done by [25]. This attempt was later extended considerably and detailed by [26] and [27].

Alsaad et al [28] presented the information needed for a prediction formulas for the various components of solar radiation.

The hourly solar radiation incident on tilted surface, I_t, is expressed as[29]

$$I_t = I_{bn}DBF + I_d \cos^2\left(\frac{\beta}{2}\right) + \rho_g I_h \sin^2\left(\frac{\beta}{2}\right) \quad \text{..... (2-40)}$$

where :

I_{bn}- is the direct hourly beam radiation incident on a normal surface. Its value is given by

$$I_{bn} = \frac{I_h - I_d}{\cos\theta_z} \quad \text{..... (2-41)}$$

where

θ_z- the angle of incidence of beam radiation on horizontal surface, which is expressed in [1] as:

$$\cos\theta_z = \cos\phi\cos\delta\cos\omega + \sin\phi\sin\delta \quad \text{..... (2-42)}$$

where

I_h-the hourly global flux on a horizontal surface.

I_d-the hourly diffuse flux on a horizontal surface.

The fraction of direct beam radiation, DBF, incident on a tilted surface is given as follows [1]:

$$DBF = \cos\beta\left[\sin\phi\sin\delta + \cos\phi\cos\delta\cos\omega\right] + \sin\beta\left\{\begin{matrix}\cos\gamma\left[\tan\phi\left(\sin\phi\sin\delta + \cos\phi\cos\delta\cos\omega\right) - \sin\delta\sec\phi\right] \\ +\sin\gamma\cos\delta\sin\omega\end{matrix}\right\} \quad \text{..... (2-43)}$$

where

ϕ-is the latitude angle

ω - the hour angle

δ-declination angle. Its value given by

$$\delta = 23.45\sin\left[\frac{360}{365}(284+n)\right] \quad \text{..... (2-44)}$$

The hourly global radiation, I_h, is expressed in [28] as:

$$I_h = A_h + B_h\sin\left(\frac{2\pi n}{365} - F_h\right) \quad \text{..... (2-45)}$$

where A_h, B_h and F_h are given below for Amman in terms, h, of the hour of the day.[28]:

$$A_h = -191.3343 + 322.8383h - 32.8510h^2 + 0.6137h^3 \quad \text{..... (2-46)}$$

$$B_h = 142.1121 + 31.9338h + 0.4338h^2 - 0.2908h^3 \quad \text{..... (2-47)}$$

$$F_h = 75.1929 + 2.1360h + 0.0779h^2 - 0.0194h^3 \quad \text{..... (2-48)}$$

The values of h are 1, 2, 3,. . ., 11, 12 for the hours 06, 07, 08, . . ., 16, 17.

The hourly diffuse radiation, I_d, is expressed as [28]:

$$\frac{I_d}{I_h} \{= 0.344 + 1.45k_T (\text{for} 0 \le k_T \le 0.137) \quad \text{..... (2-49)}$$

$$\frac{I_d}{I_h} \{= 0.636 - 0.670k_T (\text{for} 0.137 \le k_T \le 0.785) \quad \text{..... (2-50)}$$

$$\frac{I_d}{I_h} \{= 0.110 (\text{for} k_T \ge 0.785) \quad \text{..... (2-51)}$$

where, k_T, is the ratio of the global solar radiation , I_h , to the extraterrestrial radiation, I_o, for the desired hour.

$$k_T = \frac{I_h}{I_o} \quad \text{..... (2-52)}$$

The extraterrestrial radiation on a horizontal surface, I_o , is expressed in [1] as:

$$I_o = \frac{12 * G_{sc}}{\pi} * \left(1 + 0.33 \cos\left(\frac{360n}{365}\right) \left(\begin{matrix} \cos\phi \cos\delta * (\sin\omega_2 - \sin\omega_1) \\ + \frac{2\pi(\omega_2 - \omega_1)}{360} \sin\phi \sin\delta \end{matrix} \right) \right) \quad \text{.. (2-53)}$$

where

G_{sc}-is the solar constant, its current value is 1367 W/m^2 .

n- is the day of the year.

ϕ -Latitude angle .

2.7 Estimation of ambient temperature:

The values of the hourly ambient temperature can be correlated using the PeakFit soft ware for the months of August and September. The obtained equation for the month of August is:

$$T_a=T_1+T_2+T_3+T_4+T_5 \quad \text{(2-54)}$$

where

$$T_1=15.0045+0.24348X+0.00609613X^2-0.00123364X^3 \quad \text{(2-55)}$$

$$T_2 = a_o \exp\left[-0.5\left(\frac{X-a_1}{a_2}\right)^2\right] \quad \text{(2-56)}$$

a_o=1.45449 ,a_1=13.32247 and a_2=0.880859

$$T_3 = a_3 \exp\left[-0.5\left(\frac{X-a_4}{a_5}\right)^2\right] \quad \text{(2-57)}$$

a_3=13.6507 ,a_4=15.38189 and a_5=6.24817

$$T_4 = a_6 \exp\left[-0.5\left(\frac{X-a_7}{a_8}\right)^2\right] \quad \text{(2-58)}$$

a_6=1.64694 ,a_7=11.642 and a_8=0.763324

$$T_5 = a_9 \exp\left[-0.5\left(\frac{X-a_{10}}{a_{11}}\right)^2\right] \quad \text{(2-59)}$$

a_9=2.06127 ,a_{10}=9.29022 and a_{11}=0.6993

and that for September is:

$$T_a = 7.17872 - 0.388107X + 30.316504X^2 - 0.0136785X^3 \quad \text{..... (2-60)}$$

where X is the Time of the day (in 24 hour Format).

2.8 Theoretical calculations and procedures:

The results of the theoretical calculations of the performance parameters of the present study were recorded every hour from 8:00 to 17:00, using the equations of this chapter. The recorded calculations are :

1- Inlet (T_i) and outlet (T_o) water temperatures for the serpentine collectors (metallic and non-metallic).

2-Plate mean temperature (T_p) .

3-The over all heat loose coefficient (U_l) .

4- The ambient temperature (T_a) .

5- The heat removal factor (F_r) .

6- Solar incident radiation on the collector plane (I_t) .

The theoretical performance of the metallic and non- metallic collector, was obtaind for the cases of forced circulation tests with no- load and load conditions.

Chapter Three

RESULTS AND DISCUSSION

This Chapter is divided into two sections. Section (3.1) deals with the performance calculations. In section (3.2) the results are analyzed and discussed.

3.1 Performance, Calculations and Results.

The calculations of this study were performed by developing a FORTRAN Computer Program as shown in Appendix (B). The calculations are based on the performance equations introduced in section (2.4) and section (2.5) for metallic and non-metallic serpentine collector respectively. The results of these calculations are tabulated in Appendix (A). All calculations are based on the absorber plate area.

Plots and Figures of this study are prepared by using the Computer AXUM Graphics Package. In the following sub-sections, the results of all calculations are introduced.

3.1.1 Results of the forced circulation with no load condition for metallic serpentine solar collector

This calculations were performed by using two different arrangements as related to the storage tank used. The first arrangement, a storage tank of 150 Liter capacity was used. The water flow rates used are: 0.05, 0.03, 0.02, and 0.04 Kg/s. The second arrangement, uses a common storage tank of 50 Liter capacity with water flow rates of 0.03, 0.02, 0.05 and 0.07Kg/s.

All calculated temperatures of this collector models, are presented in Tables (A.1-A.8), and are plotted as a function of time as shown in Figures (3.1-3.8).

By using the calculated data of temperatures as indicated in Tables (A.1-A.8), the useful energy gain is calculated using Equation.(2-23). The variation of the useful energy gains as well as the incident solar radiation with time of day are shown in Figures (3 9. 3.16), for the serpentine solar collectors. at different flow rates.

The instantaneous efficiency is calculated using Equation.(2-25). This Equation is applied assuming constant ambient temperature and radiation during each time interval (One hour).

The variations of the instantaneous efficiency with $(T_i-T_a)/I$ at different flow rates are shown in Figures (3.17-3.24). Linear regression fitting in AXUM Graphics Package was used to express these variations linearly. According to Equation.(2-26), the intercept with the Y-Axis represents $F_R.(\tau\alpha)_e$ and the slope of the equation represents $-F_R.U_L$.

The variation of the overall heat loss coefficient with the mass flow rate is shown in Figures (3.25) and (3.26), for 50 Liter and 150 Liter storage tanks, respectively.

On the other hand, the variation of the heat removal factor against water mass flow rate is shown in Figures (3.27) and (3.28) for 50 Liter and 150 Liter storage tanks, respectively.

Table (3-1) lists the obtained instantaneous efficiency expressions for storage tank capacities of 50 Liter and 150 Litters for the serpentine metallic solar collectors. Each expression of these instantaneous efficiencies

represents a separate day, where the wind velocity is different from day to day.

Table (3.1) Instantaneous efficiency expressions for metallic serpentine collector

$\dot{m}$, Kg/s	V_s= 50 Liter	V_s=150 Liter
0.02	$\eta_i = \left[0.52245 - 4.5329\left(\frac{T_i - T_a}{I}\right)\right]$	$\eta_i = \left[0.50625 - 4.58\left(\frac{T_i - T_a}{I}\right)\right]$
0.03	$\eta_i = \left[0.5475 - 5.032\left(\frac{T_i - T_a}{I}\right)\right]$	$\eta_i = \left[0.54189 - 5.0175\left(\frac{T_i - T_a}{I}\right)\right]$
0.05	$\eta_i = \left[0.57348 - 5.605\left(\frac{T_i - T_a}{I}\right)\right]$	$\eta_i = \left[0.56943 - 5.546\left(\frac{T_i - T_a}{I}\right)\right]$

3.1.2 Results of the forced circulation with load condition for metallic serpentine solar collector

The variations of all calculated temperatures for this collector model with time of day as expressed in Tables (A.9 -A.12) are plotted in Figures (3.29-3.30). The useful energy gain for each time interval (One hour) is calculated using Equation.(2-23). The results of such calculations are shown in Tables (A.33 -A.36), in Appendix (A). The useful energy gain as well as the incident solar radiation are plotted versus time of day as shown in Figures (3.31-3.32).

The daily efficiency is calculated using Equation. (2-28) for flow rates of 0.02, 0.03, 0.04 and 0.05 Kg/s. Table (3-2) presents the daily efficiencies for this collector at two different flow rates. Finally, Figure (3.33) shows the variation of daily efficiency with mass flow rate.

Table (3.2) daily efficiency for the serpentine metallic solar collector.

Model	$\dot{m}$ Kg/s	η_d %
Serpentine Metallic Solar Collector	0.02	49.3
	0.05	56.6

To illustrate the calculation procedure of the daily efficiency, the useful energy gains, for the serpentine metallic type are considered. Referring to Table (A.33-A.36) the daily useful energy gain for 0.02 Kg/s is 12127.11 KJ and the total radiation incident on the collector area during the complete day is 21240.15 KJ, so, using Equation.(2-28) the daily efficiency would be:

$$\eta_d = \frac{Q_{ut}}{I_t . A_c} \times 100\%$$

$$\eta_d = \frac{12127.11}{21240.15 \times 1.16} \times 100\% = 49.3\%$$

3.1.3 Results of the forced circulation with no load condition for non-metallic serpentine solar collectors

As outlined earlier, the present study was performed using two arrangements related to the storage tanks used. The first arrangement, when a storage tank of 150 Liter capacity was used, the water flow rates used are, 0.02, 0.03, 0.04, and 0.06 Kg/s.

In the second arrangement, when a common storage tank of 50 Liter capacity was used, with the same mass flow rates at which 150 Liter arrangement were used.

All calculated temperatures, as presented in Tables (A.13-A.20) were plotted against time of the day, as shown in Figures (3.34-3.37) and Figures (3.38-3.41) for the 50 Liter and 150 Liter respectively.

Again, the useful energy gain and the stored energy were calculated according to Equations (2-29) and (2-32), respectively.

The variation of the useful energy gain, the stored energy and the incident solar energy with time of the day are plotted in Figures (3.42-3.45), and Figures (3.46-3.49), at different mass flow rates for 50 Liter and 150 Liter storage tanks, respectively.

The instantaneous efficiency is calculated using Equation. (2-35). The variation of the instantaneous efficiency with $(T_i-T_a)/I$ at different mass flow rates are shown in Figures (3.50-3.52). The linear regression fitting in the AXUM Graphics Package was used in these figures.

The variation of the overall heat loss coefficient against the mass flow rates is shown in Figures (3.53) and (3.54), for 50 Liter and 150 Liter storage tanks, respectively.

On the other hand, the variation of the heat removal factor against water mass flow rate is shown in Figures (3.55) and (3.56) for 50 Liter and 150 Liter storage tanks, respectively.

3.1.4 Results of the forced circulation with load condition for non-metallic serpentine solar collectors

The variations of all calculated temperatures for this model, with time of the day are plotted in Figures (3.57-3.60). The data are recorded in tables (A.21-A.24). in Appendix A.

The useful energy gain for each time interval (One hour) is calculated using Equation.(2-29) and the stored energy for the whole day was calculated according to the Equation.(2-32). Also, the useful energy gain and the incident solar radiation were plotted against time of day in Figures (3.61-3.64).

Finally, Figure (3.65) shows the variation of daily efficiency with mass flow rate

The calculation of daily efficiency was based on Equation.(2-39), for various mass flow rates, as shown in Table (3-4).

As a samples calculation, the 0.02 Kg/s mass flow rate for non-metallic collector with galvanized steel serpentine tubes is selected. The daily efficiency, η_d, is calculated from Equation.(2-39), the result is:

$$\eta_d = \frac{Q_{ut}}{I_t . A_c} \times 100\%$$

$$\eta_d = \frac{10957.9}{24057.8 \times 1.0725} \times 100\% = 42.47\%$$

Table (3-3) Daily efficiency of the serpentine non-metallic solar collector

	$\dot{m}$, Kg/s			
Model	0.01	0.02	0.04	0.06
Serpentine non-metallic solar collector	30.5	42.47	54.23	59.18

3-2 Discussion of Results.

In the present study, the performance parameters are studied with all design parameters kept constant, while the mass flow rates were varied over a wide range. The discussion of the obtained performance parameters is outlined for the metallic and non-metallic serpentine solar collector in the following subsections.

3-2-1 Temperature Distributions

The calculated inlet, outlet and ambient temperatures are presented in Tables (A1-A24). The variation of these temperatures with the time of day are presented in Figures (3.1-3.8), and Figures (3.34-3.41), for forced circulation, with no-load condition, for metallic and non-metallic serpentine solar collector, respectively. For open loop, Figures (3.29-30), and Figures (3.57-3.60) , shows the variation of these temperatures for metallic and non-metallic serpentine solar collector, respectively.

When a small capacity storage tank (50 Liter) was used, it was noticed that the temperature difference for both models increases gradually starting

from the morning until it reaches a maximum value at the mid of the day, then, it begins to diminish gradually until it reaches a relatively small value at the end of the day. The maximum outlet temperature for both models was reached during the 15:00-16:00 and 16:00-17:00 hours intervals, at a mass flow rate of 0.07 Kg/s for metallic serpentine solar collector and a flow rate of 0.06 Kg/s for non-metallic serpentine solar collector.

When a large capacity storage tank (150 Liter) was used, the temperature difference followed the same behavior like that of the small storage tank, (50 Liter) case.

The maximum outlet temperature in the present case occurred during the 15:00-16:00 hours interval for both models and a mass flow rate of 0.05 Kg/s for metallic serpentine collector and 0.06 Kg/s for the non-metallic. The maximum temperature difference for both models, was attained during the 13:00 -14:00 hours interval.

On the other hand, Tables (A13-A24), show that the maximum plate temperature was reached during the time interval of 13:00-14:00 for the non-metallic serpentine solar collector.

3-2-2 Useful Heat Gain and Stored Energy.

The useful heat energy for each model was calculated using Equation (2-23) and Equation (2-29) for serpentine metallic and non-metallic solar collector, respectively.

For the non-metallic serpentine solar collector, the stored energy calculated using equation (2-32). For no-load forced circulation case, the variation of the useful heat gain and solar intensity with time of day are shown in Figures (3.9-3.16) for metallic serpentine solar collector. Also, the variation of the useful heat gain and solar intensity and stored energy with time of the day are shown in Figures (3.42-3.49) for the non-metallic serpentine solar collector.

The results of the no-load, forced circulation case, shows that the useful heat gain of both models, increases gradually from the start of the day, till it attains a maximum value at the mid of the day, thereafter it drops gradually. This is due to the decreasing value of the incident solar flux during the afternoon hours.

When a (150 Liter) capacity storage tank was used for each model, the maximum heat gain was attained at the time interval 11:00-12:00 hours for

the metallic serpentine solar collector, and 13:00-14:00 hours for the non-metallic serpentine solar collector.

For the open loop arrangement with load, and forced circulation, the variation of the useful heat gain and solar intensity with time of the day are shown in Figures (3.31- 3.32) for the metallic serpentine solar collector, and at a flow rates of 0.05 and 0.02 Kg/s. The maximum useful heat gain was attained at 11:00-12:00 hours interval. Also, for the non-metallic serpentine solar collector, the variation of the useful heat gain, solar intensity, and stored energy with time of the day are shown in Figures (3.61 - 3.64). The maximum useful heat gain, was attained at the interval 14:00-15:00 hours.

It is also observed that, for the non-metallic model, the collector continued to deliver useful energy for a considerable time even at the end of the day. This is due to the energy which has been stored in the collector before noon. This energy besides the incident solar radiation becomes a significant input source to the collector.

represents an increase of 7.3 % for metallic serpentine solar collector. For non-metallic collector, as the flow rate increases from 0.02 to 0.06 Kg/s, the daily efficiency increases by 28.68 % the daily efficiency clearly.

3-2-4 Heat Removal Factors And Overall Heat Loss Coefficients.

The variation of the heat removal factors with mass flow rate are presented in Figures (3.27-3.28) and Figures (3.55-3.56) for metallic and non-metallic serpentine solar collector respectively .

These Figures show that the heat removal factor of metallic serpentine solar collector is higher than that of the non-metallic serpentine solar collector for all flow rates investigated.

These Figures show that the heat removal factor, F_R is more sensitive to flow rate variations when small storage tanks are used. When (150 Liter) capacity storage tank was used for each model, as the flow rate was increased from 0.02 to 0.07 Kg/s, the improvement for heat removal factor for both models is very small.

Figures. (3.25 - 3.26) and Figures (3.53-3.54) show the variation of the overall heat loss coefficients of both models with the mass flow rates. These

figures show that the dependence of the overall eat loss coefficient on the flow rate is poor. Results show that the overall heat loss coefficient depends mainly on the wind velocity.

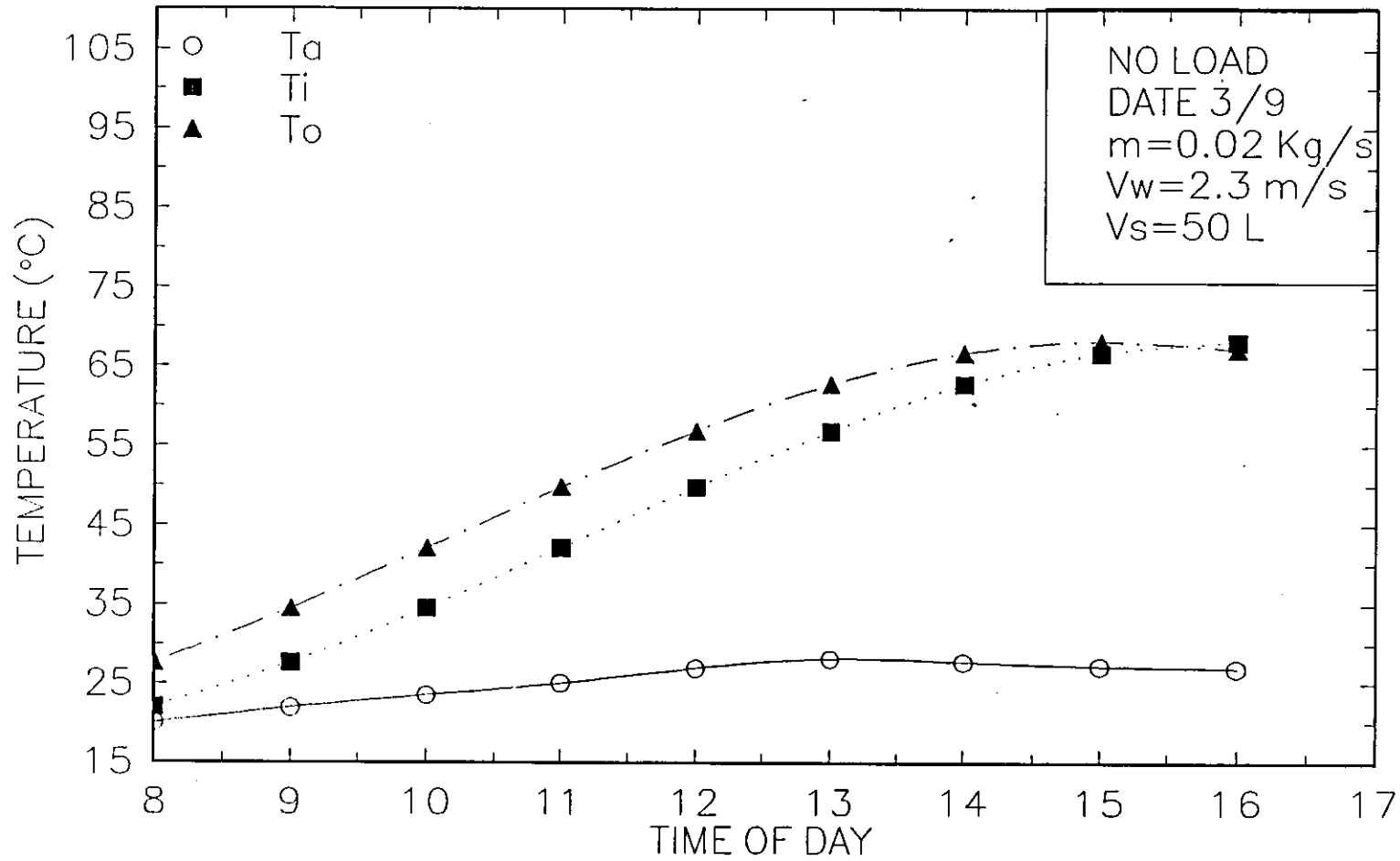

FIG (3.1). Variation of Inlet Temp. Outlet Temp. and the Amb. Temp. with Time for the Serpentine Tube Flat Metallic Plate Solar Colectors.

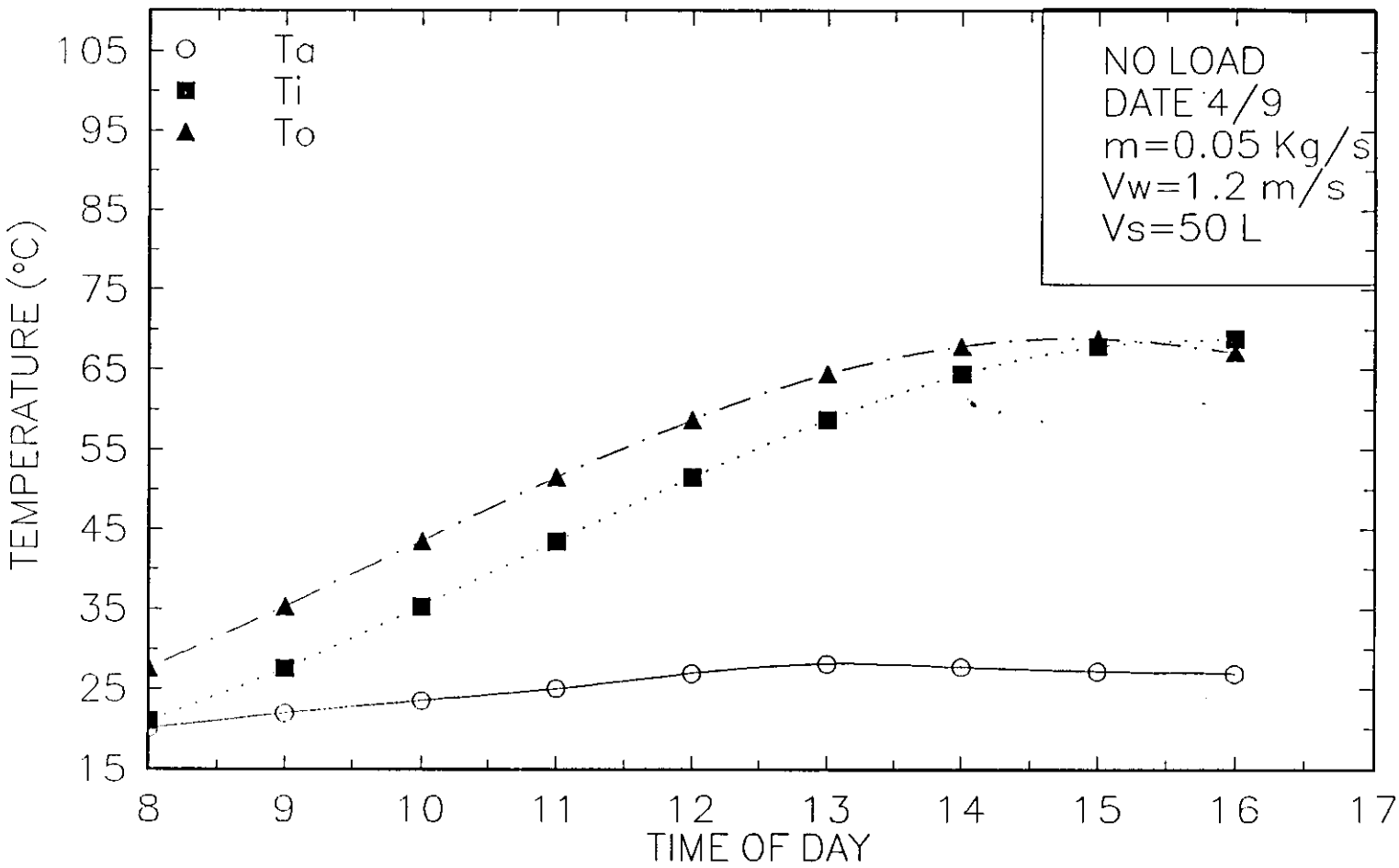

FIG (3.3). Variation of Inlet Temp. Outlet Temp. and the Amb. Temp. with Time for the Serpentine Tube Flat Metallic Plate Solar Colectors.

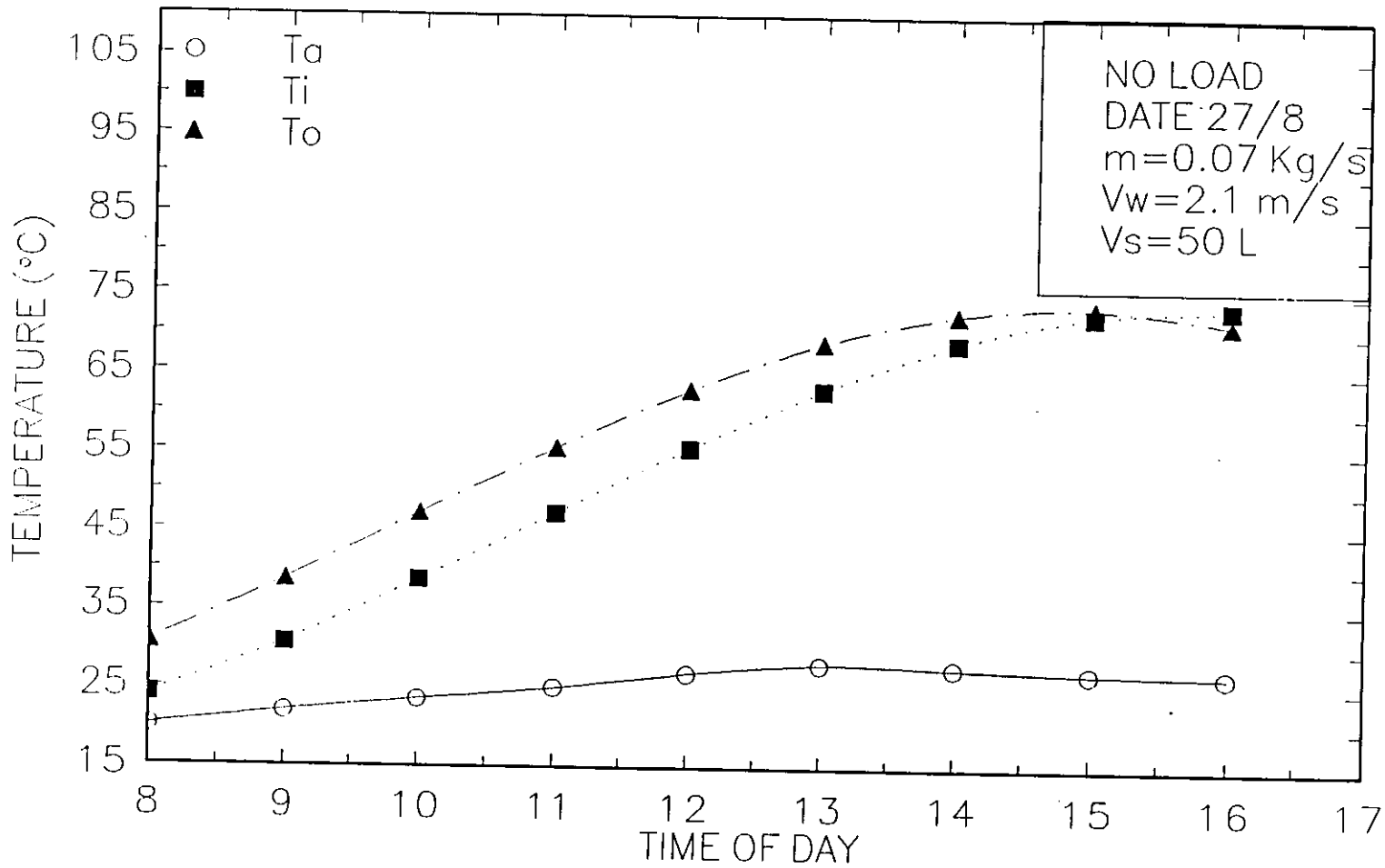

FIG (3.4). Variation of Inlet Temp. Outlet Temp. and the Amb. Temp. with Time for the Serpentine Tube Flat Metallic Plate Solar Colectors.

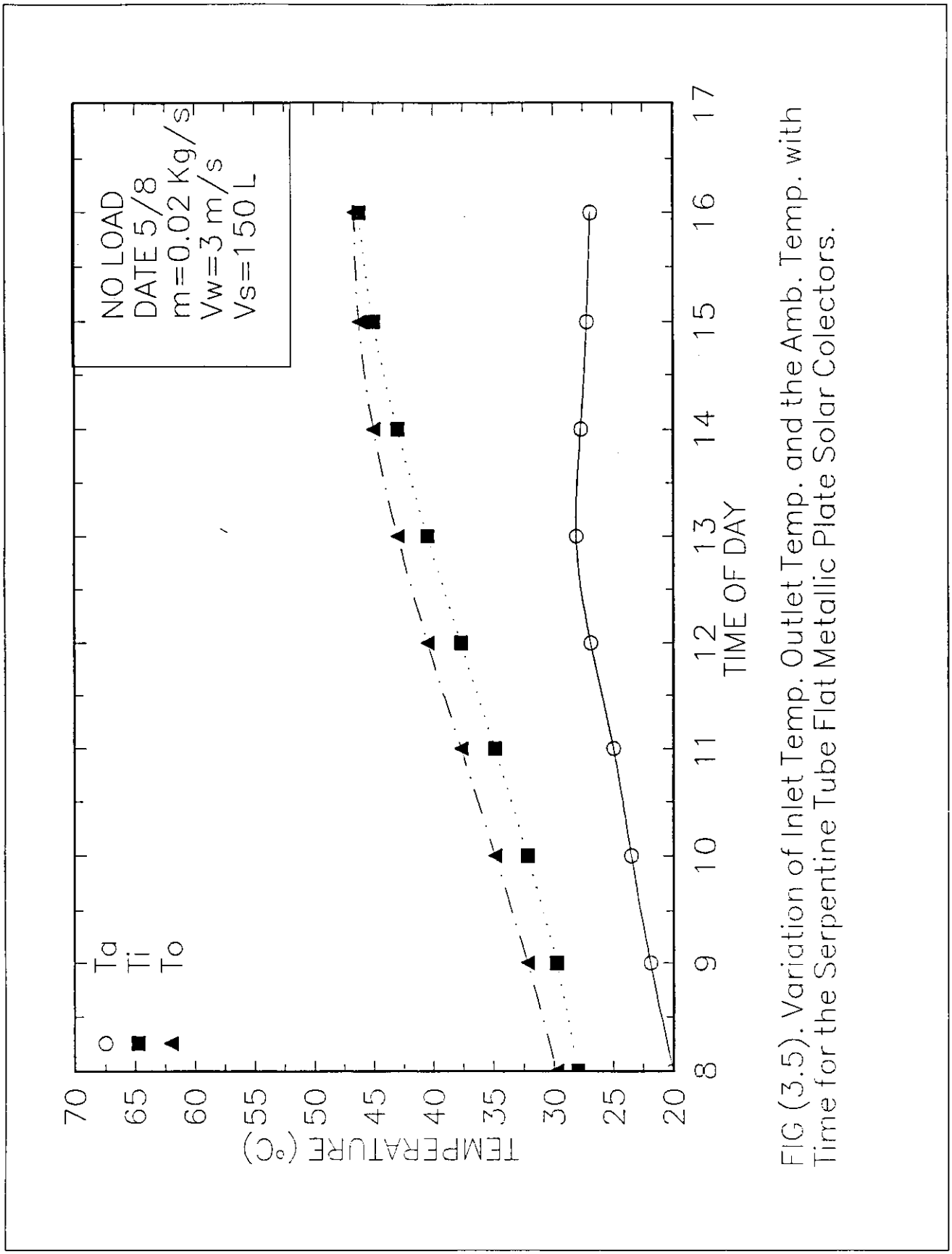

FIG (3.5). Variation of Inlet Temp. Outlet Temp. and the Amb. Temp. with Time for the Serpentine Tube Flat Metallic Plate Solar Colectors.

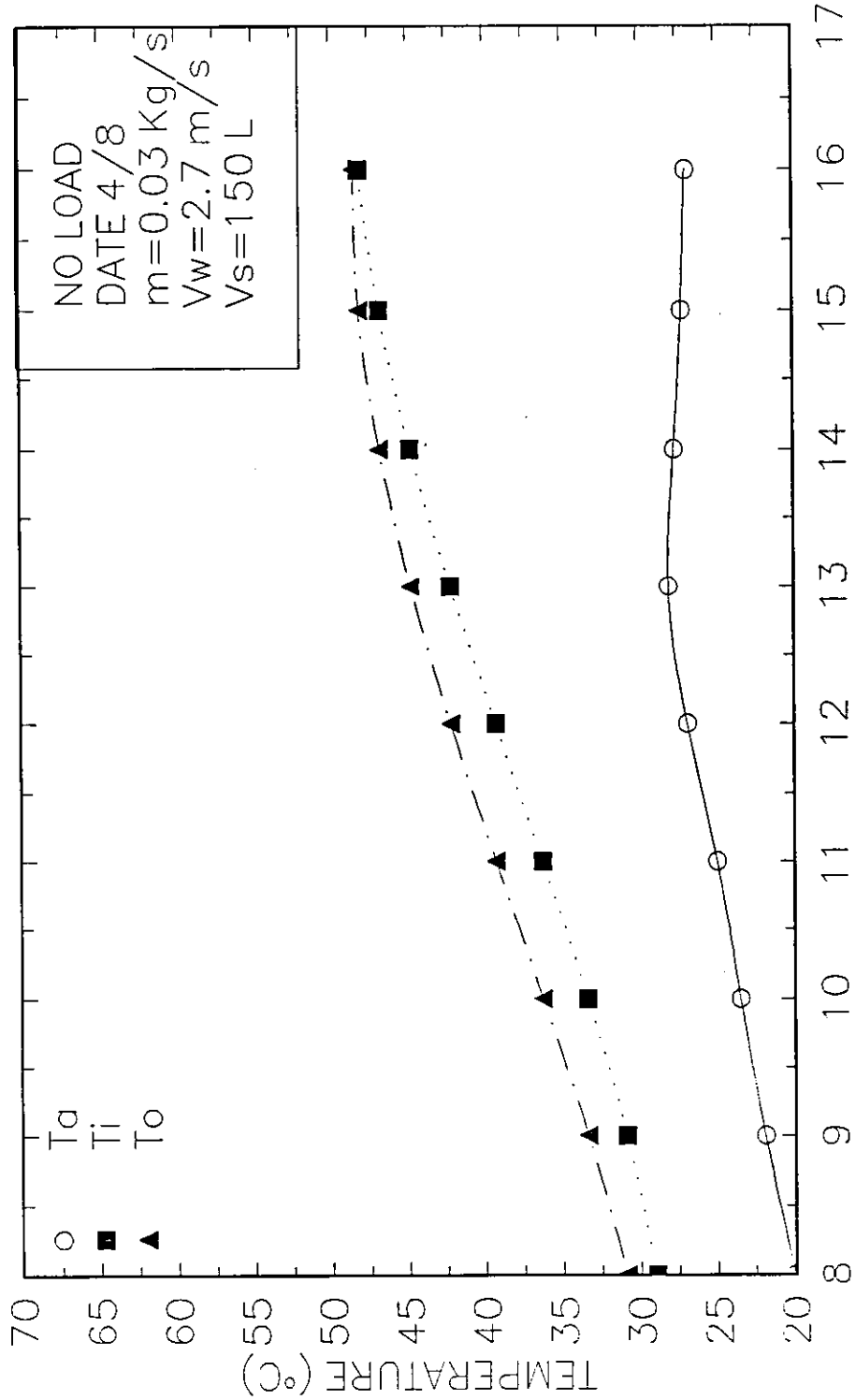

FIG (3.6). Variation of Inlet Temp. Outlet Temp. and the Amb. Temp. with Time for the Serpentine Tube Flat Metallic Plate Solar Colectors.

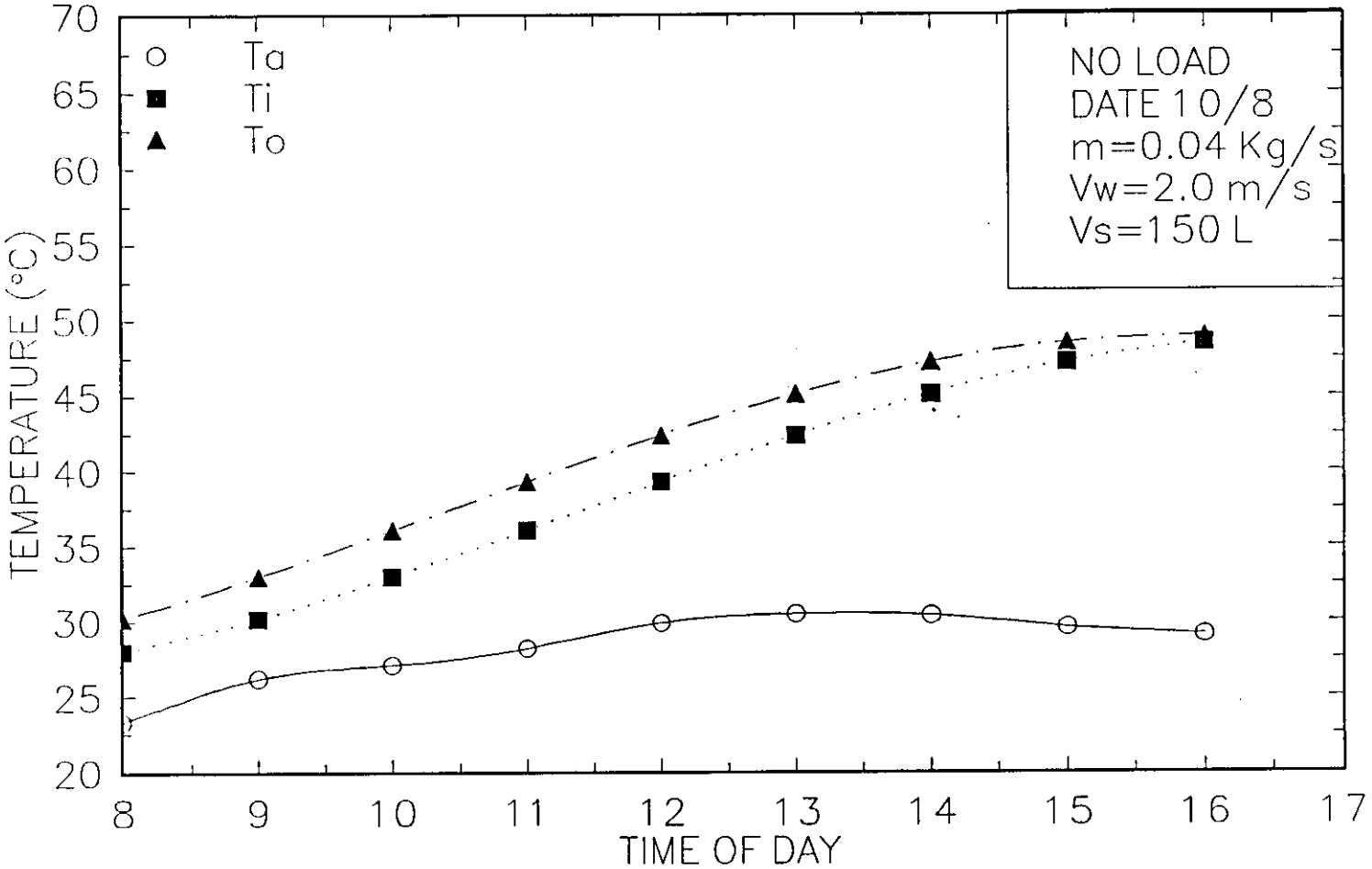

FIG (3.7). Variation of Inlet Temp. Outlet Temp. and the Amb. Temp. with Time for the Serpentine Tube Flat Metallic Plate Solar Colectors.

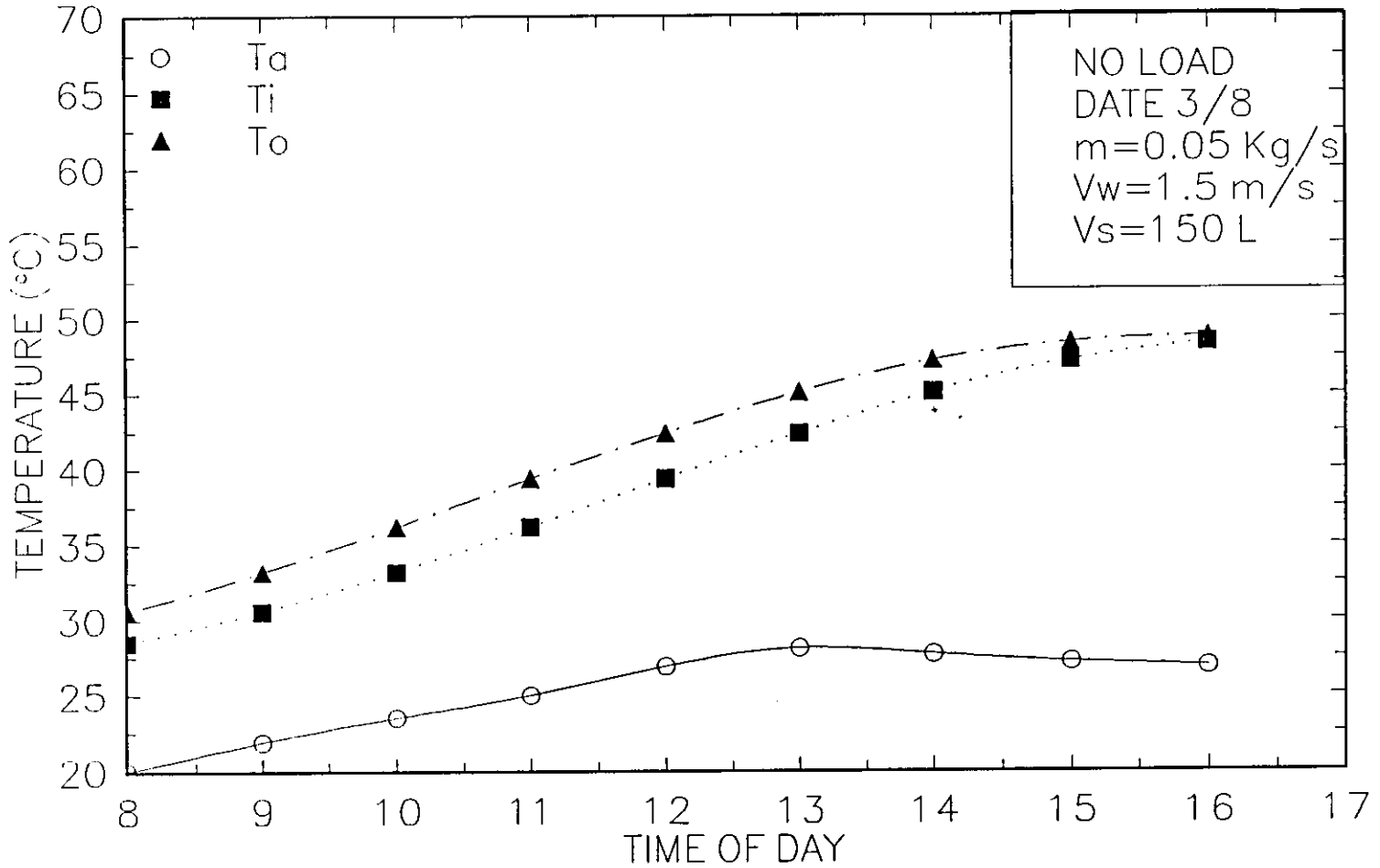

FIG (3.8). Variation of Inlet Temp. Outlet Temp. and the Amb. Temp. with Time for the Serpentine Tube Flat Metallic Plate Solar Colectors.

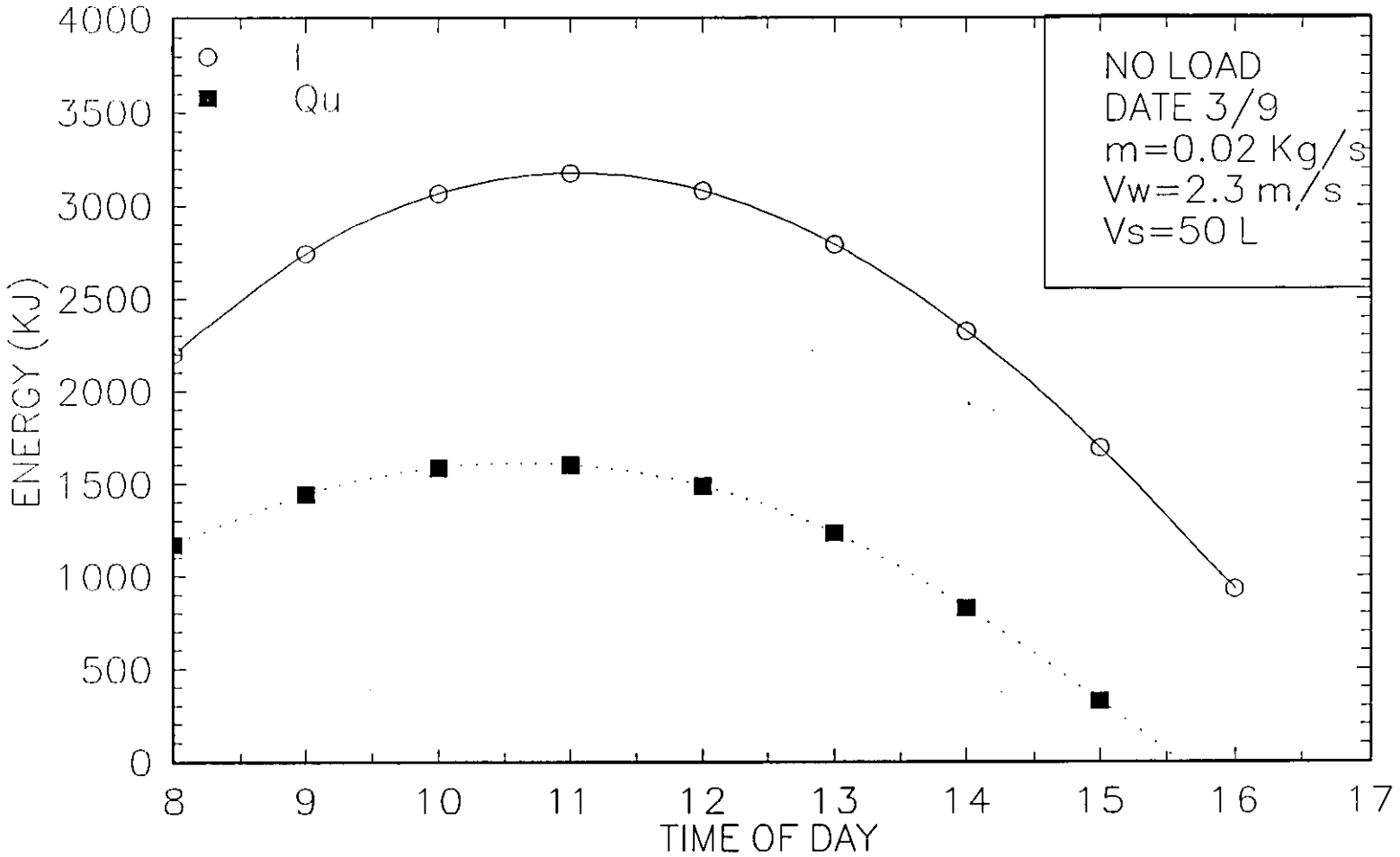

FIG (3.9). Variation of Incident Energy and Useful Energy with Time for the Serpentine Tube Flat Metallic Plate Solar Colectors.

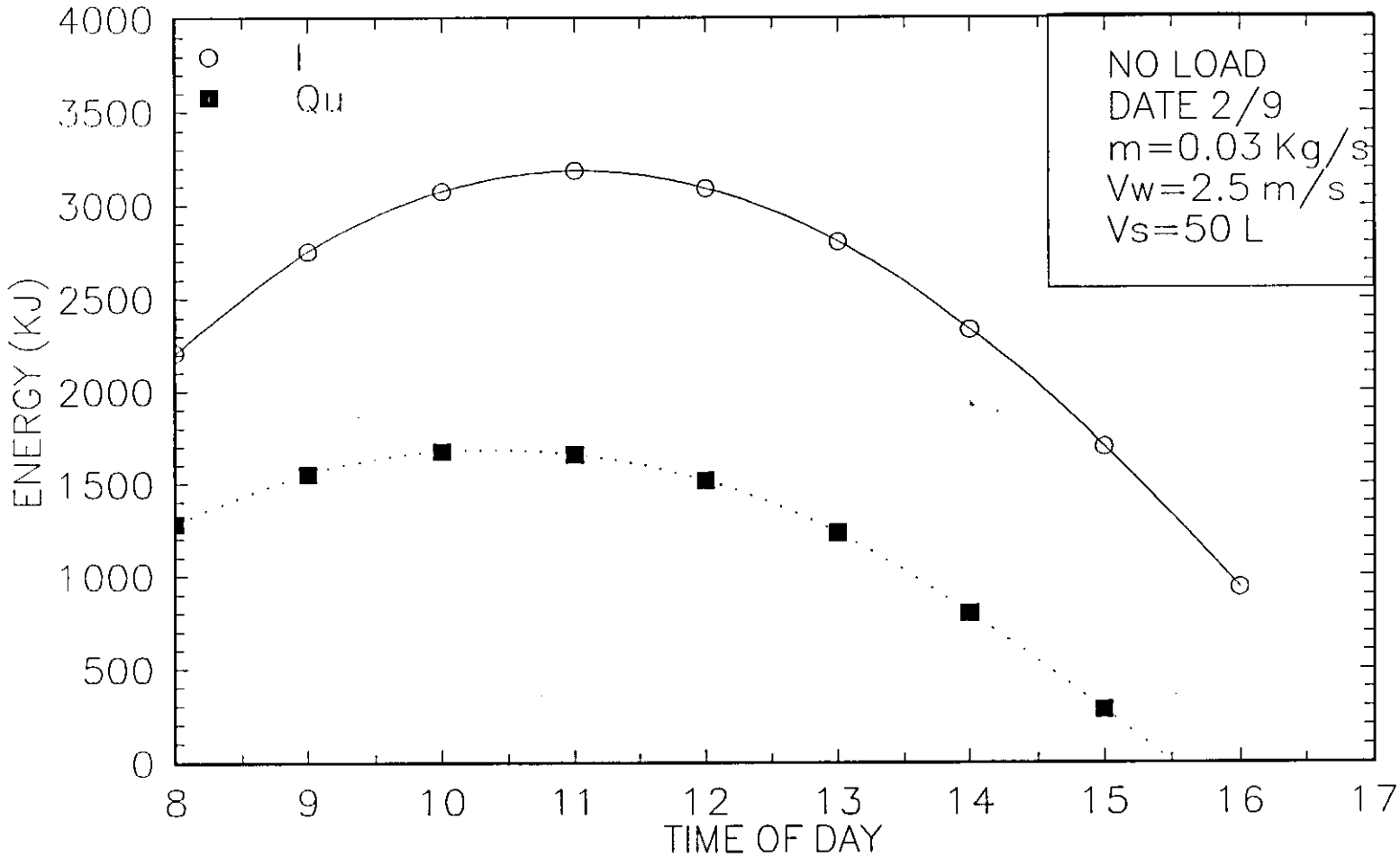

FIG (3.10). Variation of Incident Energy and Useful Energy with Time for the Serpentine Tube Flat Metallic Plate Solar Colectors.

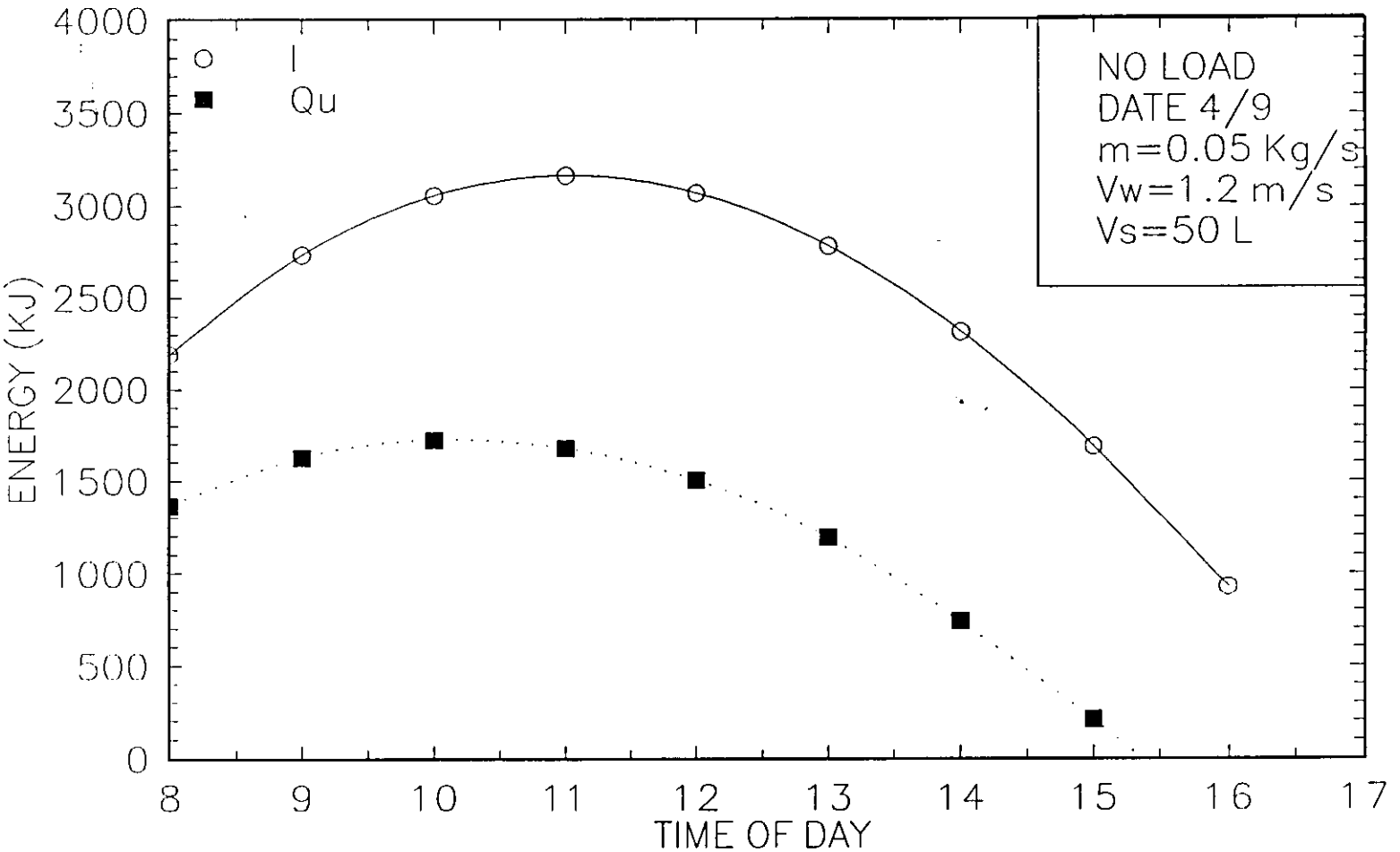

FIG (3.11). Variation of Incident Energy and Useful Energy with Time for the Serpentine Tube Flat Metallic Plate Solar Colectors.

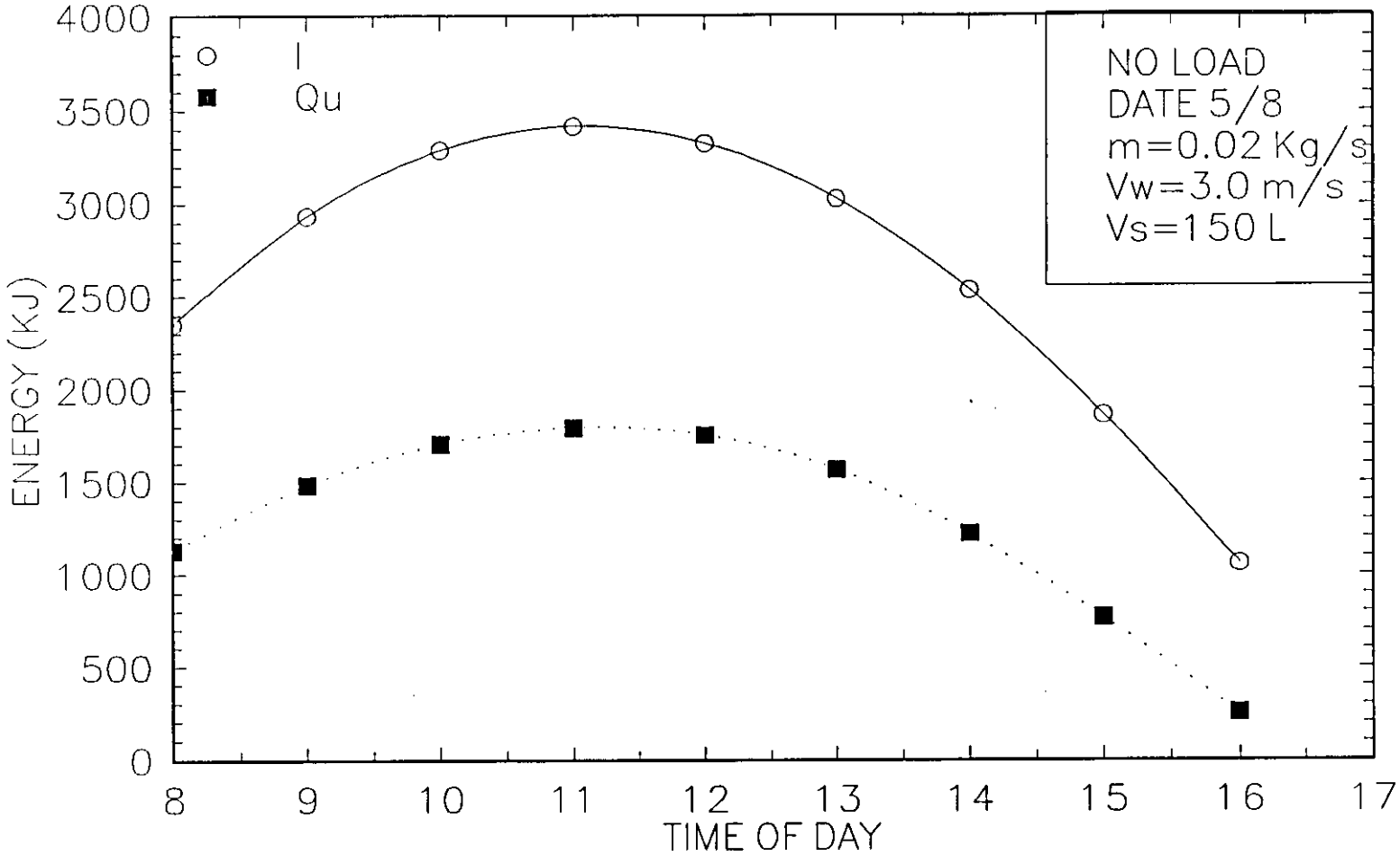

FIG (3.13). Variation of Incident Energy and Useful Energy with Time for the Serpentine Tube Flat Metallic Plate Solar Colectors.

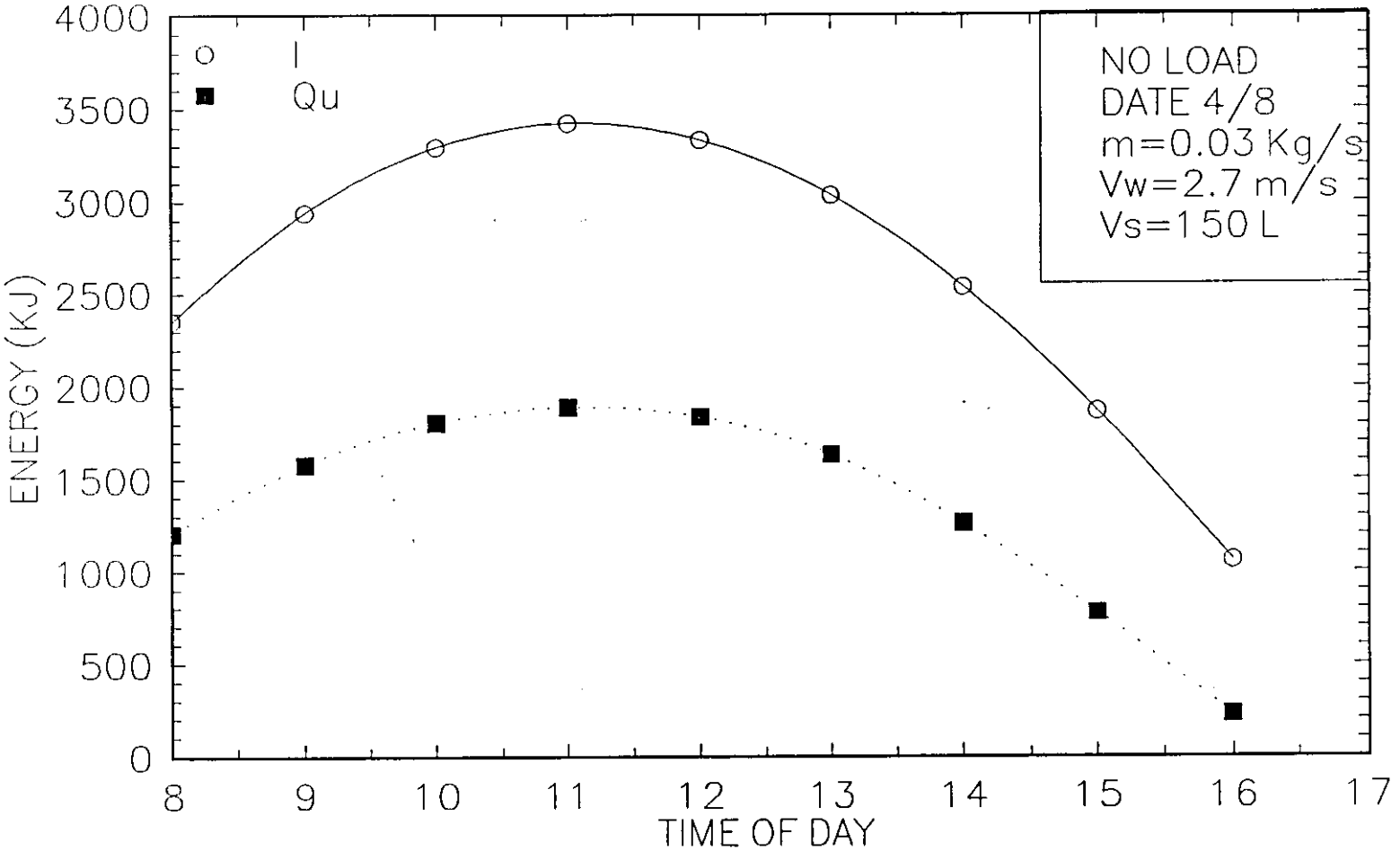

FIG (3.14). Variation of Incident Energy and Useful Energy with Time for the Serpentine Tube Flat Metallic Plate Solar Colectors.

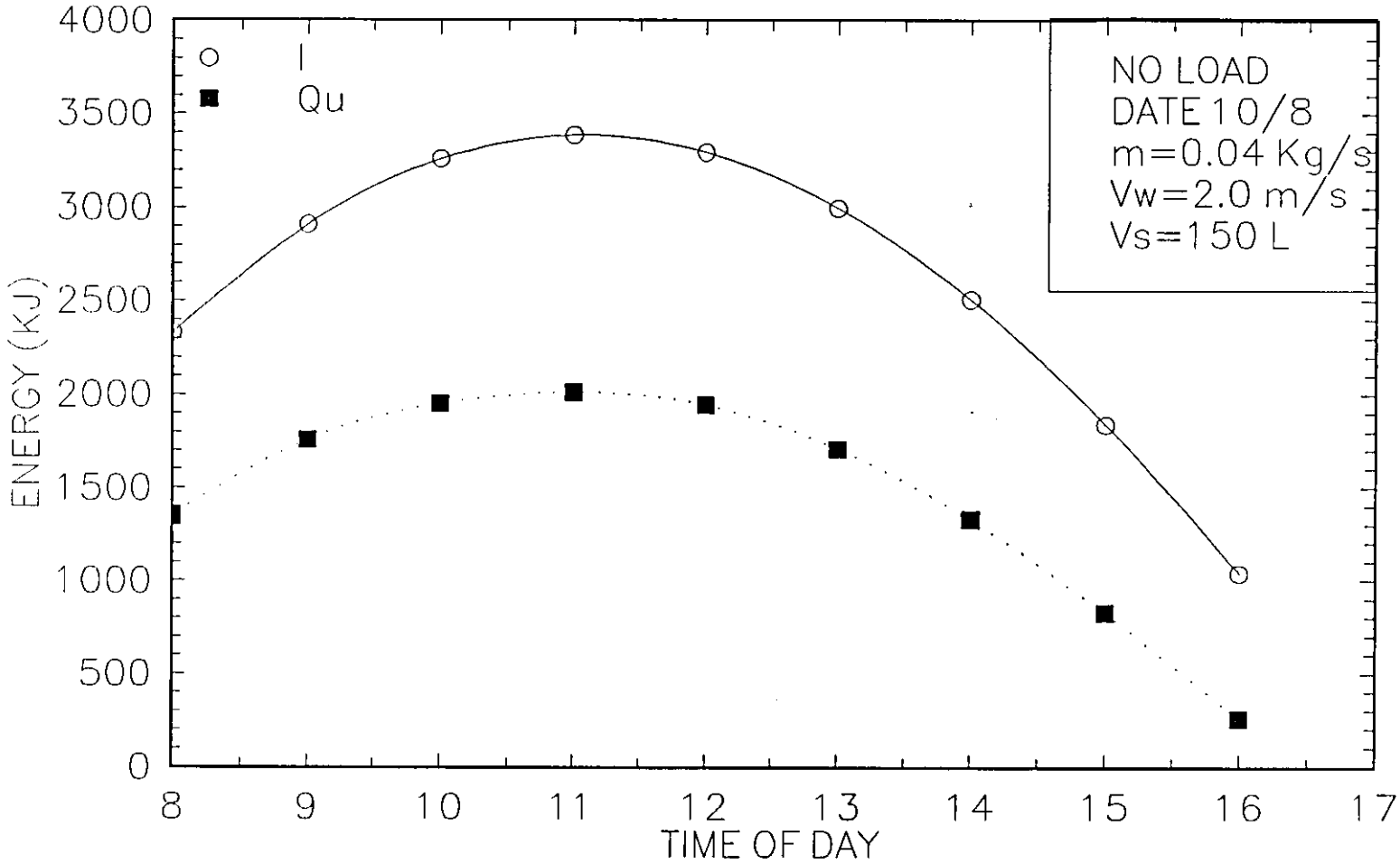

FIG (3.15). Variation of Incident Energy and Useful Energy with Time for the Serpentine Tube Flat Metallic Plate Solar Colectors.

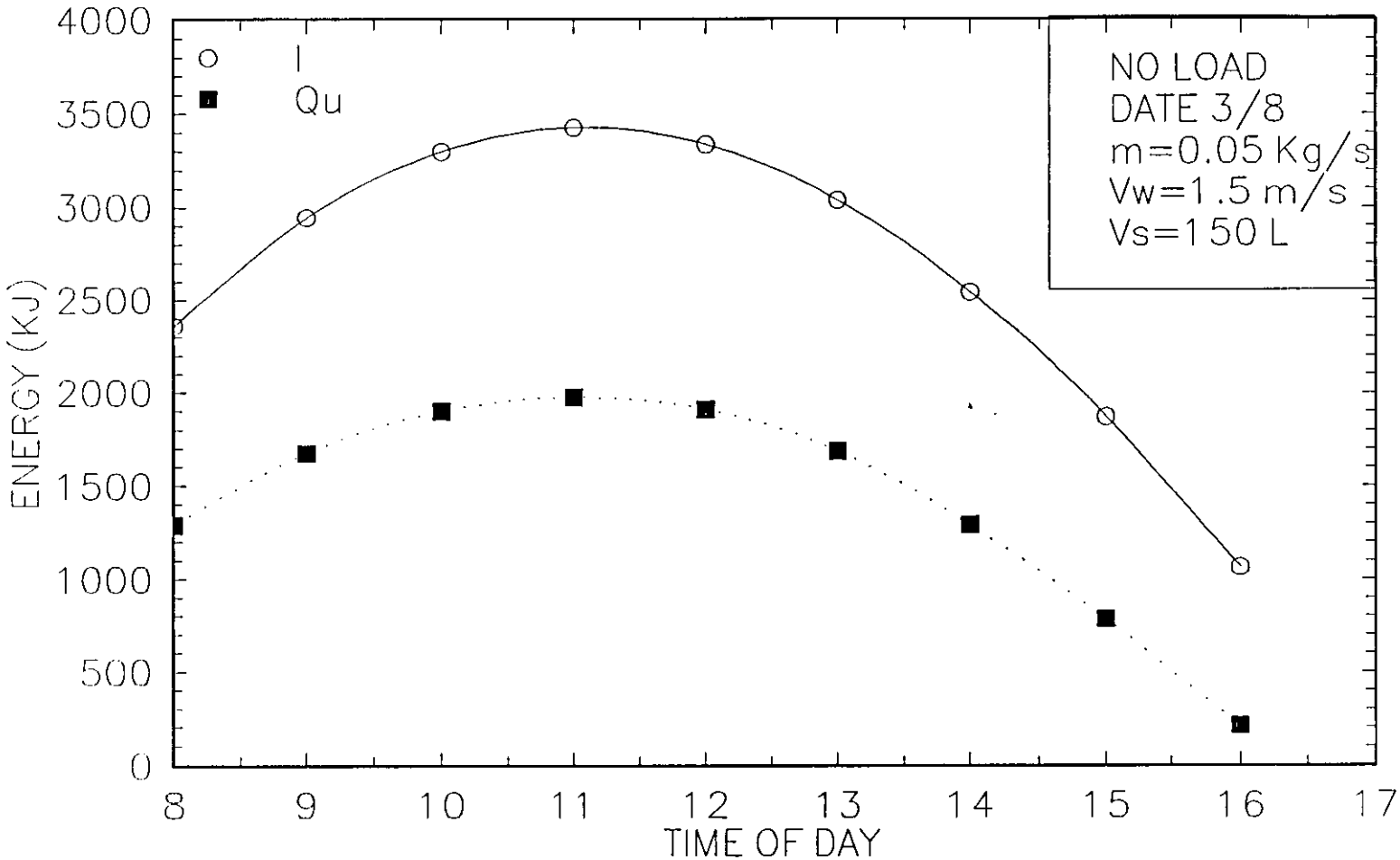

FIG (3.16). Variation of Incident Energy and Useful Energy with Time for the Serpentine Tube Flat Metallic Plate Solar Colectors.

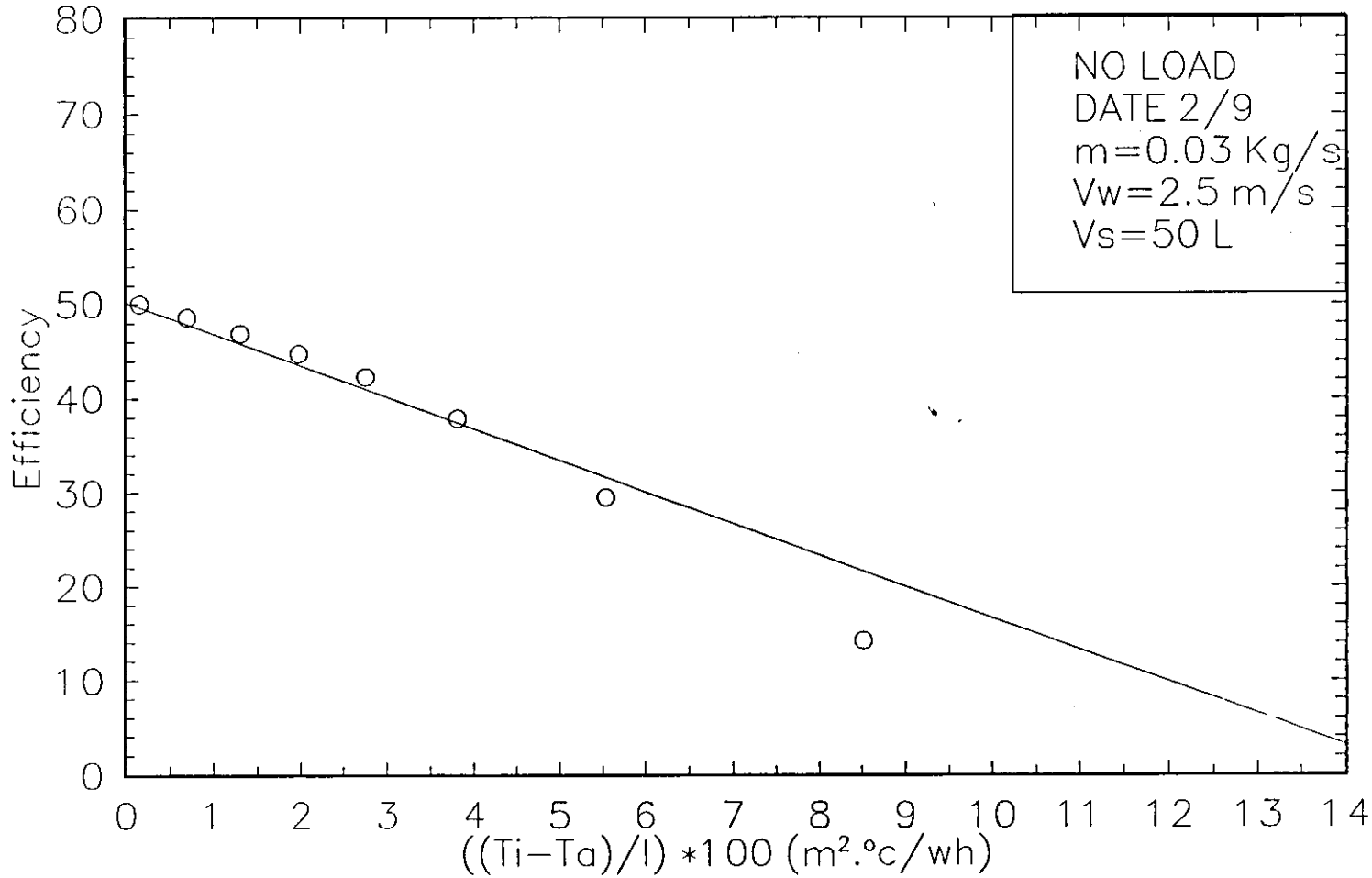

FIG (3.18). Variation of Instantaneous Efficiency against ((Ti−Ta)/I) for the Serpentine Tube Flat Metallic Plate Solar Colectors.

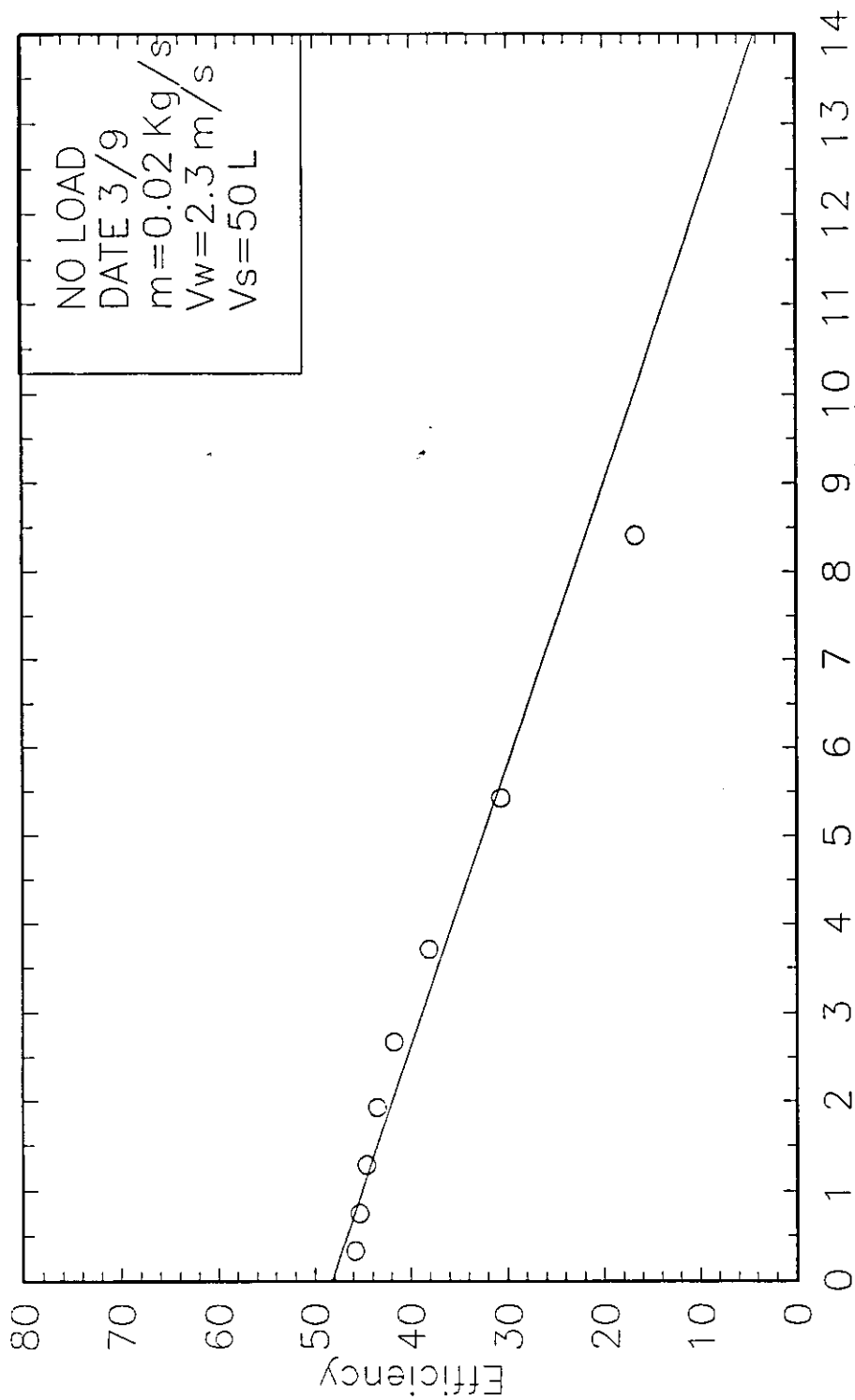

FIG (3.17). Variation of Instantaneous Efficiency against ((Ti−Ta)/I) for the Serpentine Tube Flat Metallic Plate Solar Colectors.

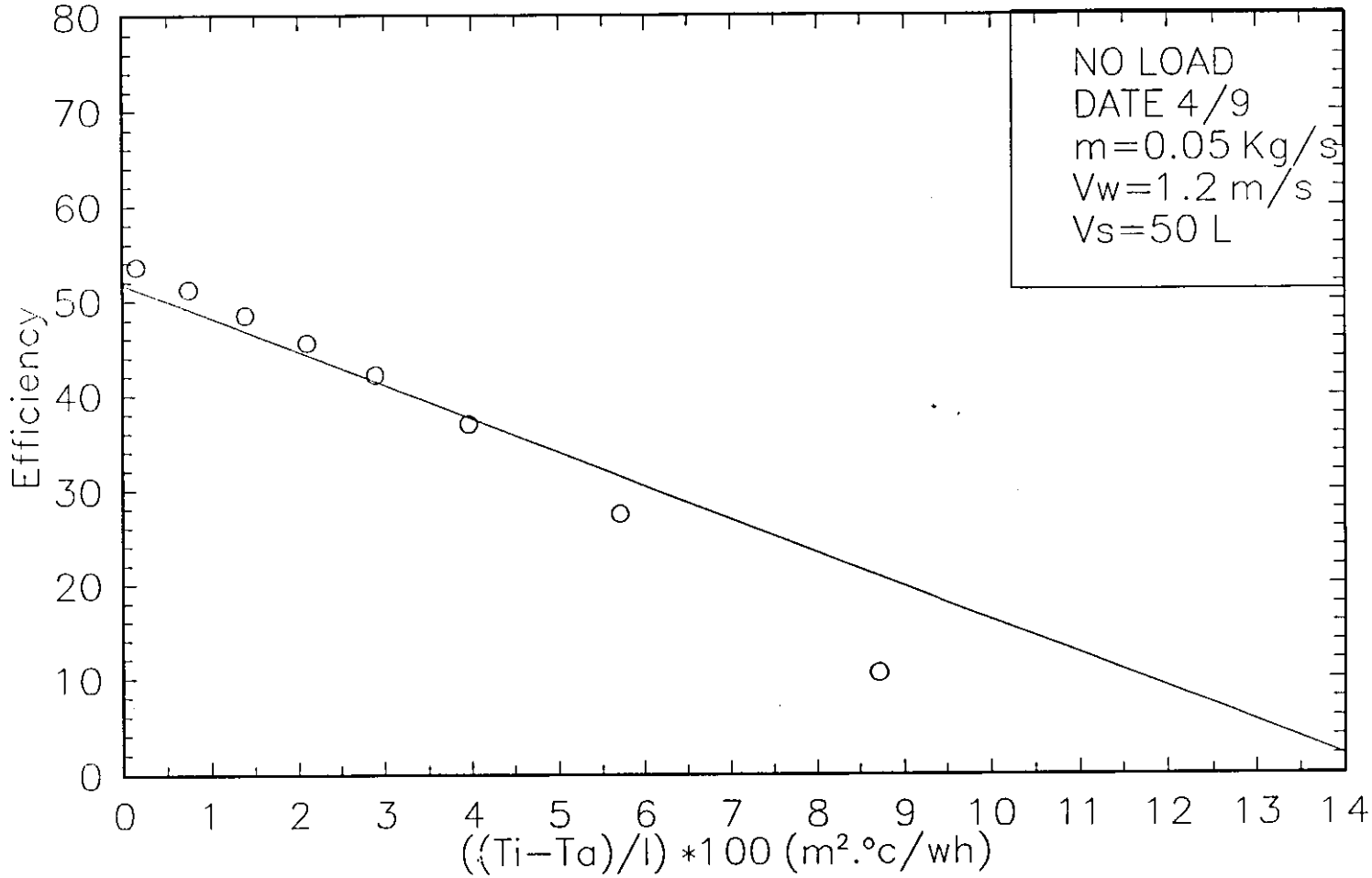

FIG (3.19). Variation of instantaneous Efficiency against ((Ti−Ta)/I) for the Serpentine Tube Flat Metallic Plate Solar Colectors.

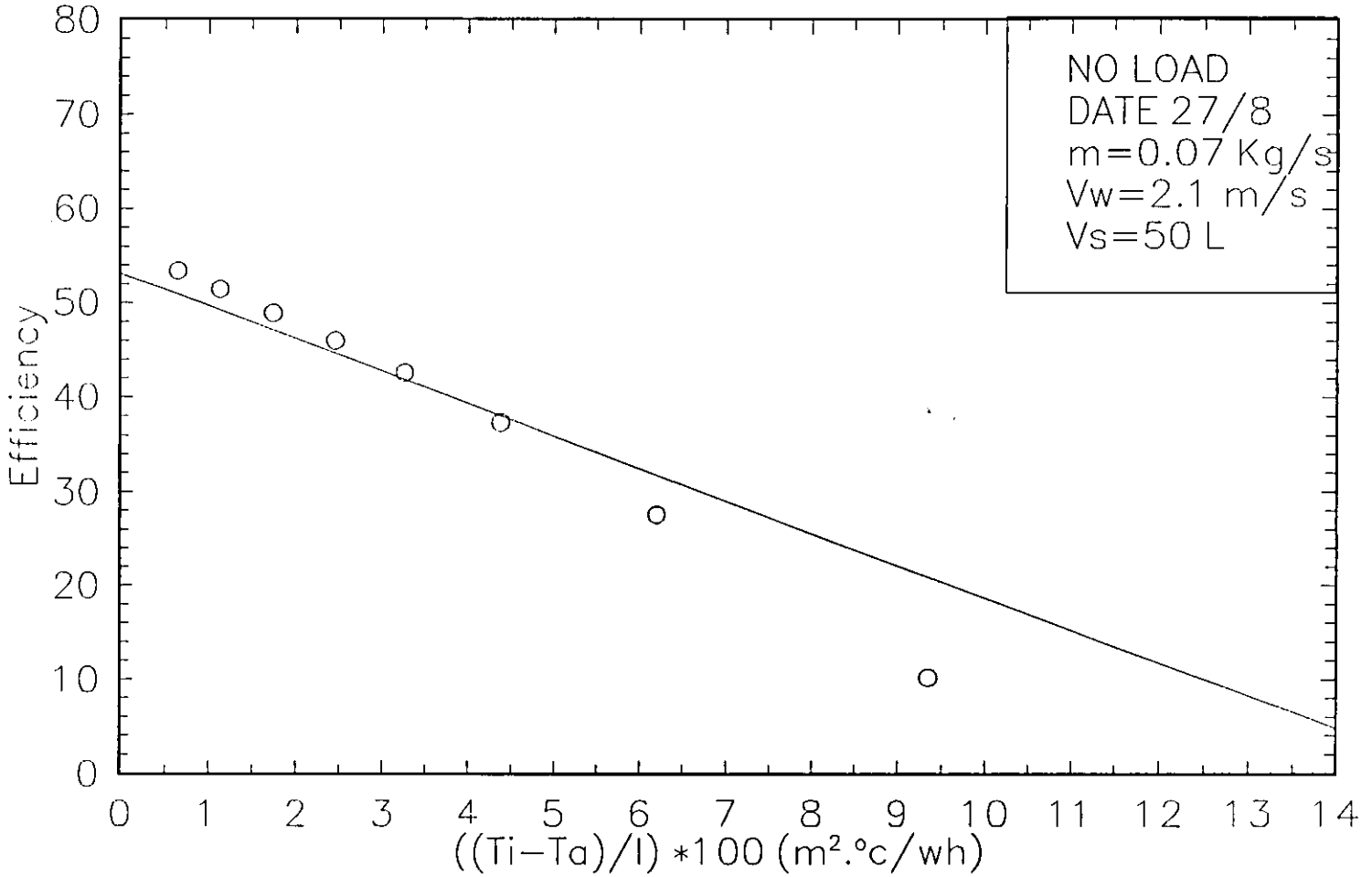

FIG (3.20). Variation of Instantaneous Efficiency against ((Ti−Ta)/I) for the Serpentine Tube Flat Metallic Plate Solar Colectors.

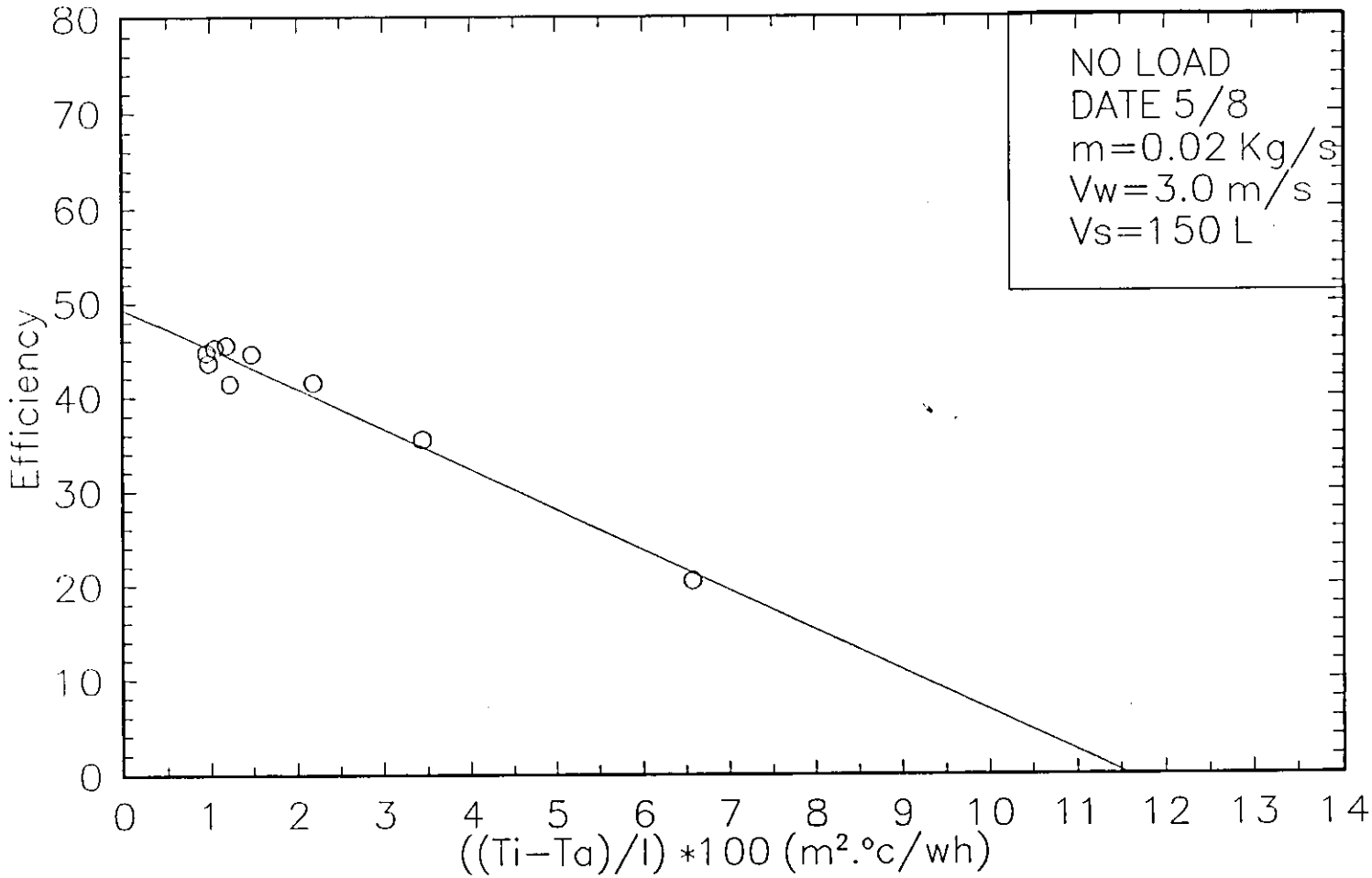

FIG (3.21). Variation of Instantaneous Efficiency against ((Ti−Ta)/I) for the Serpentine Tube Flat Metallic Plate Solar Colectors.

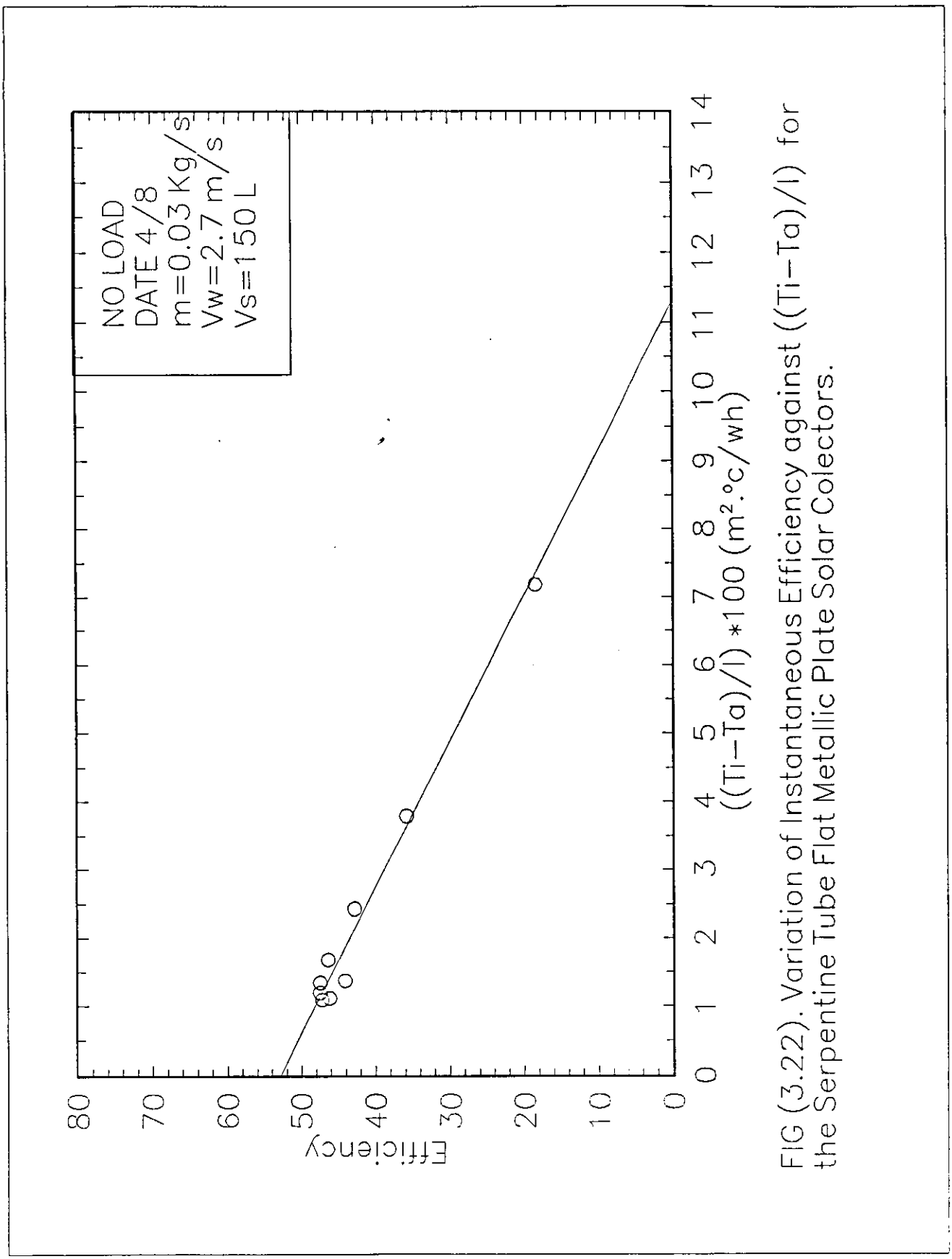

FIG (3.22). Variation of Instantaneous Efficiency against ((Ti−Ta)/I) for the Serpentine Tube Flat Metallic Plate Solar Colectors.

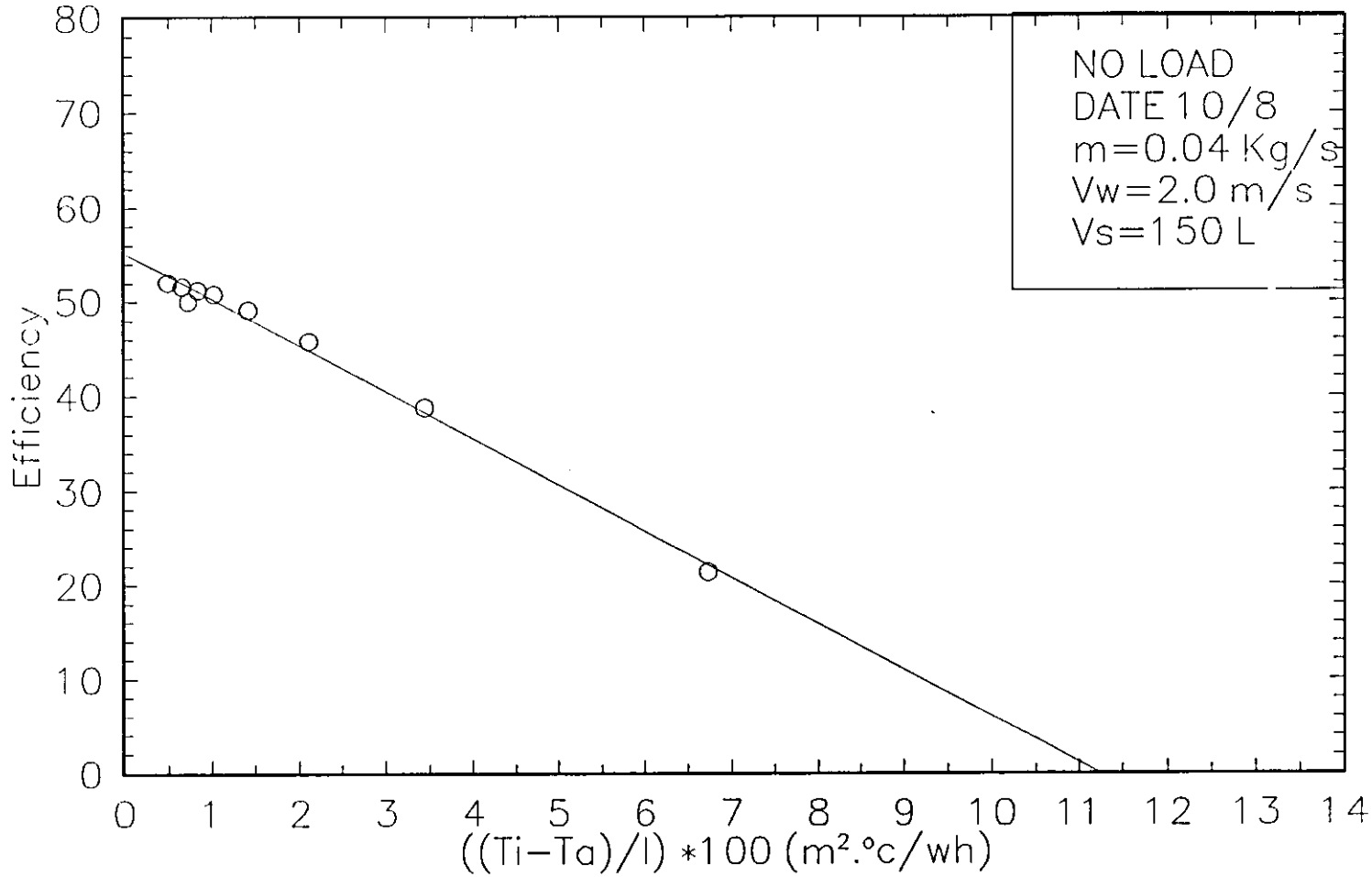

FIG (3.23). Variation of Instantaneous Efficiency against ((Ti−Ta)/I) for the Serpentine Tube Flat Metallic Plate Solar Colectors.

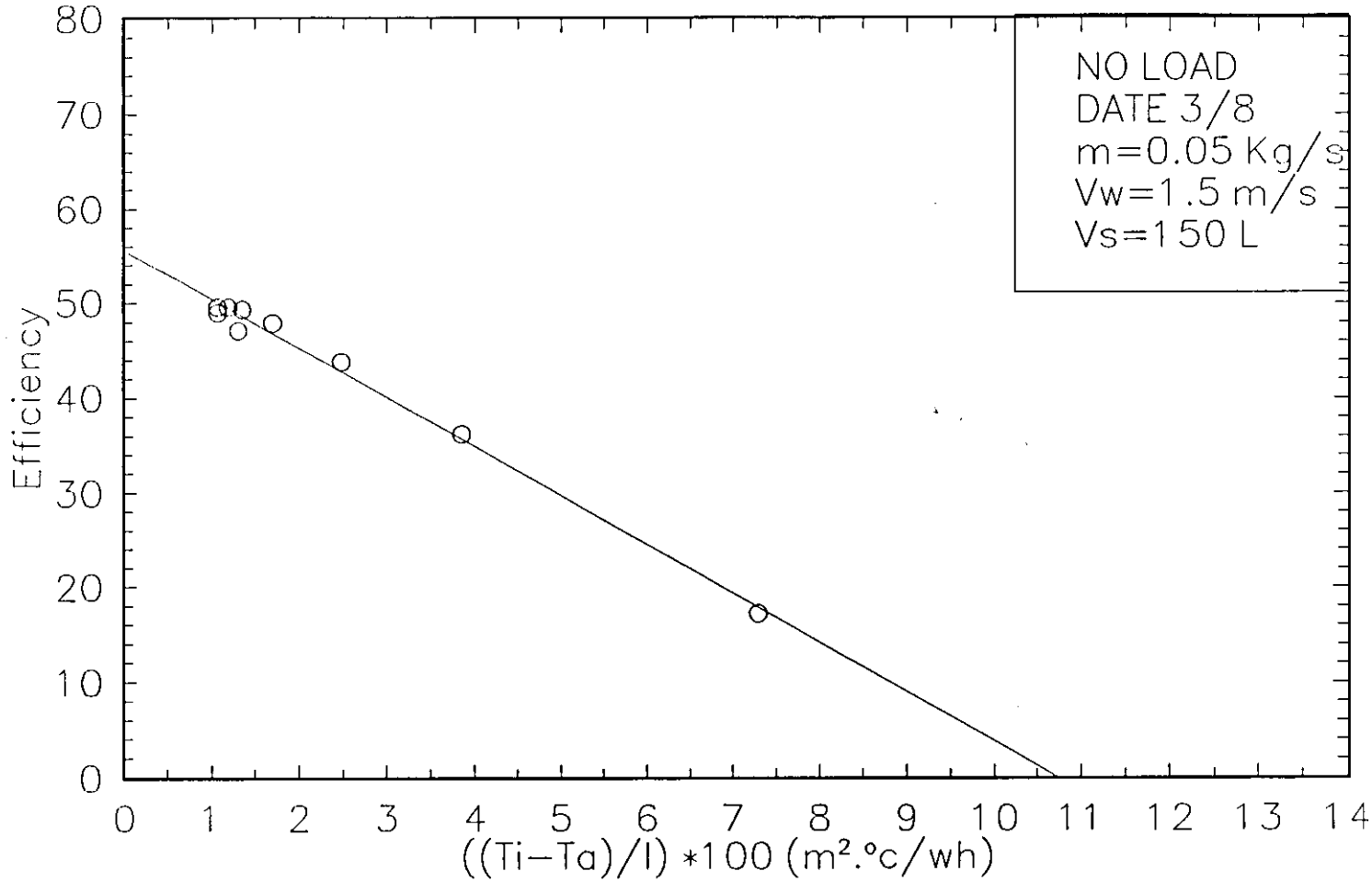

FIG (3.24). Variation of Instantaneous Efficiency against ((Ti−Ta)/I) for the Serpentine Tube Flat Metallic Plate Solar Colectors.

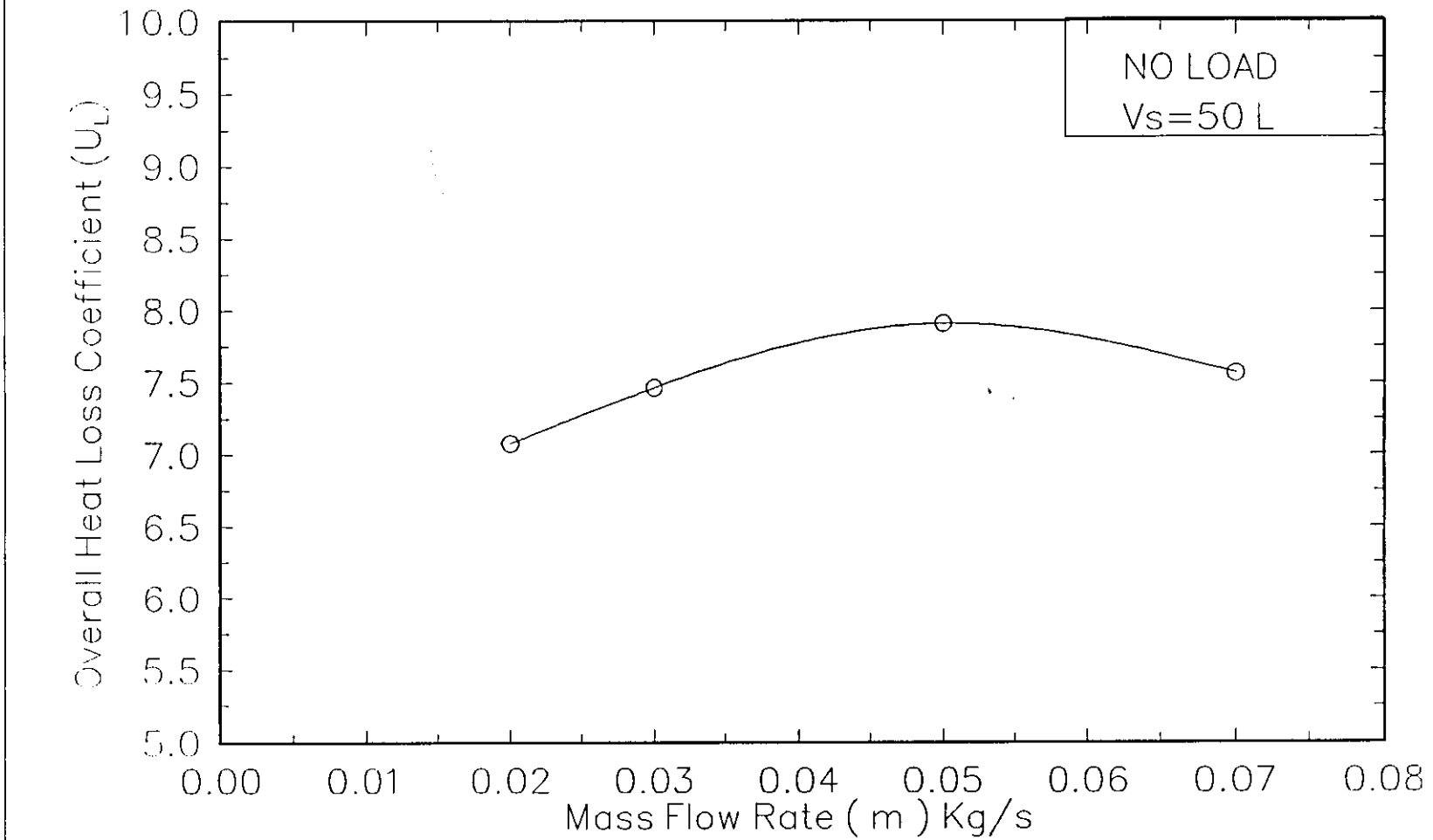

FIG (3.25). Variation of Overall Heat Loss Coefficient with Mass flow Rate for Serpentine Tube Flat (Metallic) Plate Solar Collector

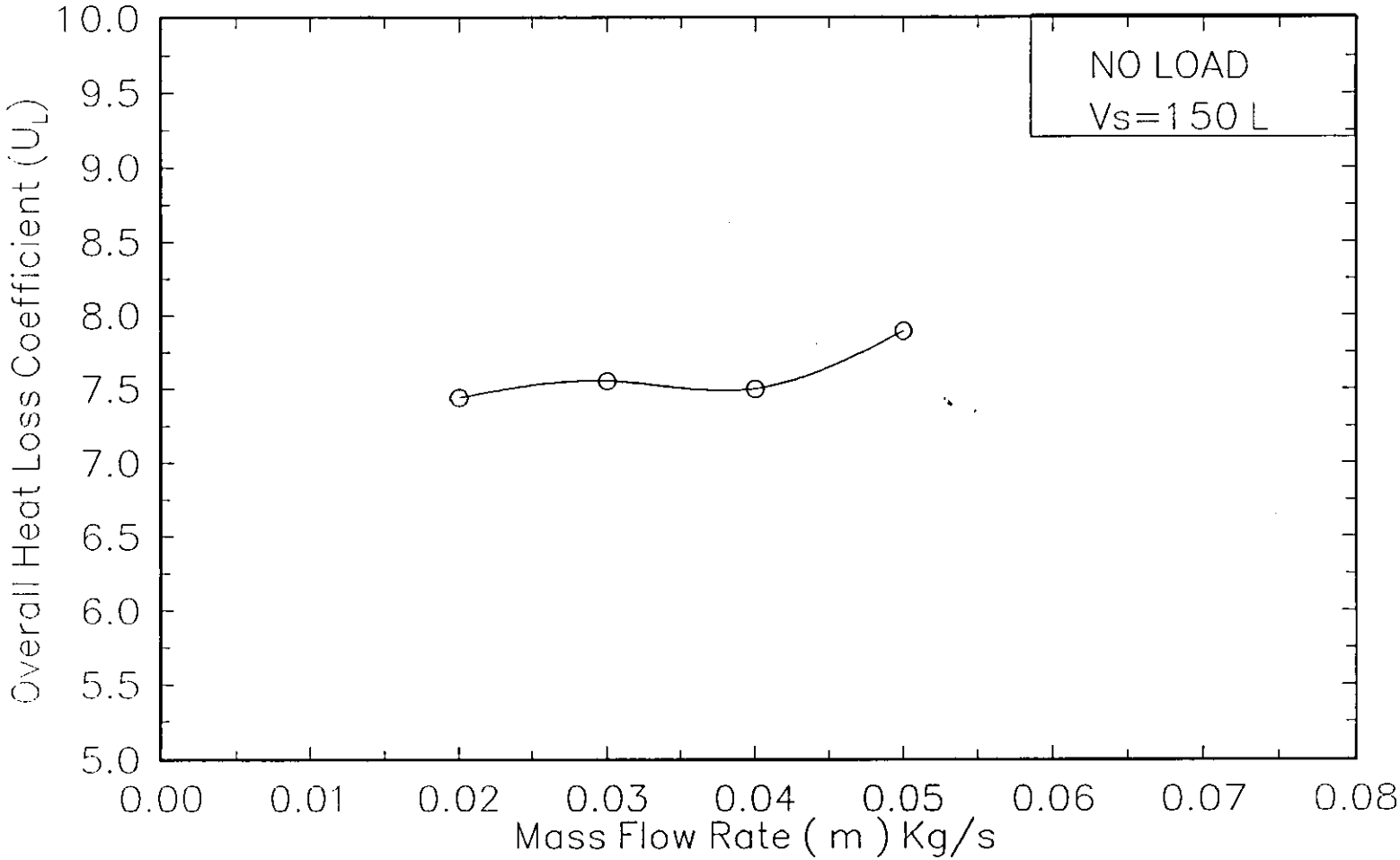

FIG (3.26). Variation of Overall Heat Loss Coefficient with Mass flow Rate for Serpentine Tube Flat (Metallic) Plate Solar Collector

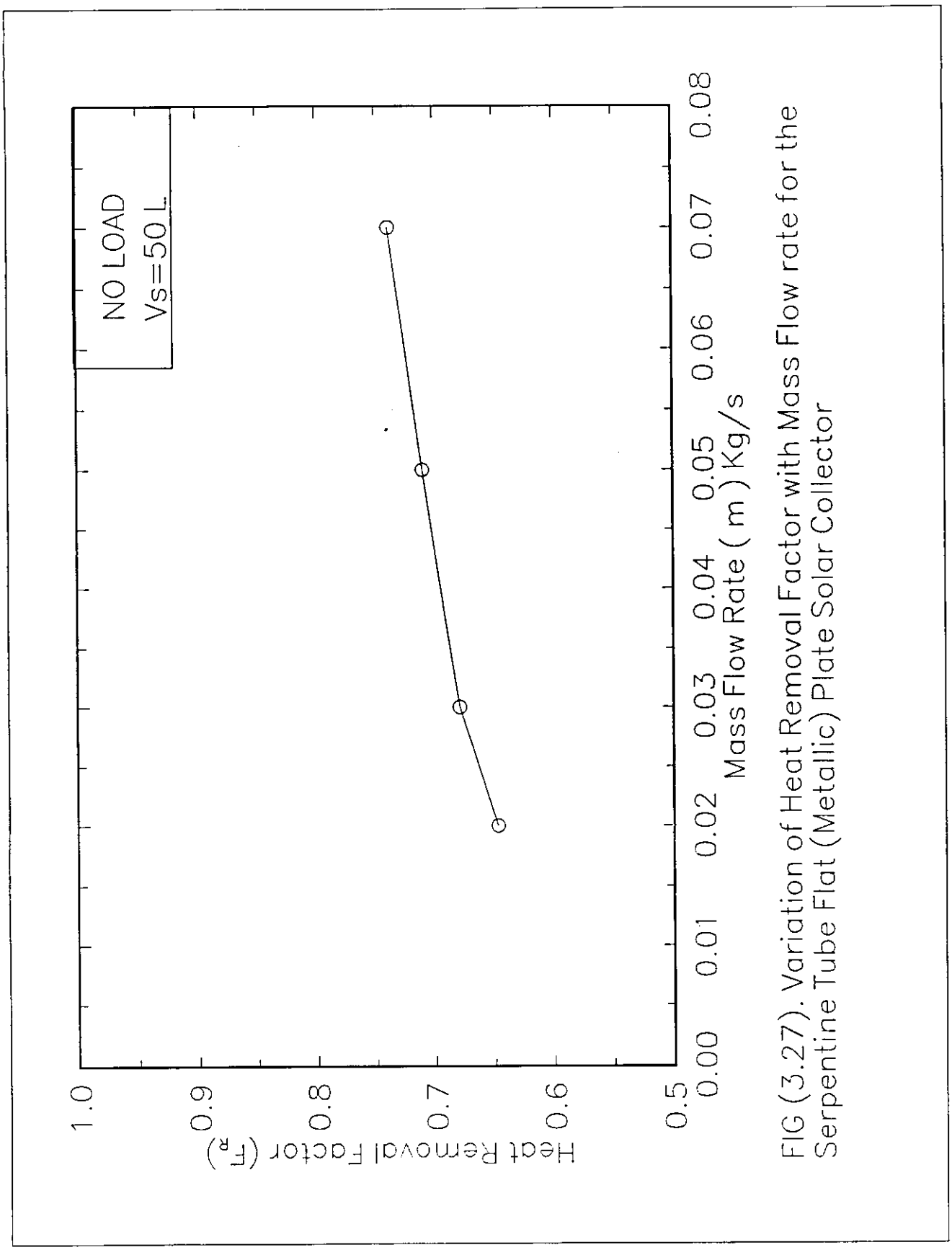

FIG (3.27). Variation of Heat Removal Factor with Mass Flow rate for the Serpentine Tube Flat (Metallic) Plate Solar Collector

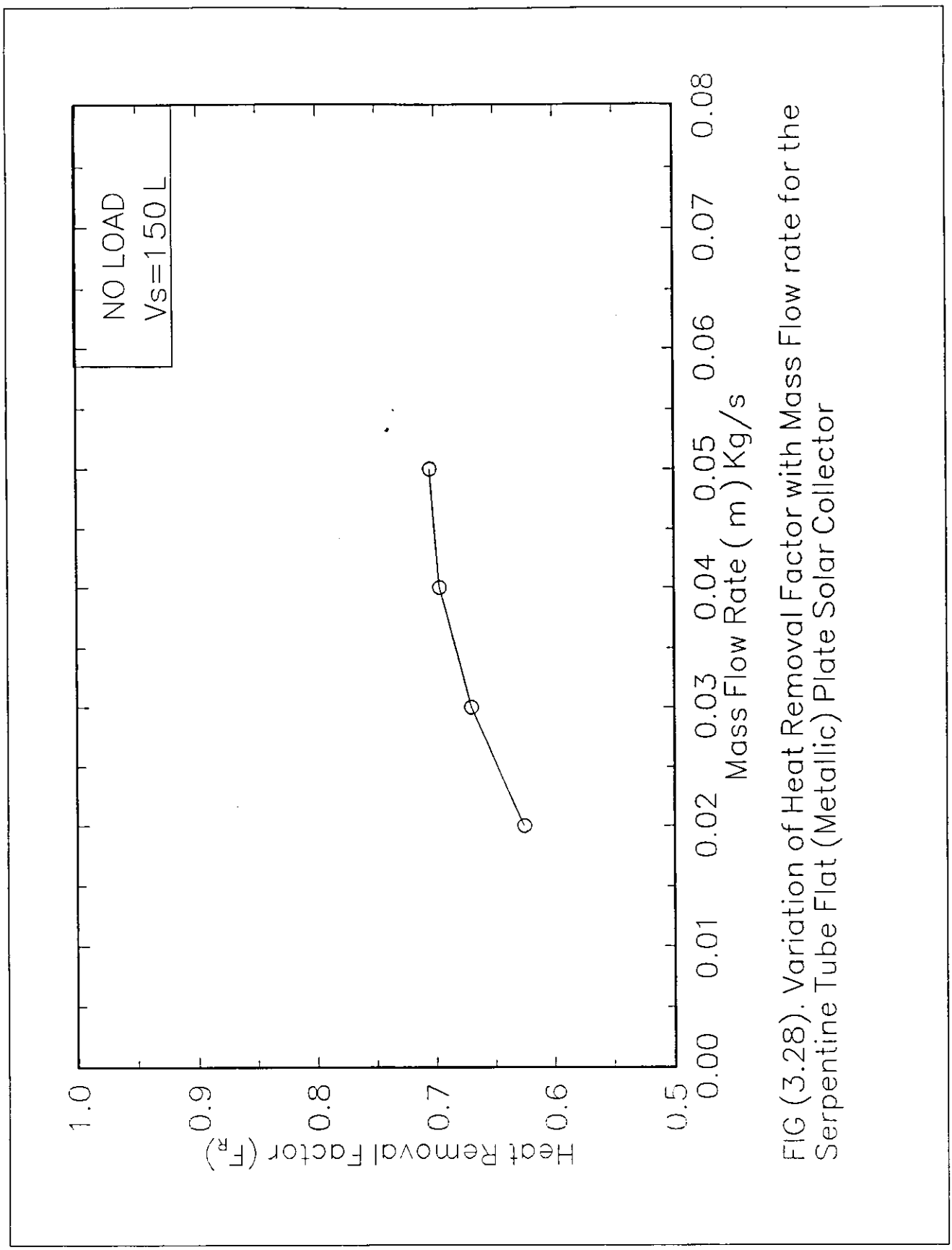

FIG (3.28). Variation of Heat Removal Factor with Mass Flow rate for the Serpentine Tube Flat (Metallic) Plate Solar Collector

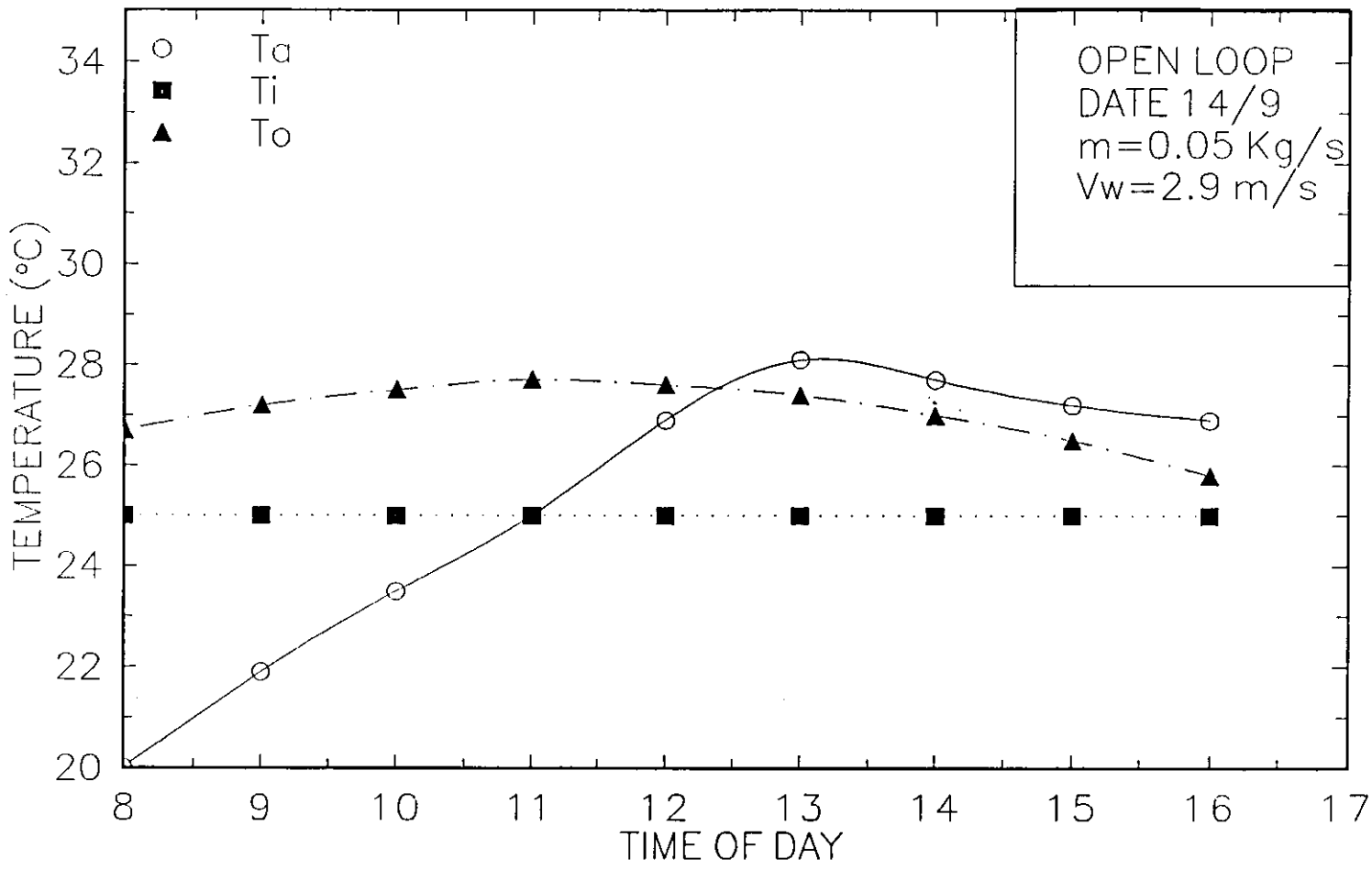

FIG (3.30). Variation of Inlet Temp. Outlet Temp. and the Amb. Temp. with Time for the Serpentine Tube Flat Metallic Plate Solar Colectors.

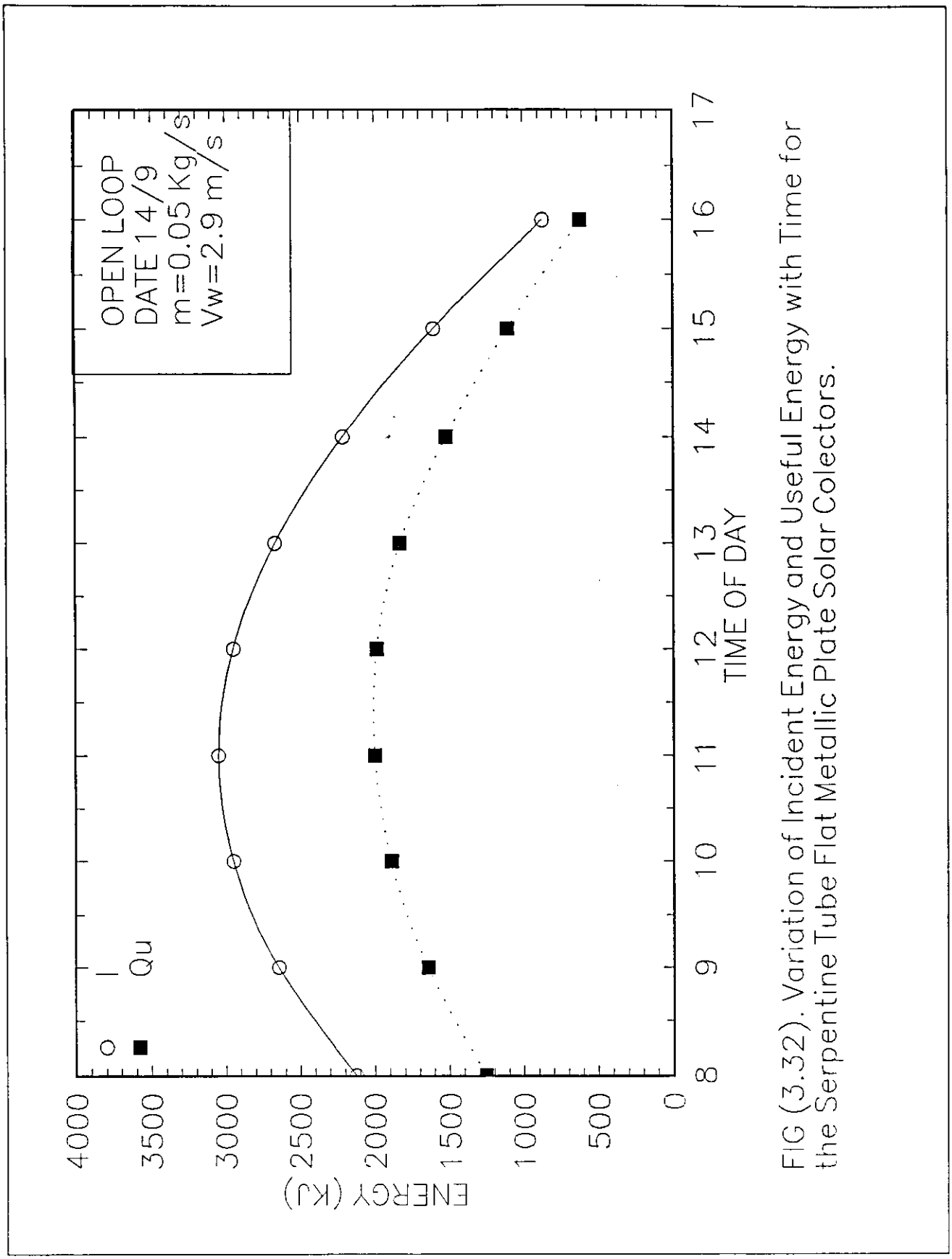

FIG (3.32). Variation of Incident Energy and Useful Energy with Time for the Serpentine Tube Flat Metallic Plate Solar Colectors.

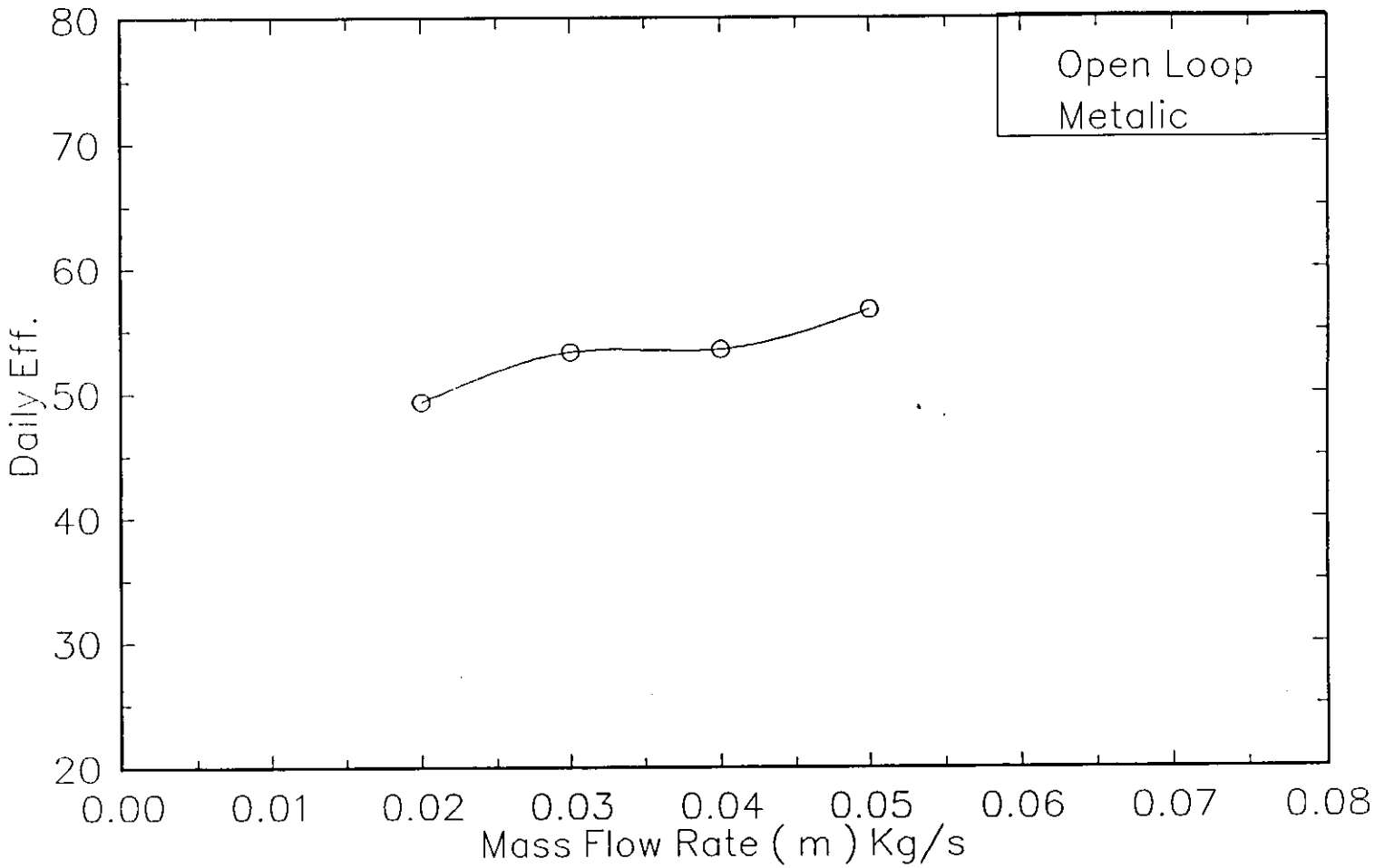

FIG (3.33). Variation of Daily Eff. with Mass Flow rate for the Serpentine Metallic Plate Solar Collector

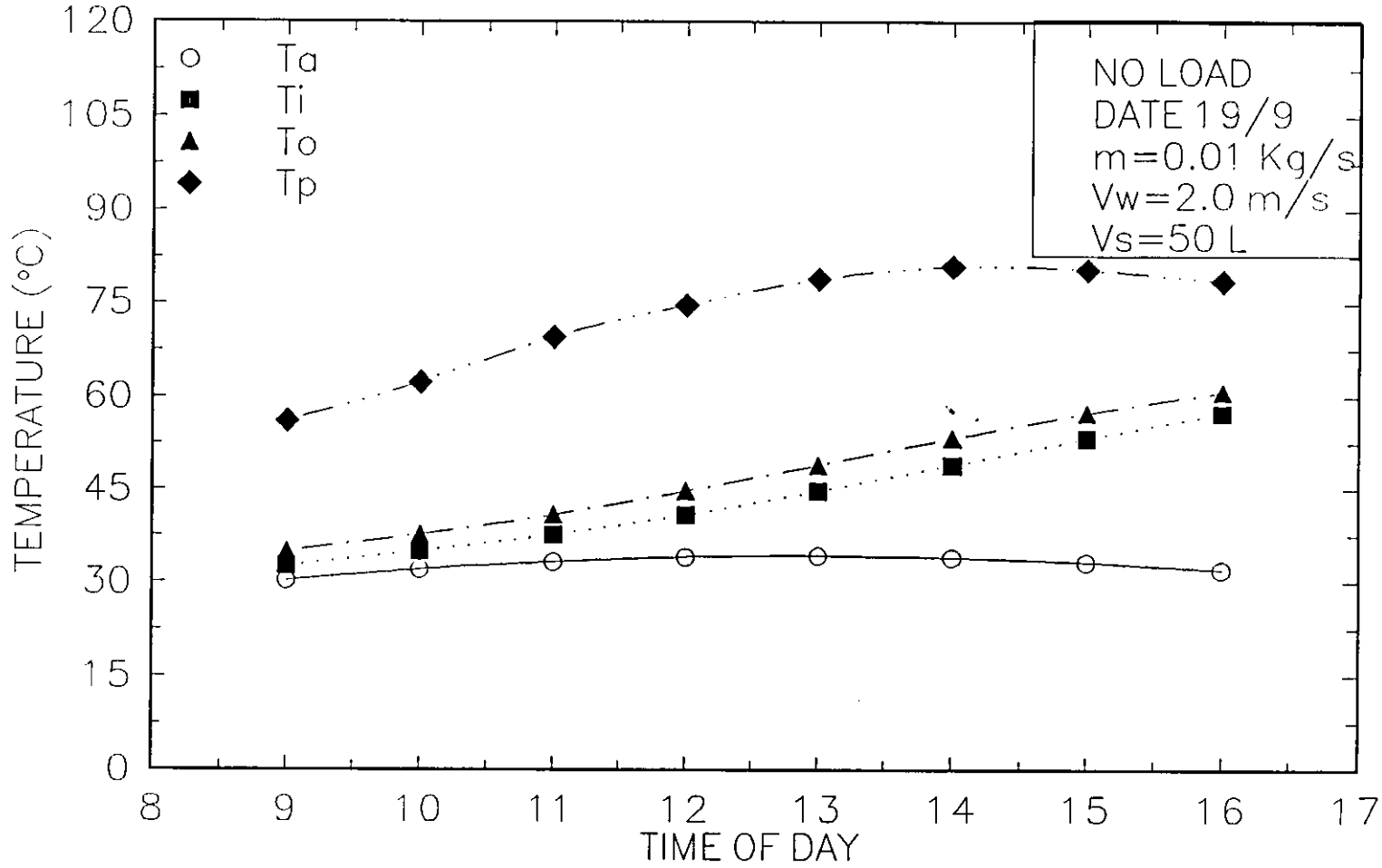

FIG (3.34). Variation of Inlet Temp., Outlet Temp., Amb. Temp. and the Plate Temp. with Time for the Serpentine Tube Flat (Non_Metallic) Plate Solar Collectors.

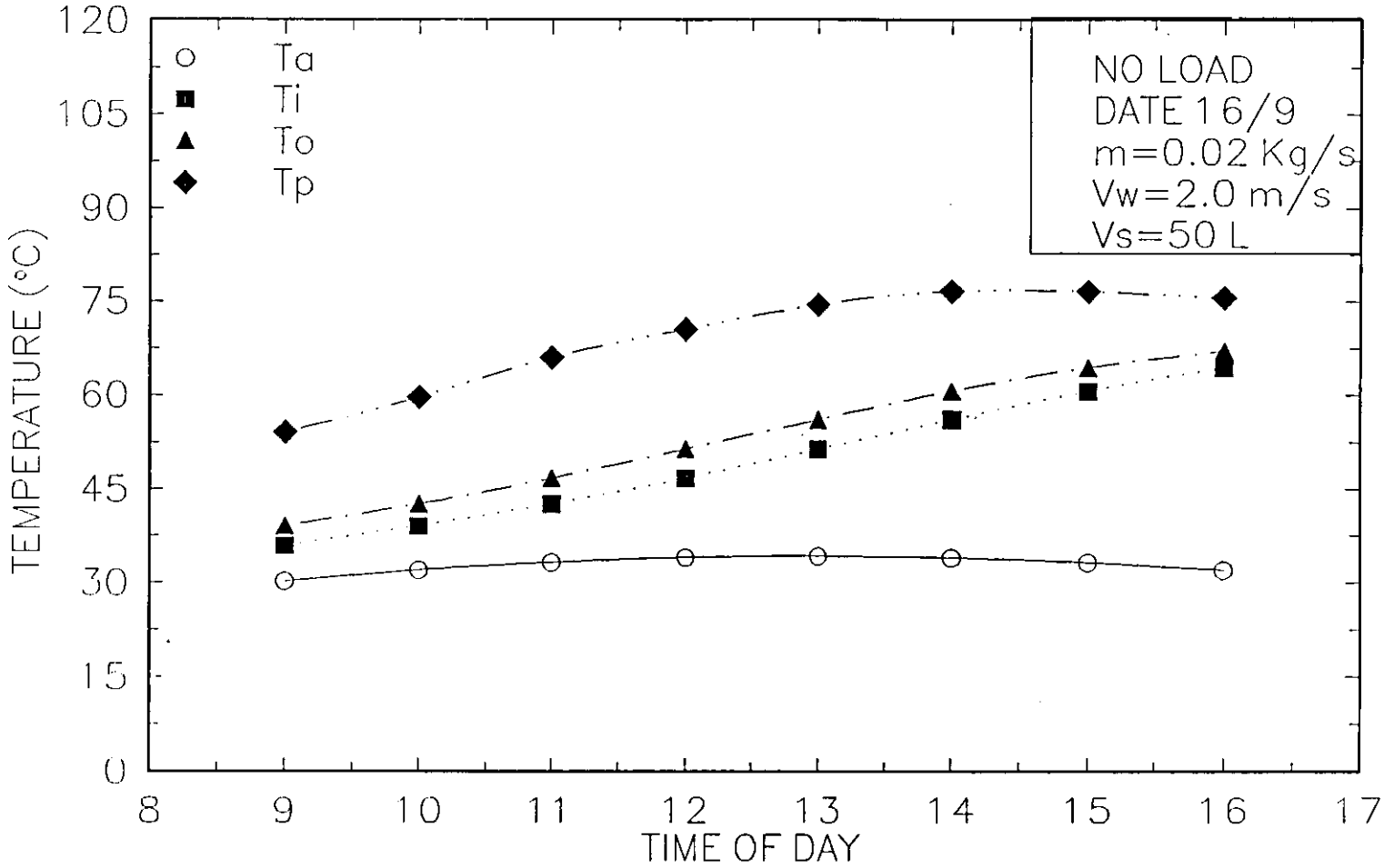

FIG (3.35). Variation of Inlet Temp., Outlet Temp., Amb. Temp. and the Plate Temp. with Time for the Serpentine Tube Flat (Non_Metallic) Plate Solar Collectors.

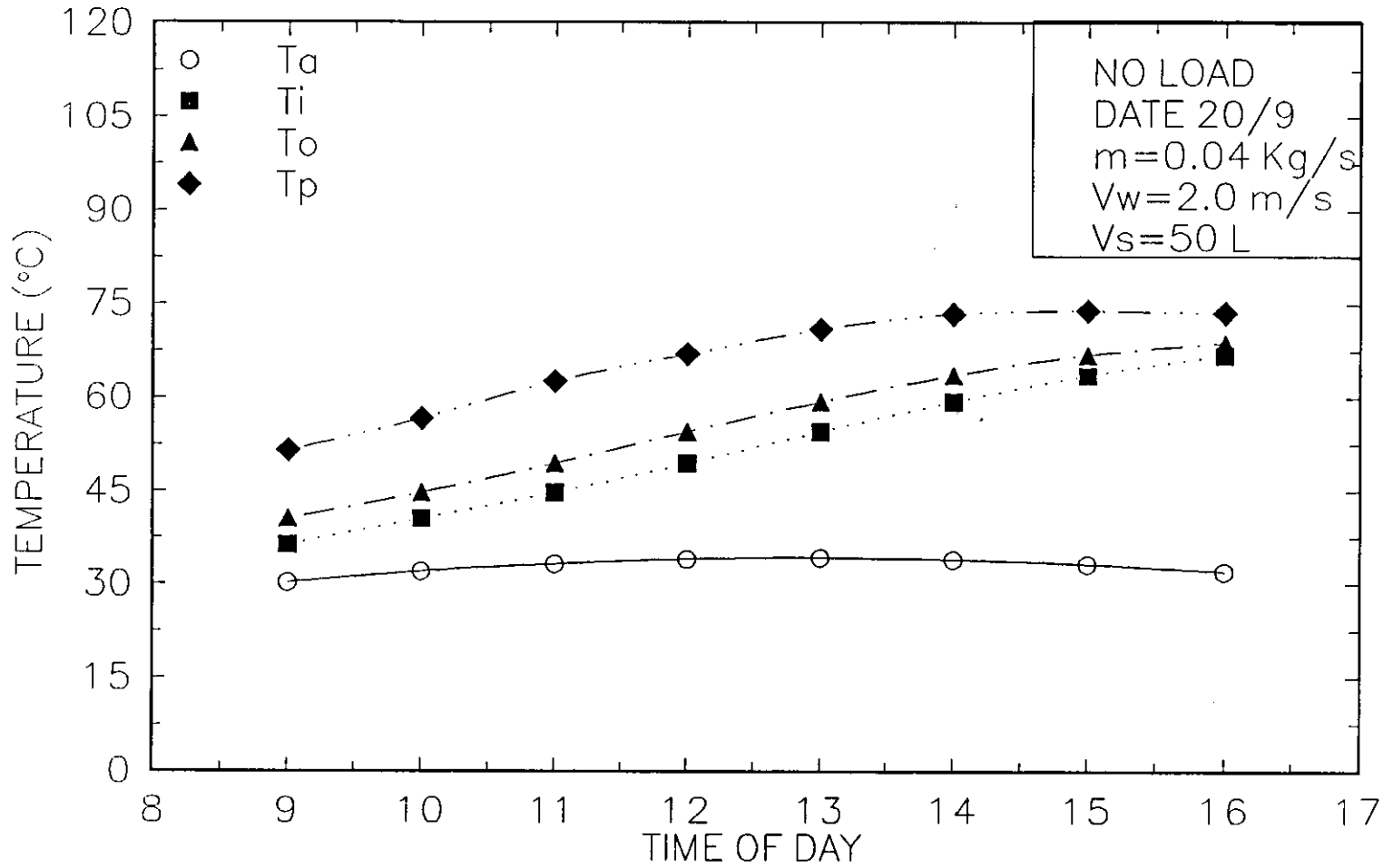

FIG (3.36). Variation of Inlet Temp., Outlet Temp., Amb. Temp. and the Plate Temp. with Time for the Serpentine Tube Flat (Non_Metallic) Plate Solar Collectors.

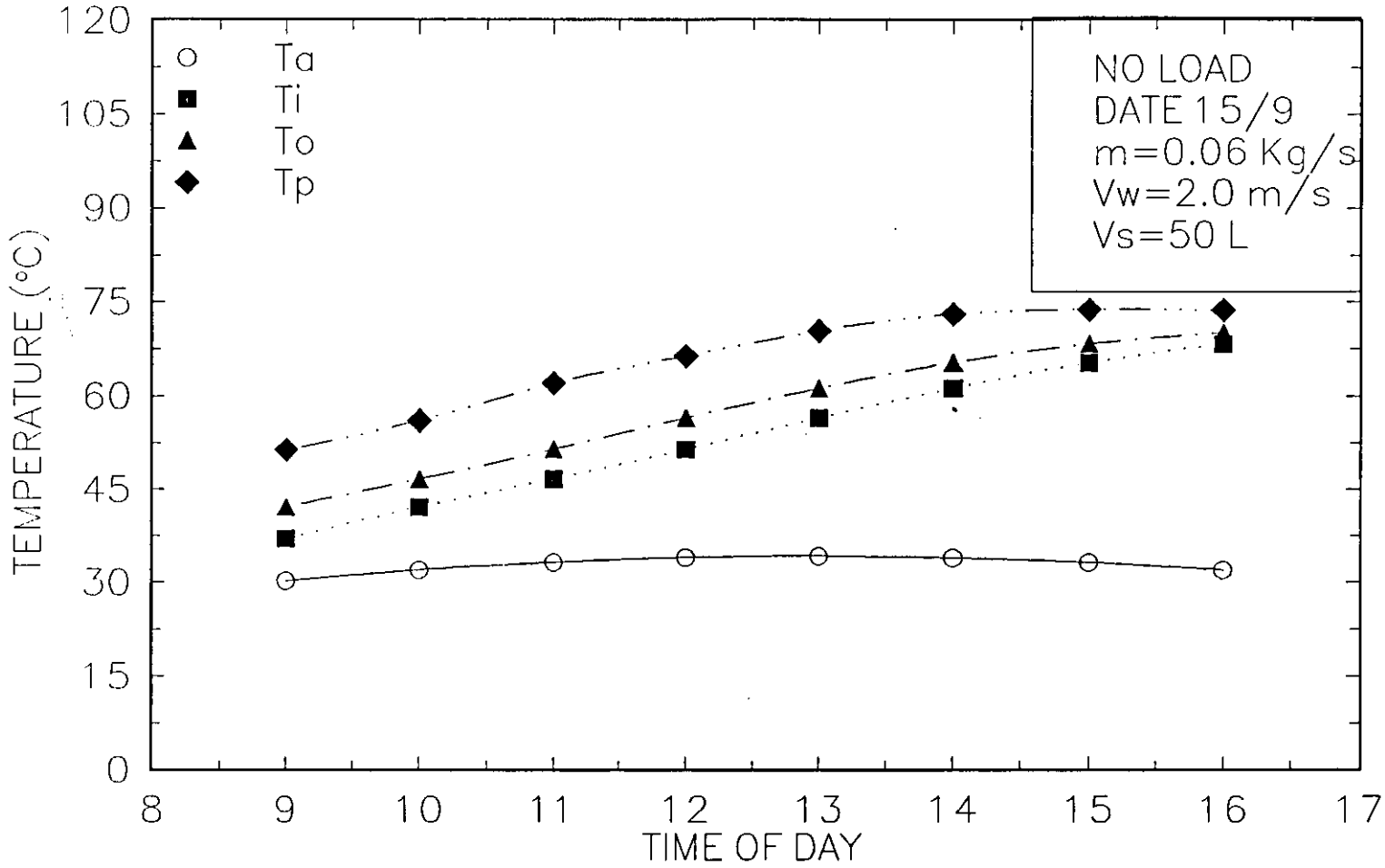

FIG (3.37). Variation of Inlet Temp., Outlet Temp., Amb. Temp. and the Plate Temp. with Time for the Serpentine Tube Flat (Non_Metallic) Plate Solar Collectors.

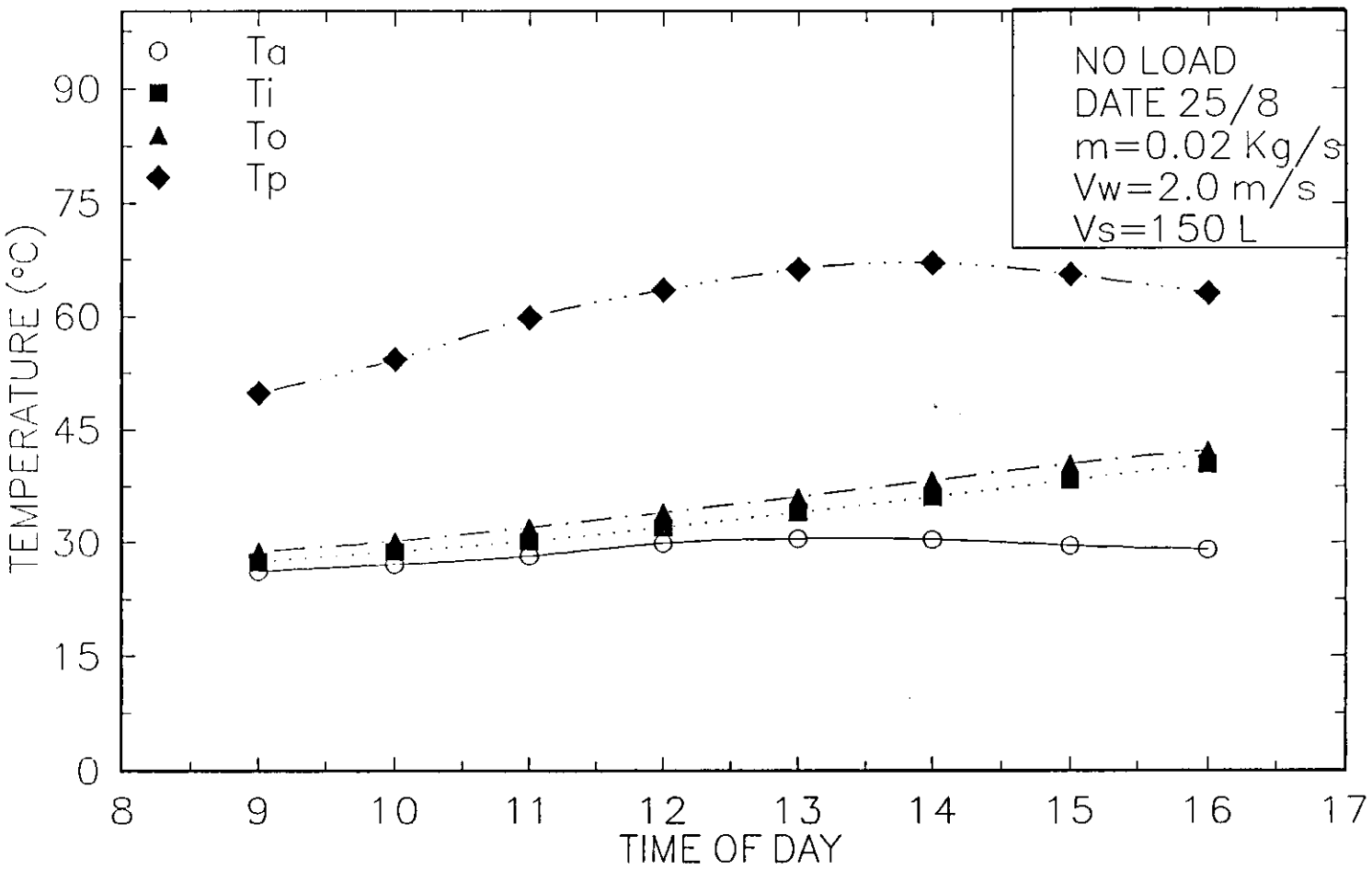

FIG (3.38). Variation of Inlet Temp., Outlet Temp., Amb. Temp. and the Plate Temp. with Time for the Serpentine Tube Flat (Non_Metallic) Plate Solar Collectors.

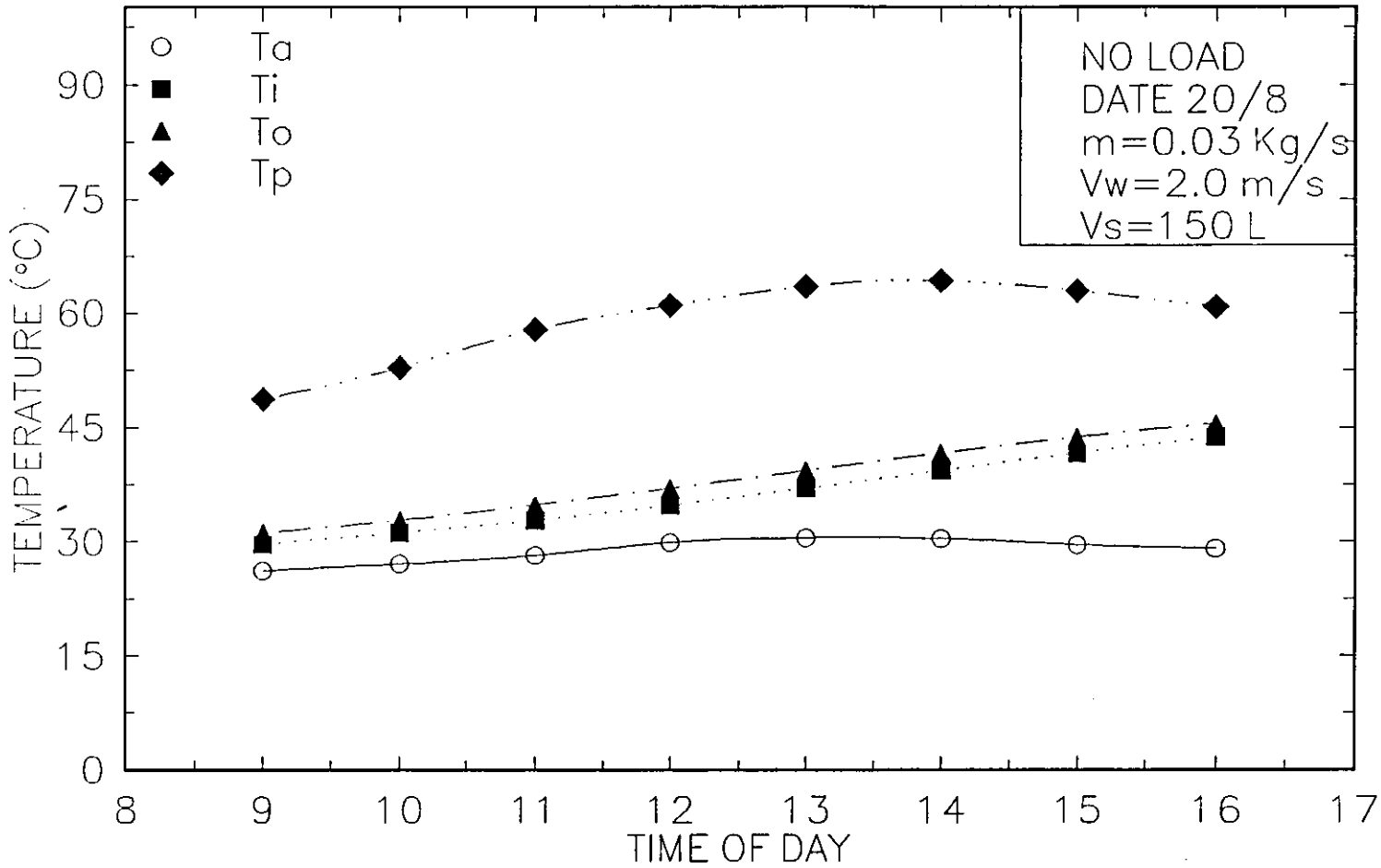

FIG (3.39). Variation of Inlet Temp., Outlet Temp., Amb. Temp. and the Plate Temp. with Time for the Serpentine Tube Flat (Non_Metallic) Plate Solar Collectors.

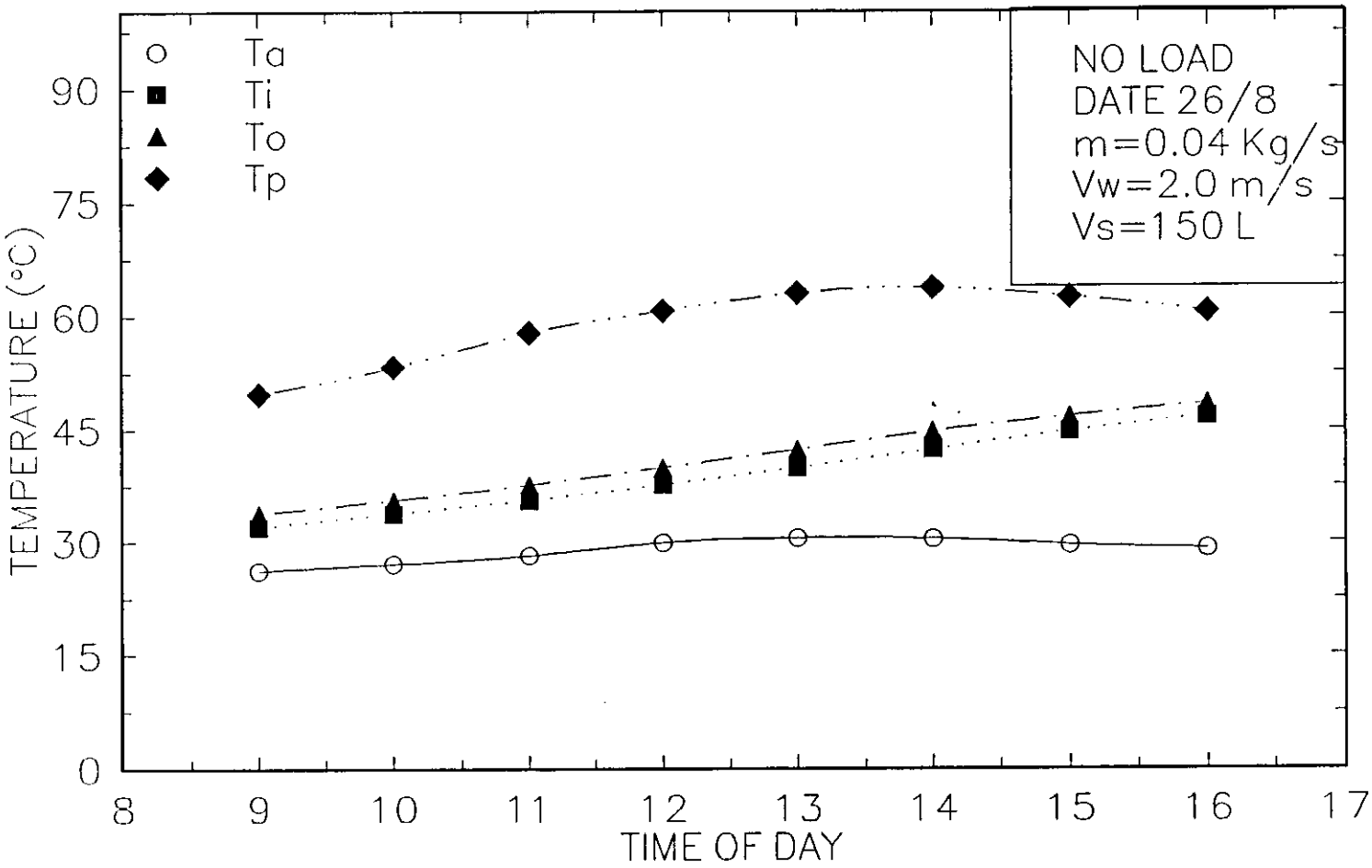

FIG (3.40). Variation of Inlet Temp., Outlet Temp., Amb. Temp. and the Plate Temp. with Time for the Serpentine Tube Flat (Non_Metallic) Plate Solar Collectors.

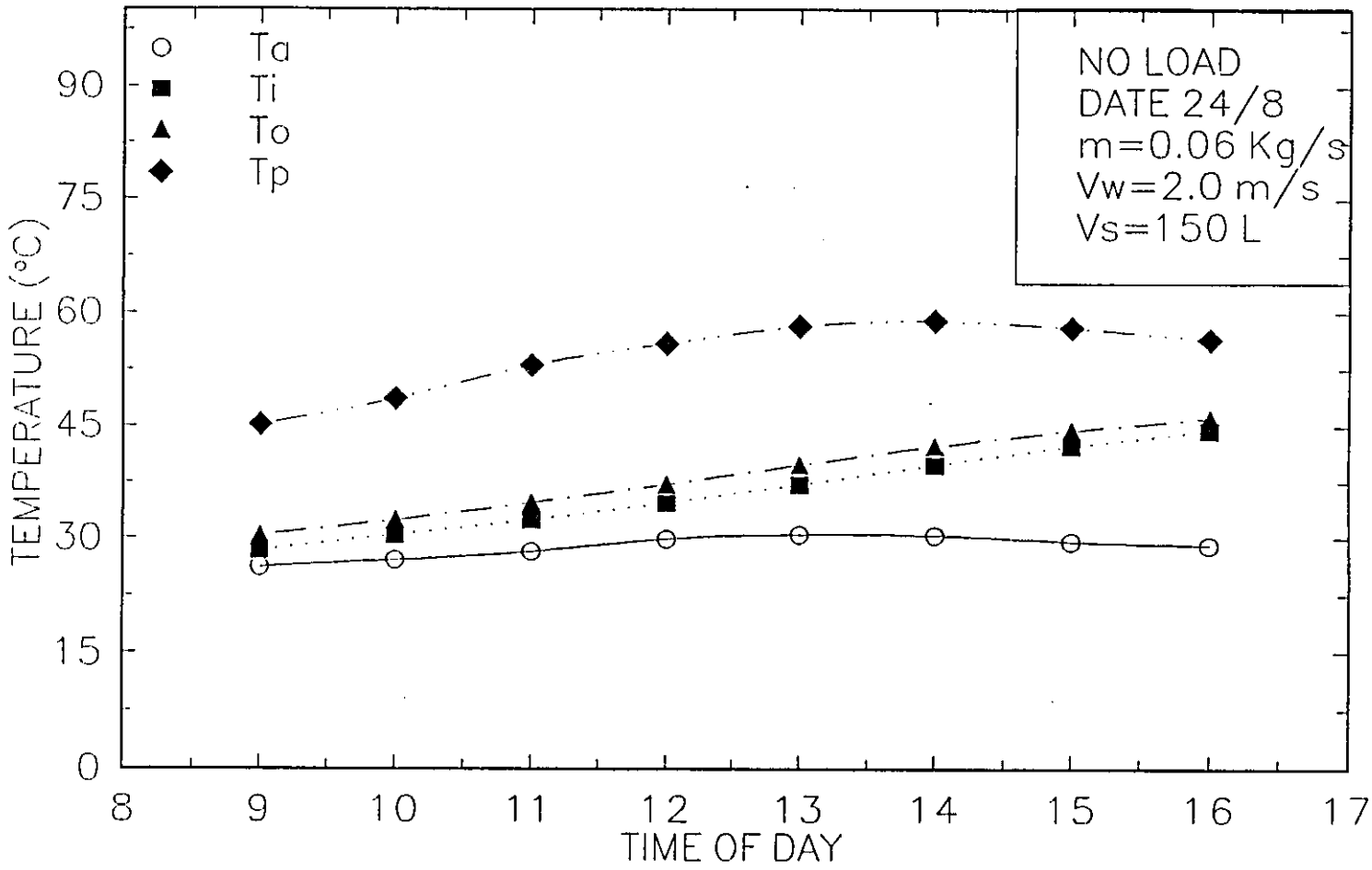

FIG (3.41). Variation of Inlet Temp., Outlet Temp., Amb. Temp. and the Plate Temp. with Time for the Serpentine Tube Flat (Non_Metallic) Plate Solar Collectors.

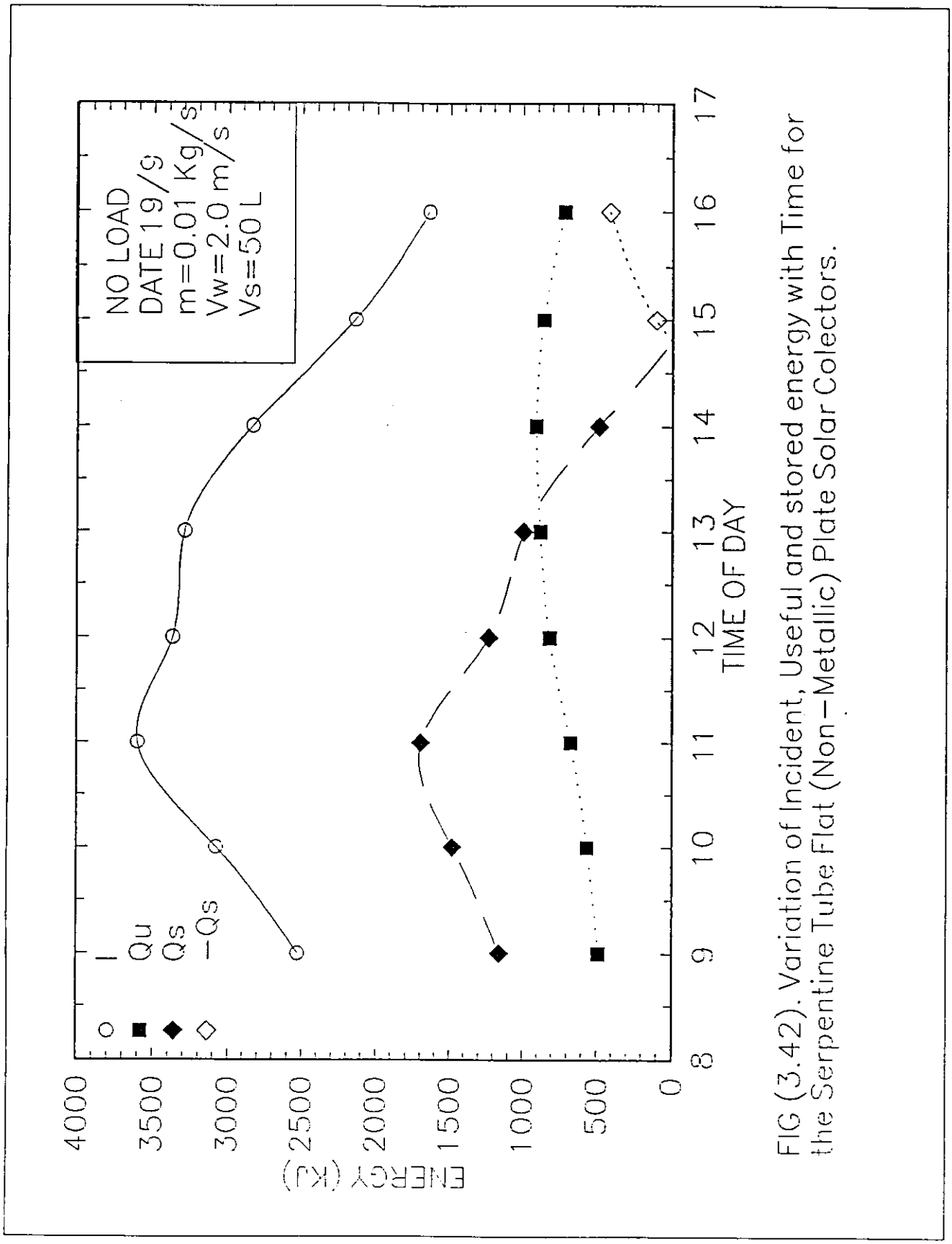

FIG (3.42). Variation of Incident, Useful and stored energy with Time for the Serpentine Tube Flat (Non-Metallic) Plate Solar Colectors.

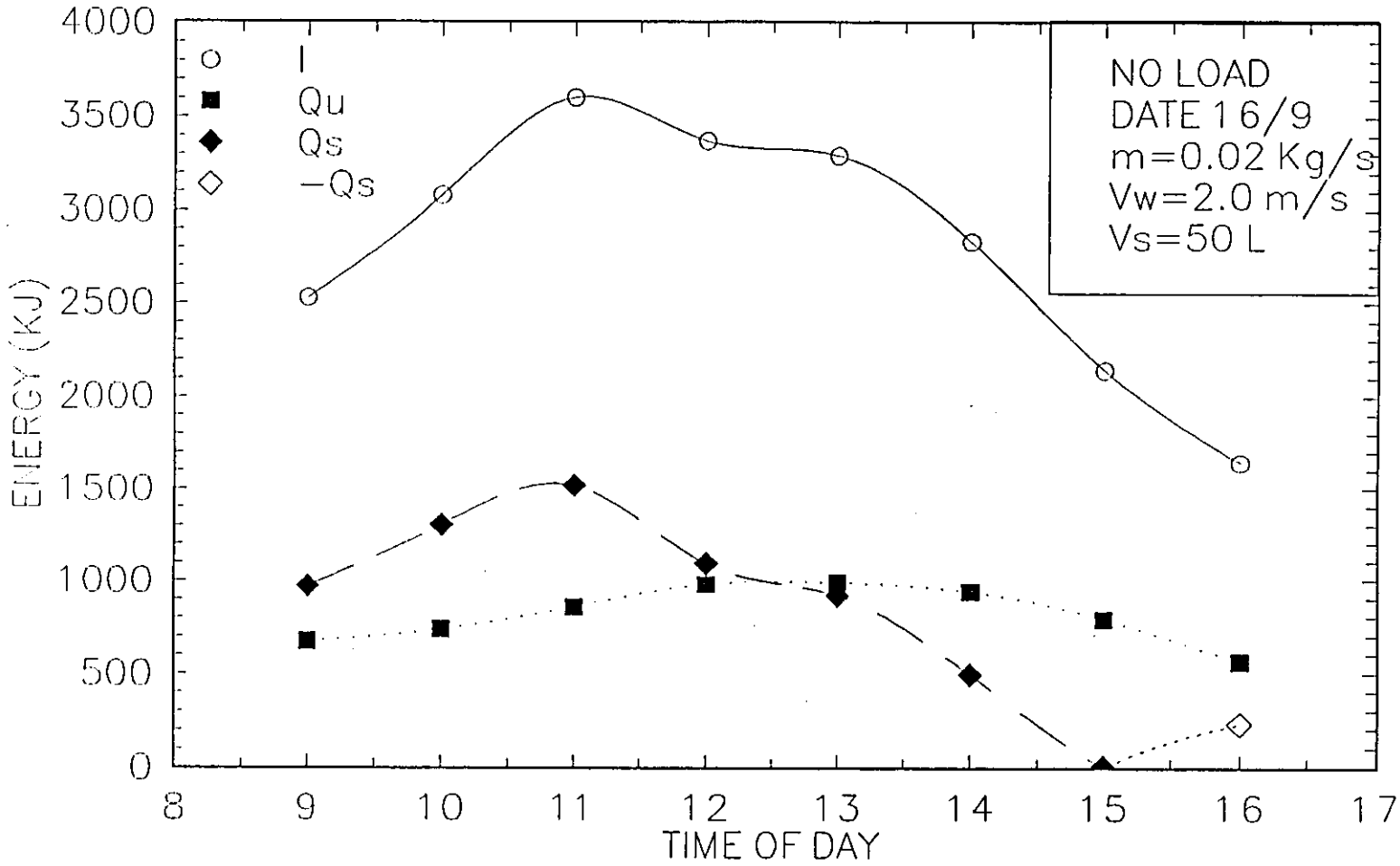

FIG (3.43). Variation of Incident, Useful and stored energy with Time for the Serpentine Tube Flat (Non-Metallic) Plate Solar Colectors.

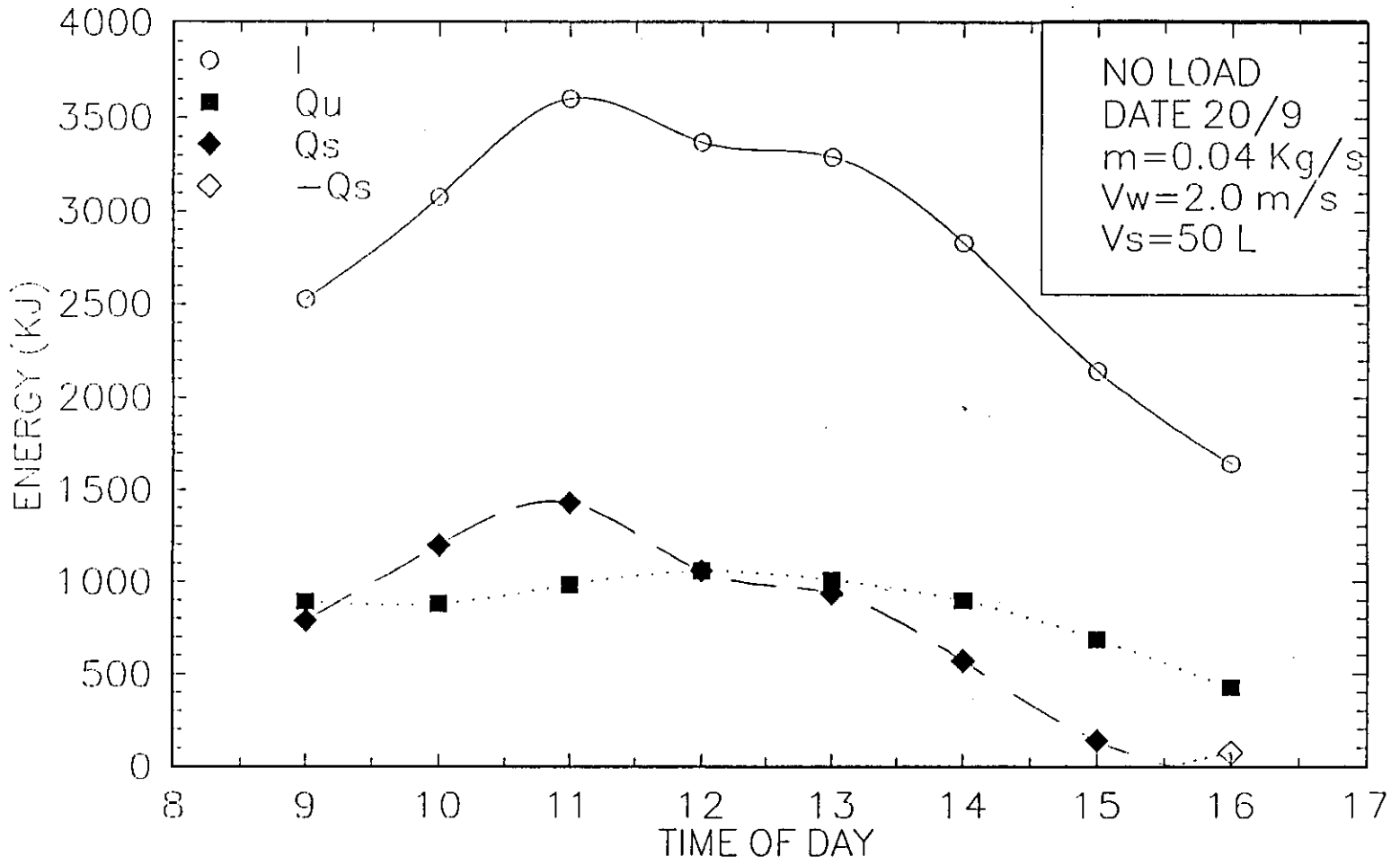

FIG (3.44). Variation of Incident, Useful and stored energy with Time for the Serpentine Tube Flat (Non−Metallic) Plate Solar Colectors.

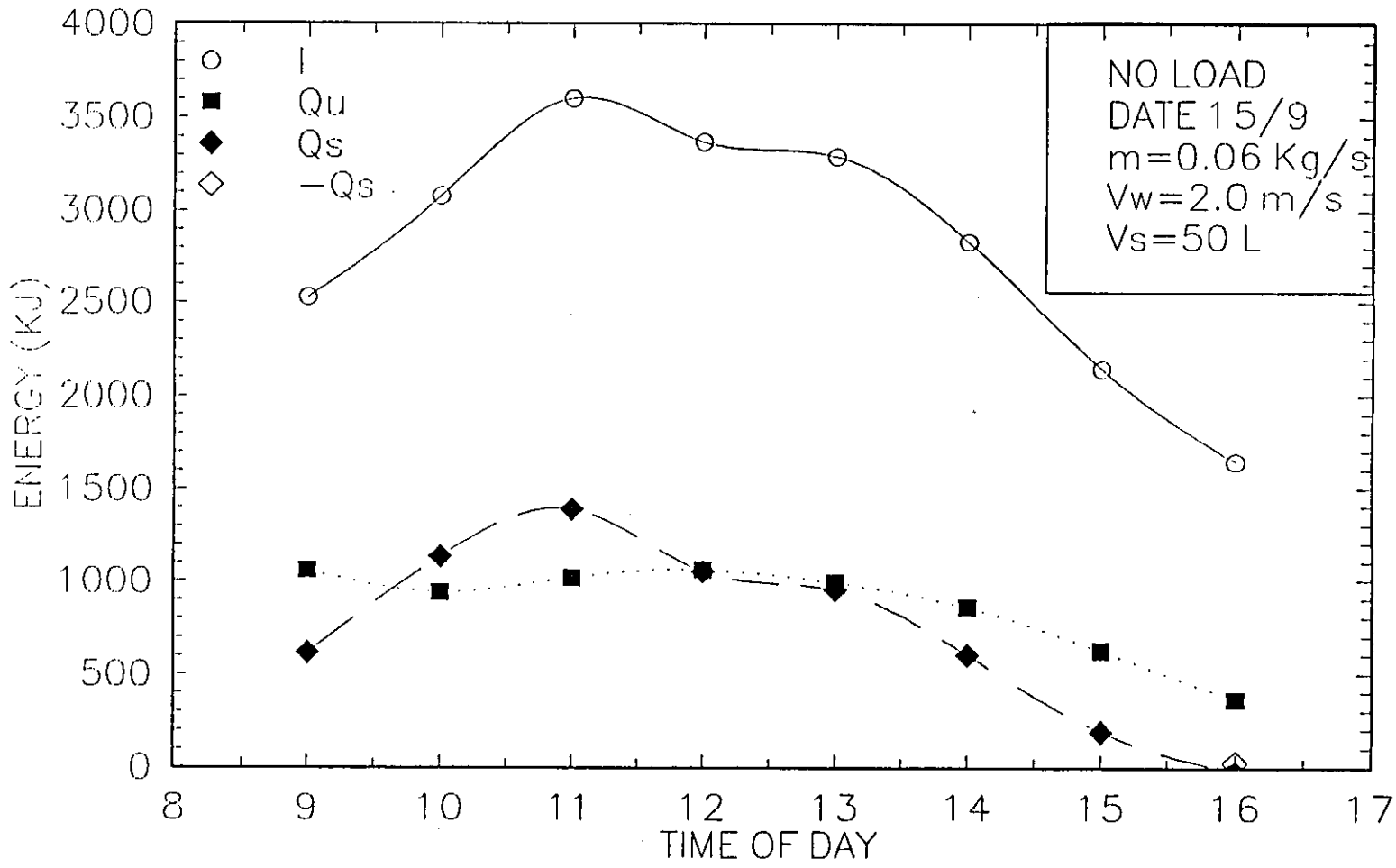

FIG (3.45). Variation of Incident, Useful and stored energy with Time for the Serpentine Tube Flat (Non−Metallic) Plate Solar Colectors.

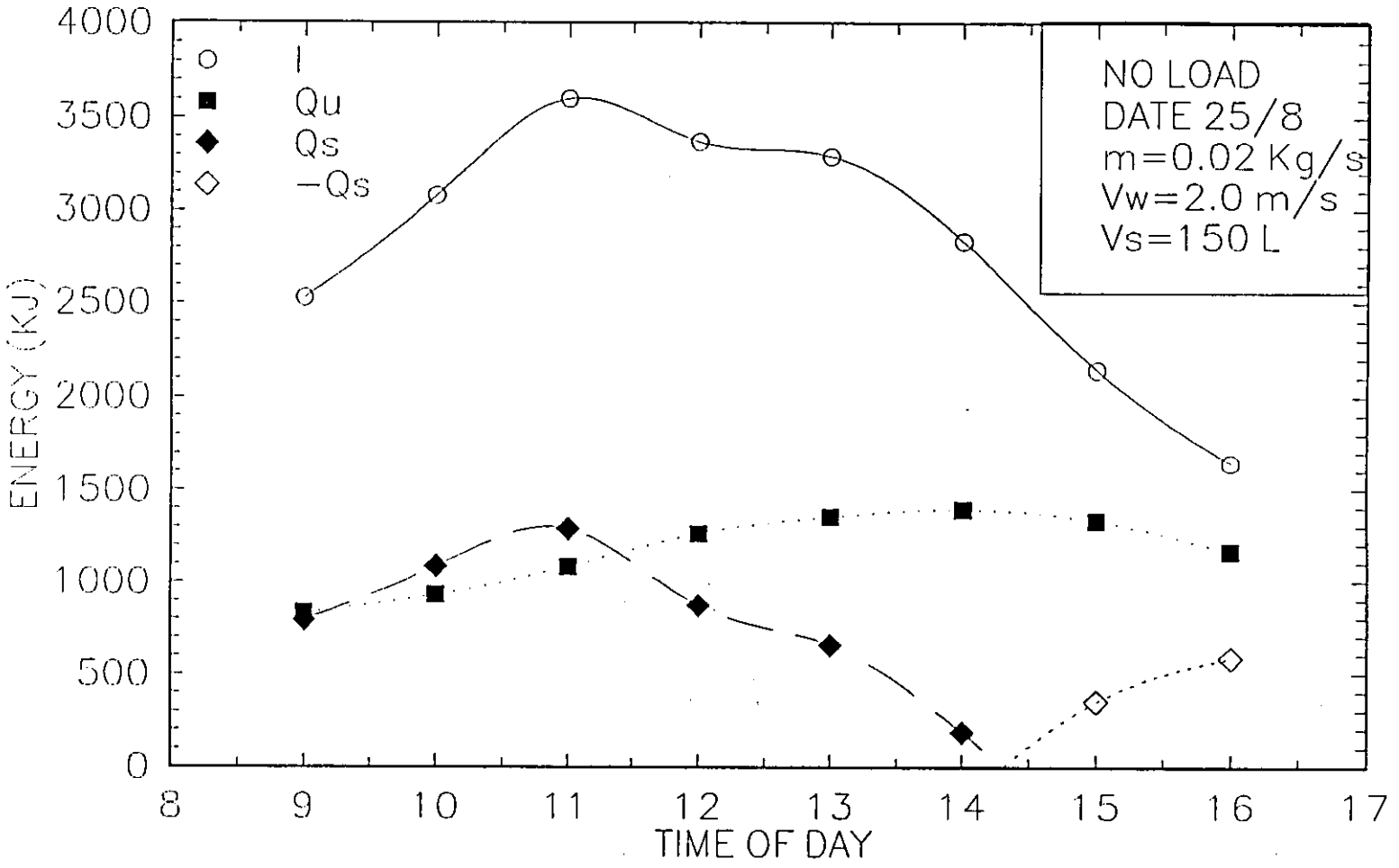

FIG (3.46). Variation of Incident, Useful and stored energy with Time for the Serpentine Tube Flat (Non−Metallic) Plate Solar Colectors.

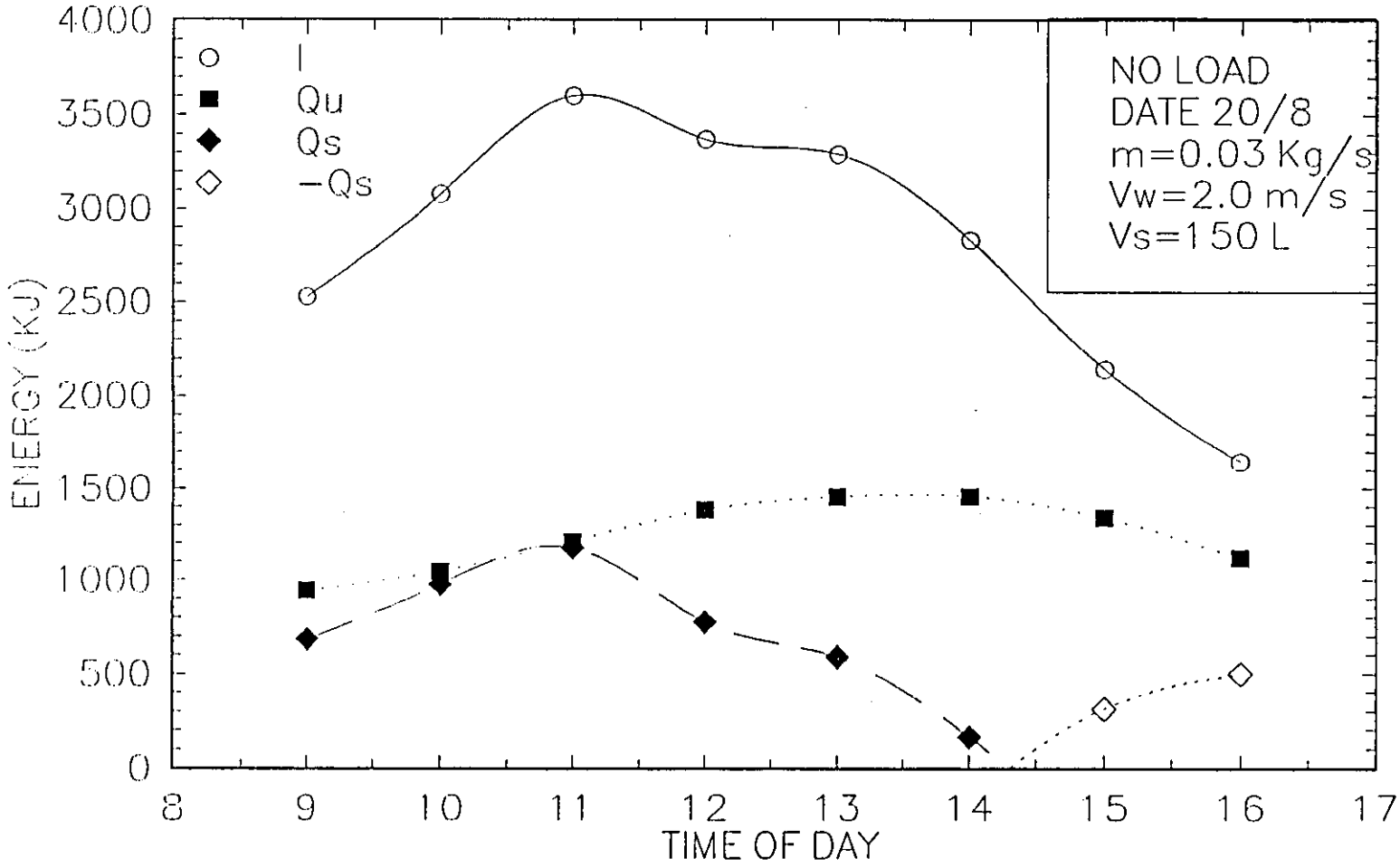

FIG (3.47). Variation of Incident, Useful and stored energy with Time for the Serpentine Tube Flat (Non−Metallic) Plate Solar Colectors.

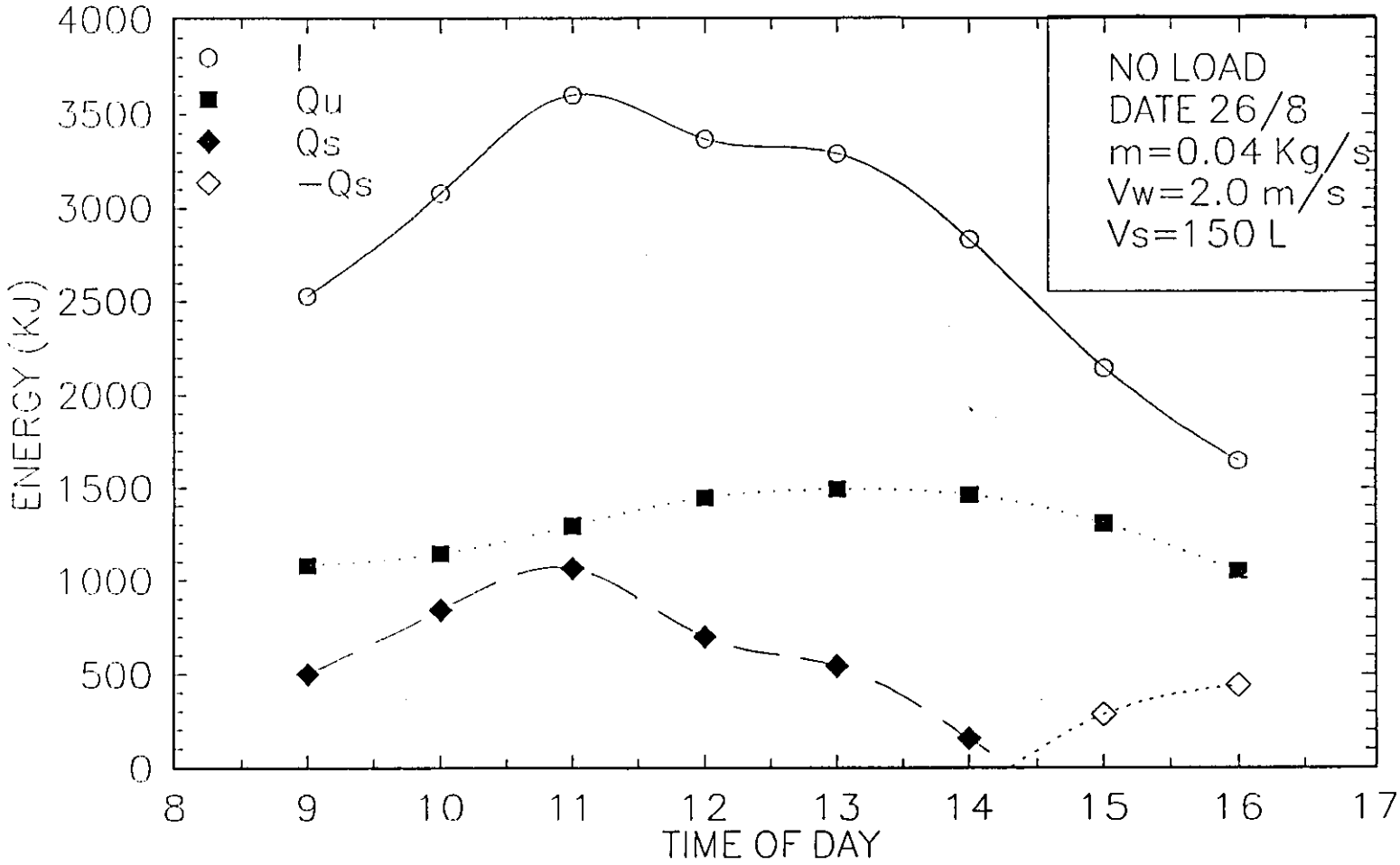

FIG (3.48). Variation of Incident, Useful and stored energy with Time for the Serpentine Tube Flat (Non−Metallic) Plate Solar Colectors.

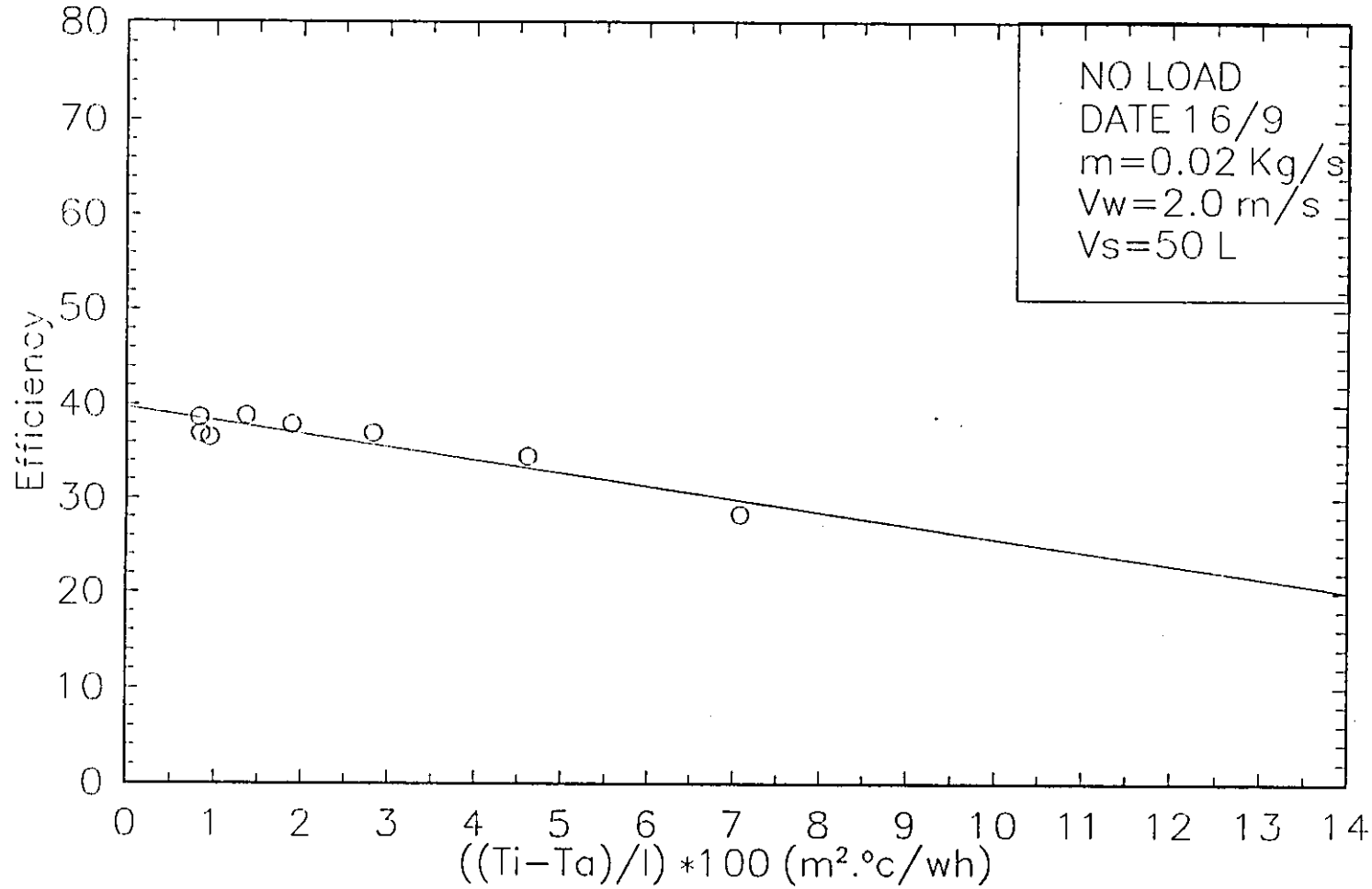

FIG (3.50). Variation of Instantaneous Efficiency against ((Ti−Ta)/I) for the Serpentine Tube Flat (Non−Metallic) Plate Solar Colectors.

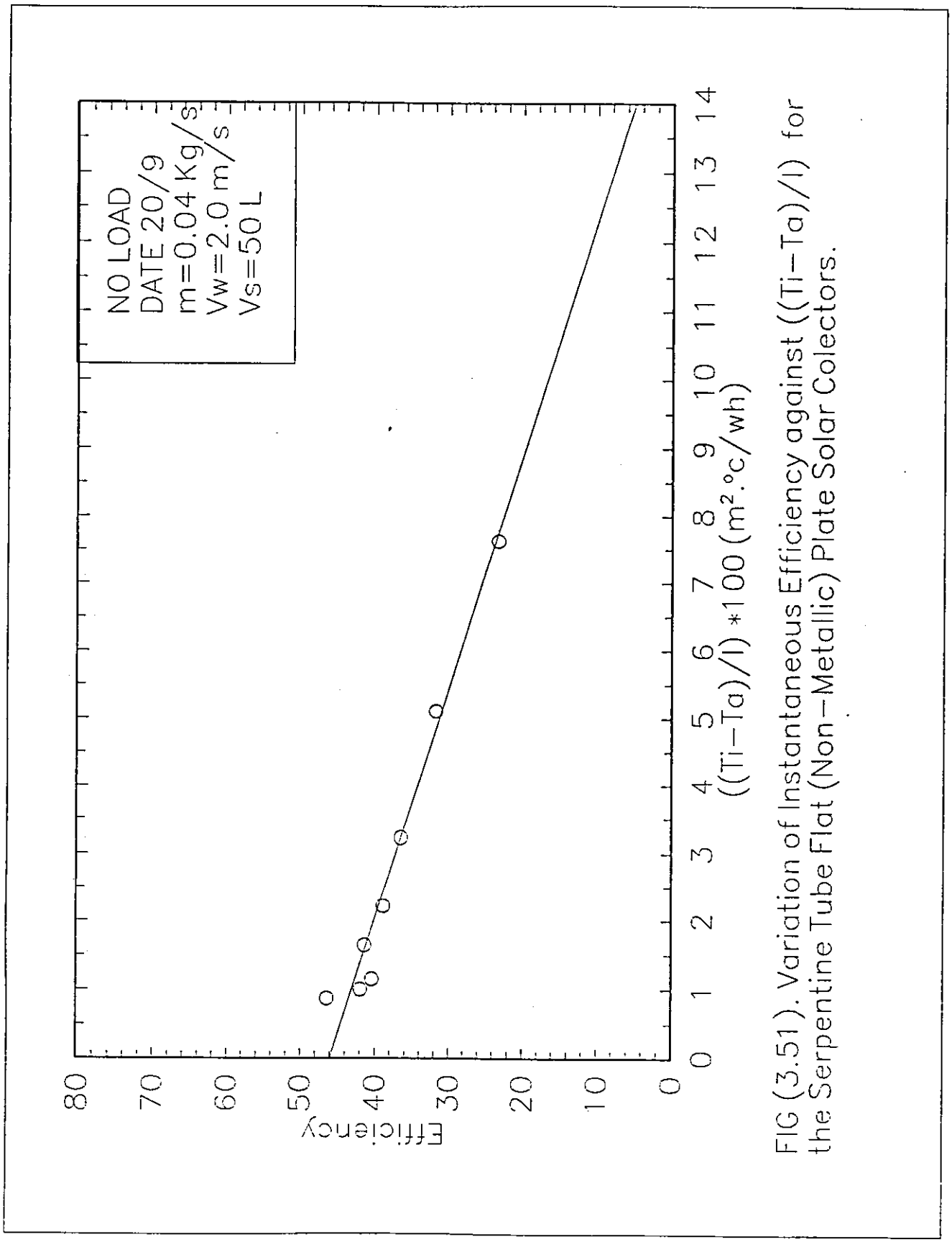

FIG (3.51). Variation of Instantaneous Efficiency against ((Ti−Ta)/I) for the Serpentine Tube Flat (Non−Metallic) Plate Solar Colectors.

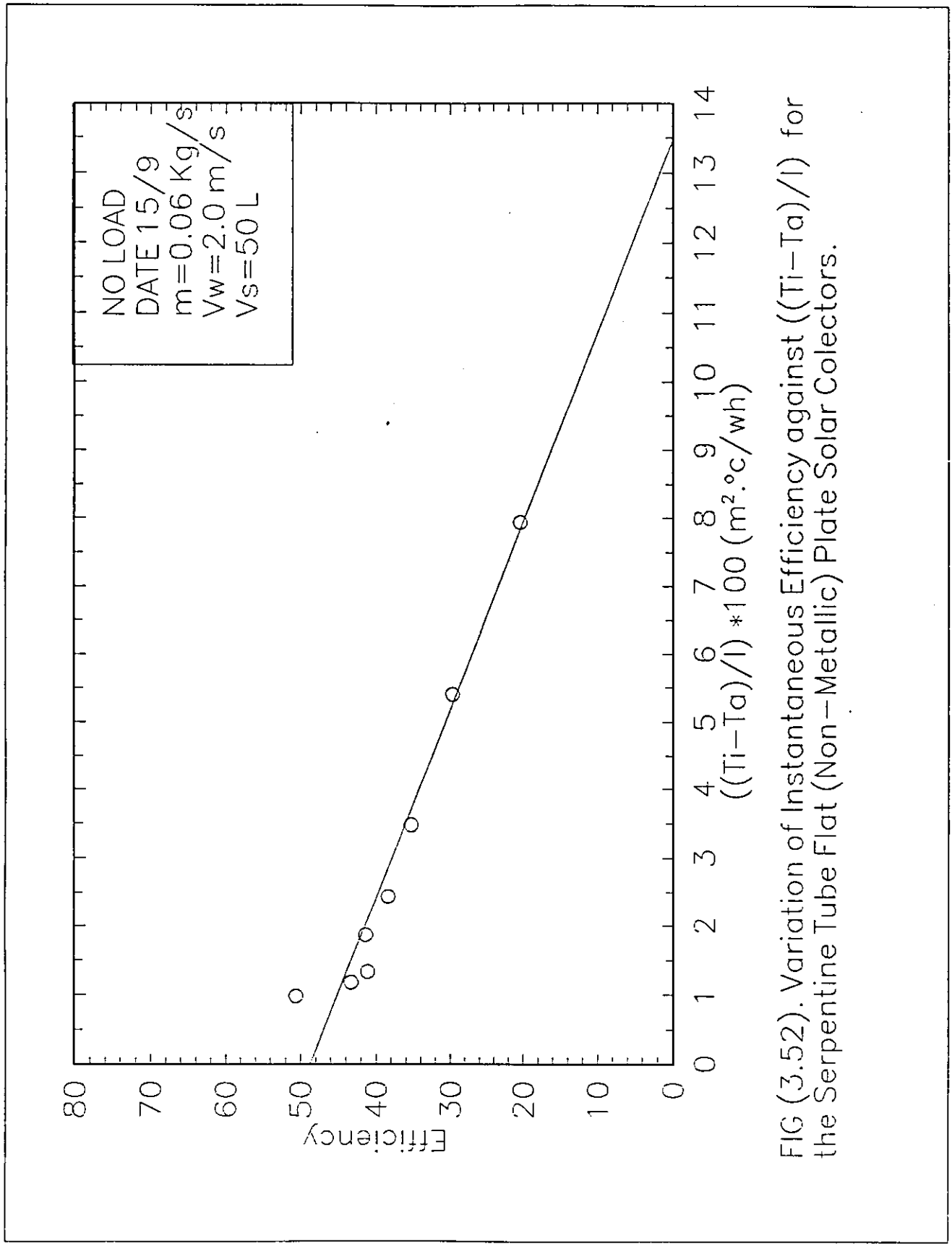

FIG (3.52). Variation of Instantaneous Efficiency against ((Ti−Ta)/I) for the Serpentine Tube Flat (Non−Metallic) Plate Solar Colectors.

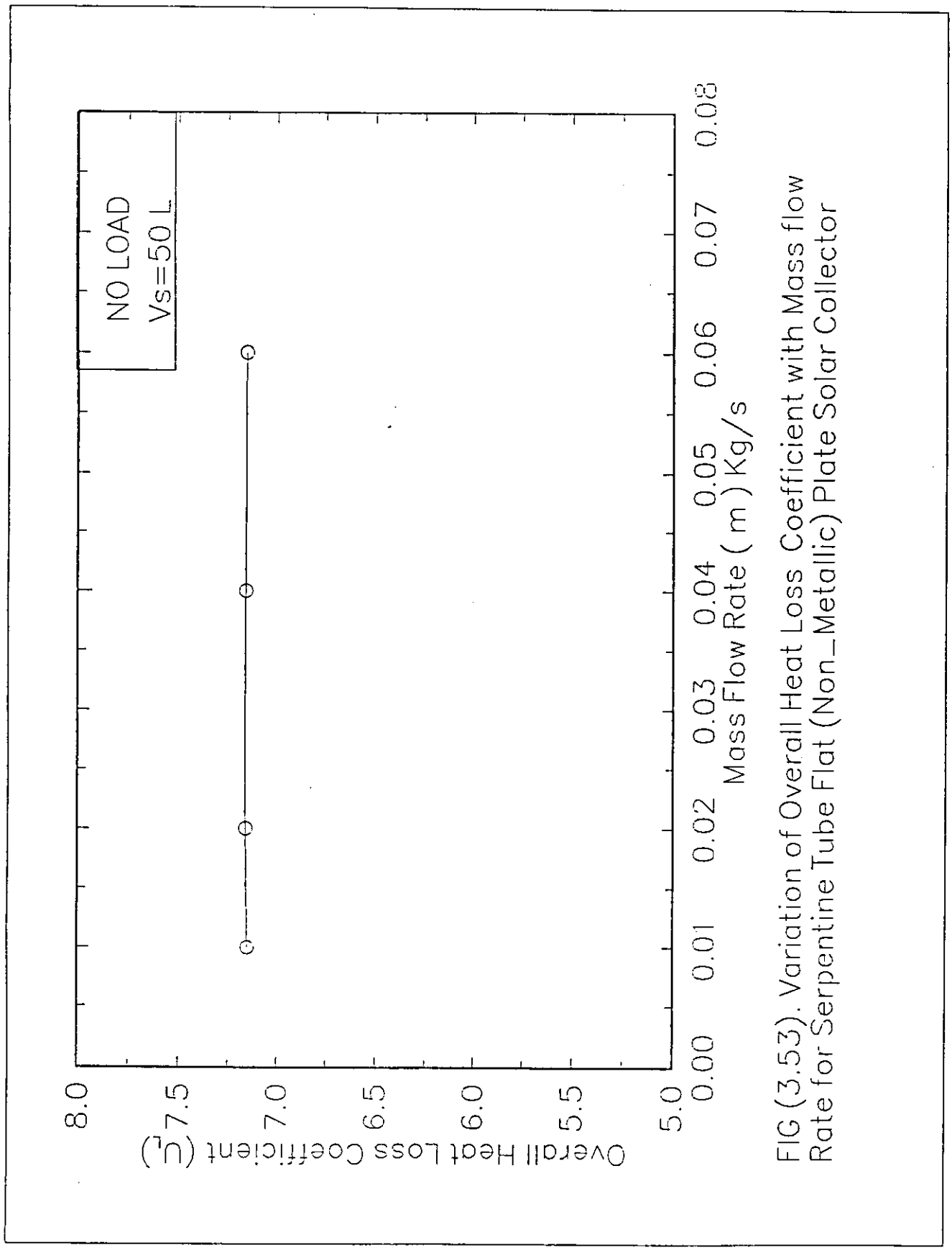

FIG (3.53). Variation of Overall Heat Loss Coefficient with Mass flow Rate for Serpentine Tube Flat (Non_Metallic) Plate Solar Collector

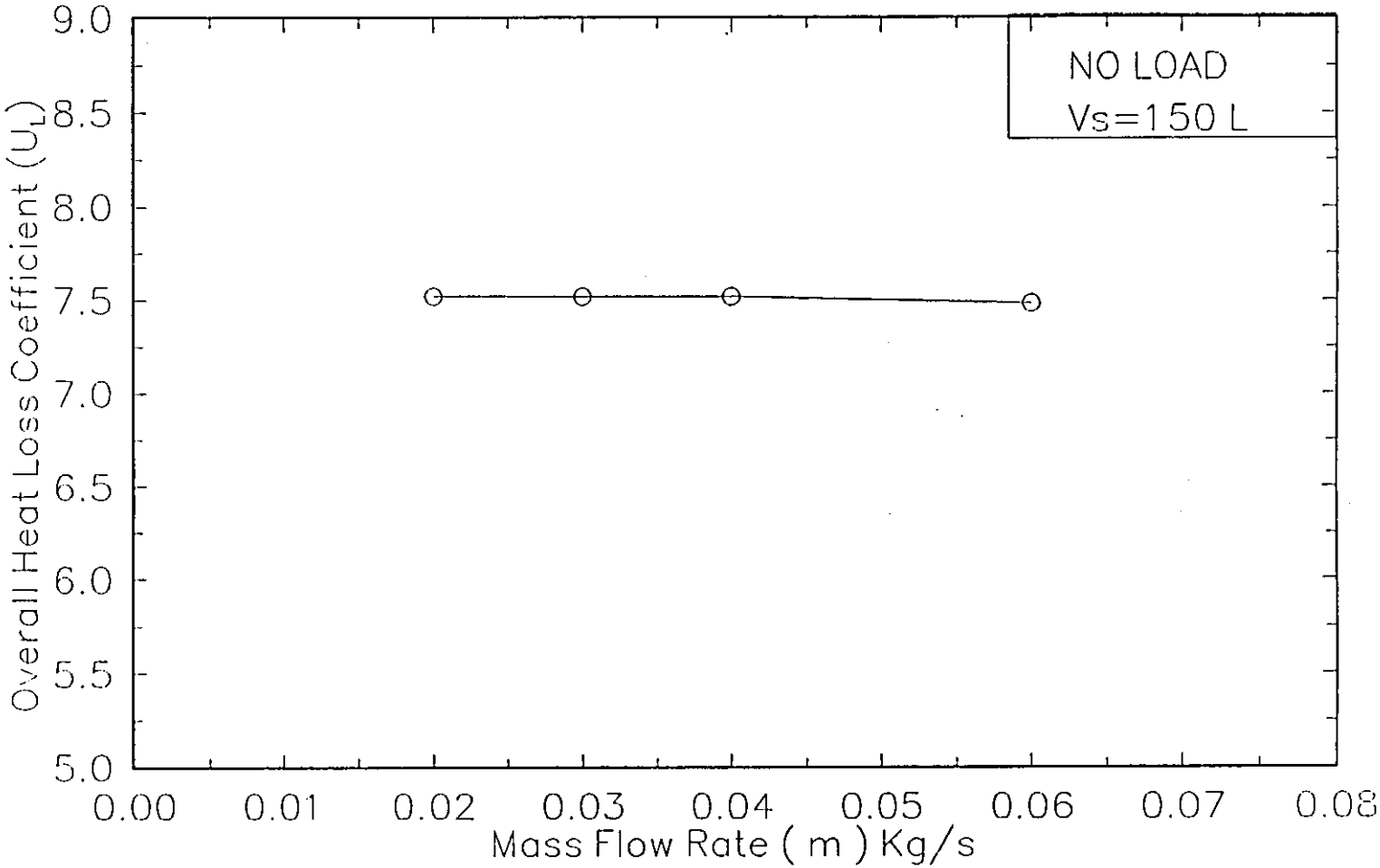

FIG (3.54). Variation of Overall Heat Loss Coefficient with Mass flow Rate for Serpentine Tube Flat (Non_Metallic) Plate Solar Collector

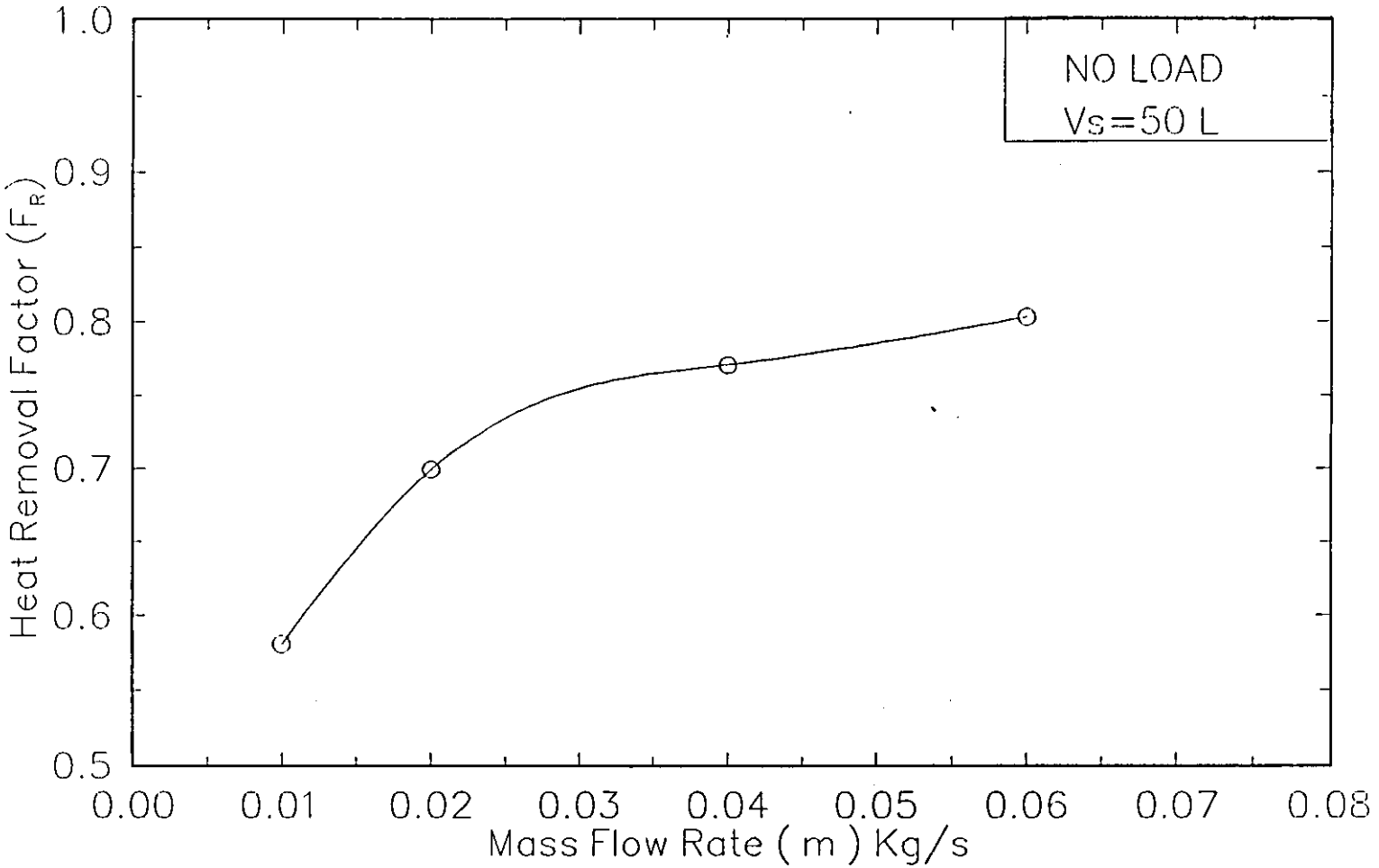

FIG (3.55). Variation of Heat Removal Factor with Mass Flow rate for the Serpentine Tube Flat (Non_Metallic) Plate Solar Collector

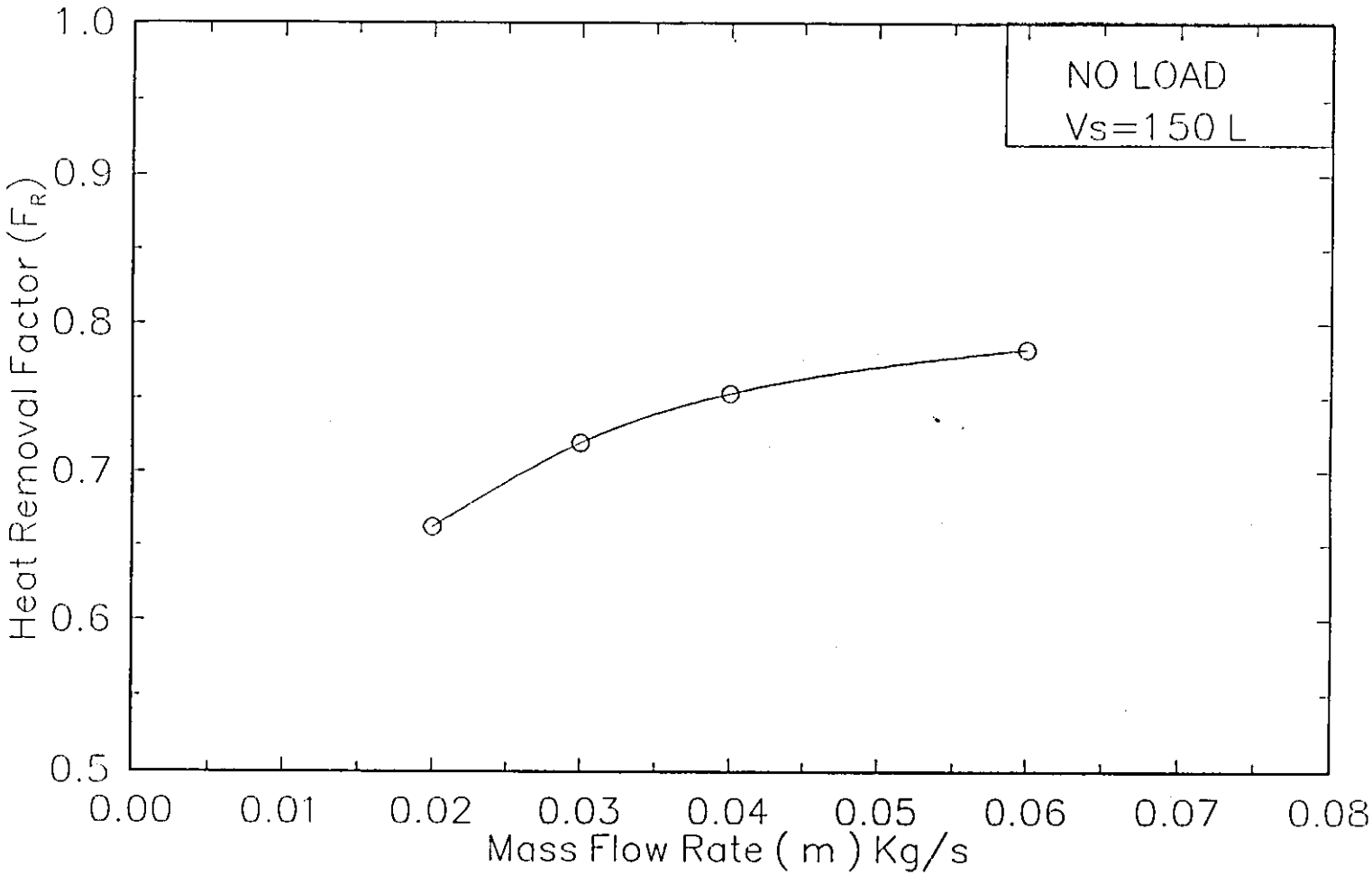

FIG (3.56). Variation of Heat Removal Factor with Mass Flow rate for the Serpentine Tube Flat (Non_Metallic) Plate Solar Collector

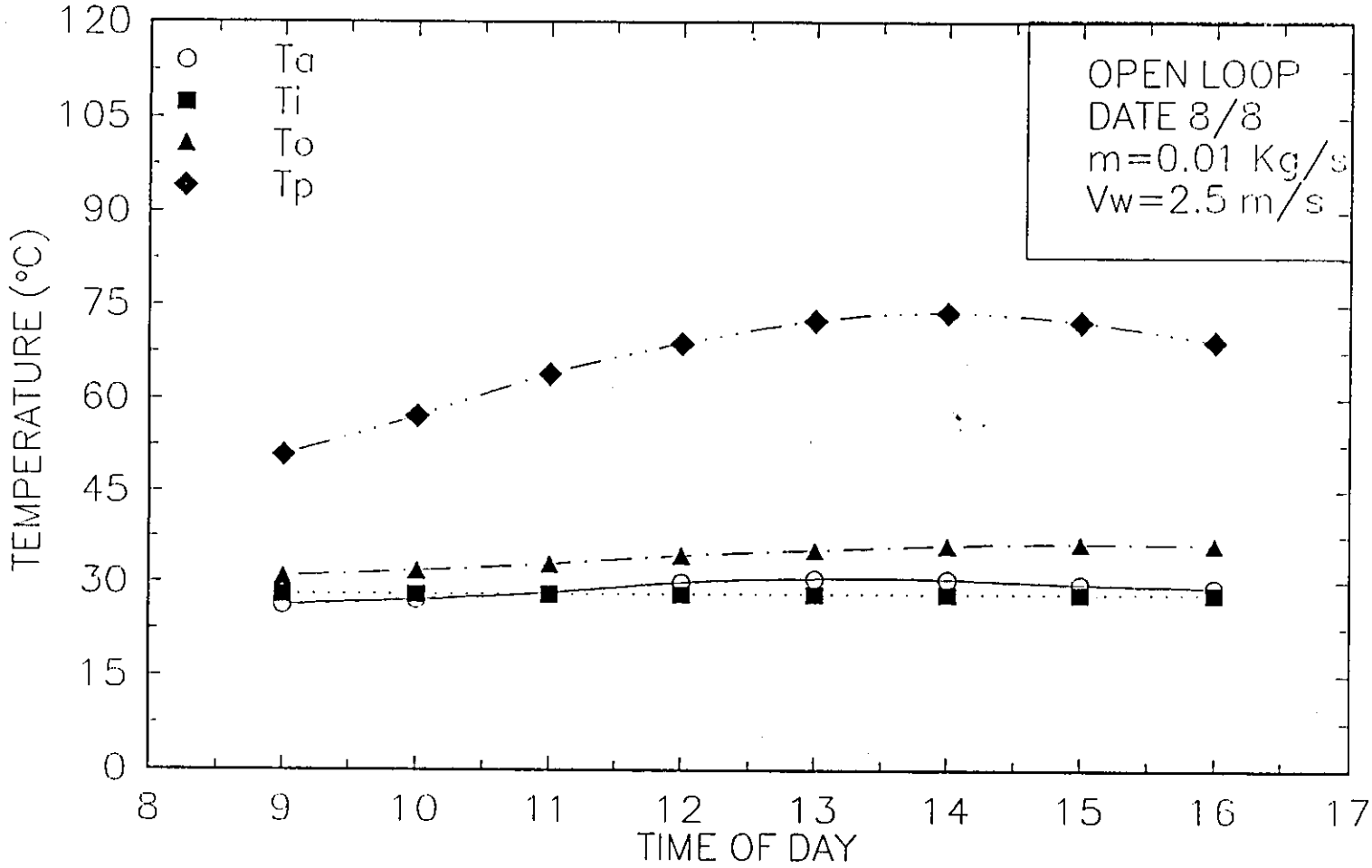

FIG (3.57). Variation of Inlet Temp., Outlet Temp., Amb. Temp. and the Plate Temp. with Time for the Serpentine Tube Flat (Non_Metallic) Plate Solar Collectors.

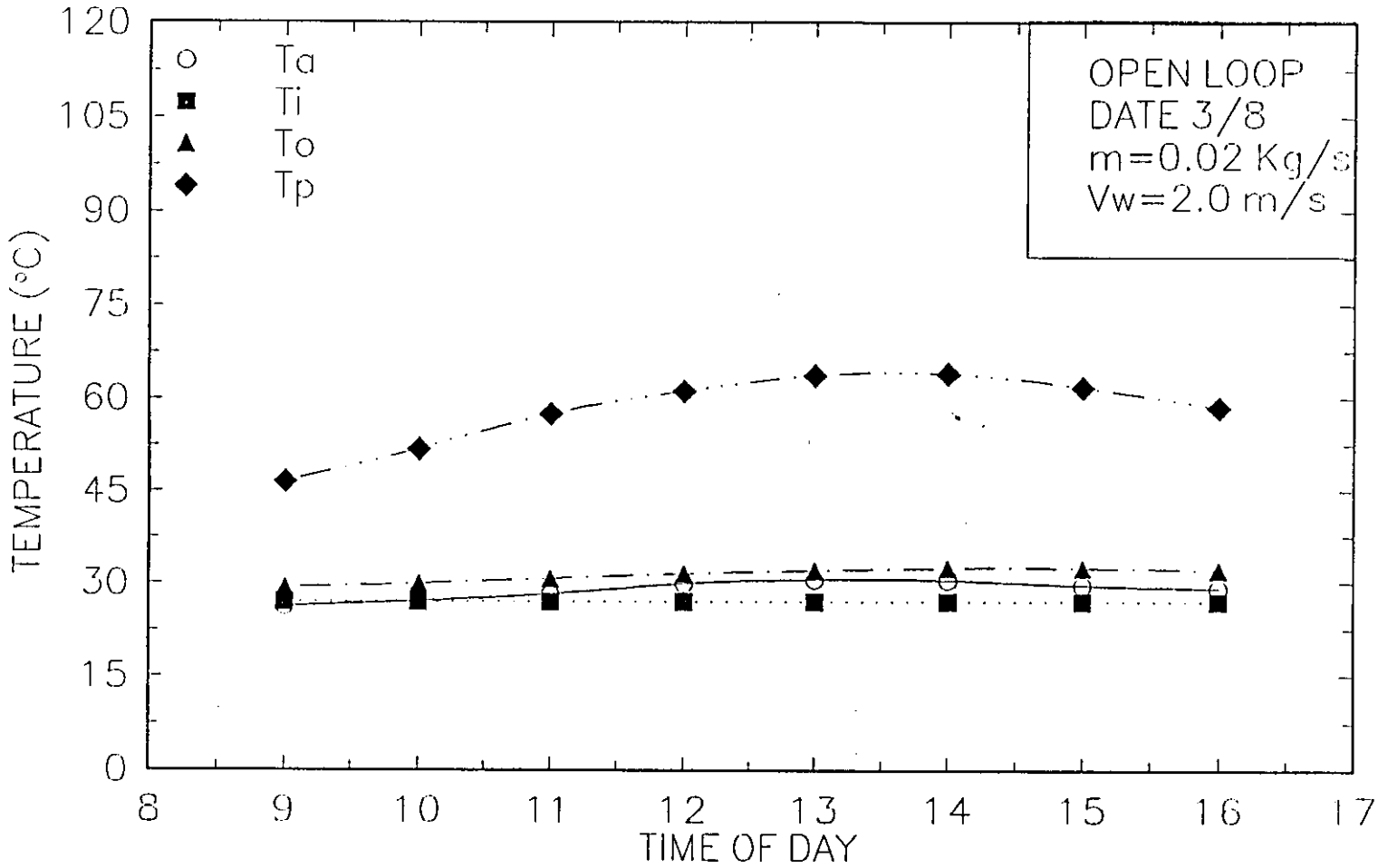

FIG (3.58). Variation of Inlet Temp., Outlet Temp., Amb. Temp. and the Plate Temp. with Time for the Serpentine Tube Flat (Non_Metallic) Plate Solar Collectors.

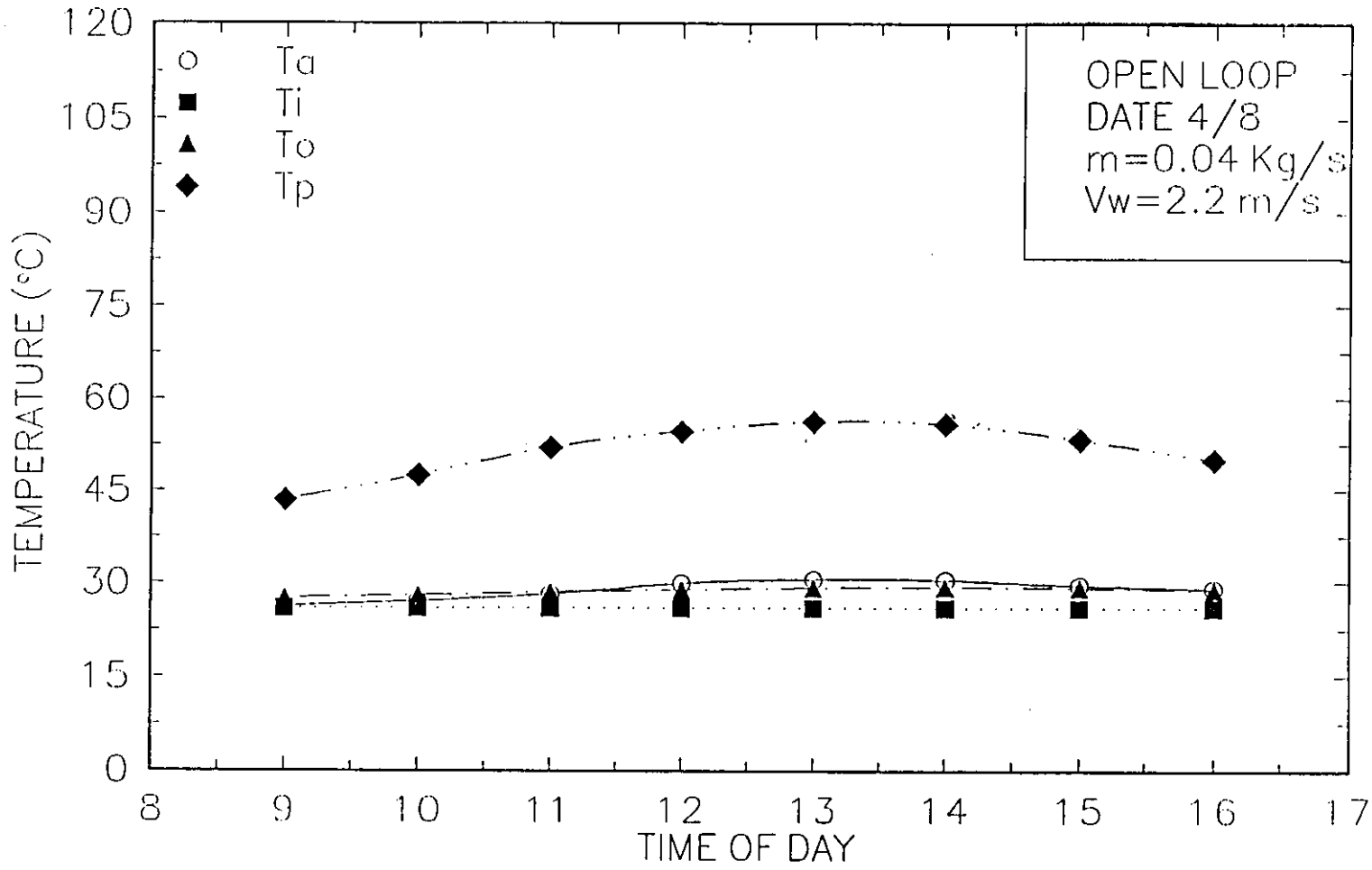

FIG (3.59). Variation of Inlet Temp., Outlet Temp., Amb. Temp. and the Plate Temp. with Time for the Serpentine Tube Flat (Non_Metallic) Plate Solar Collectors.

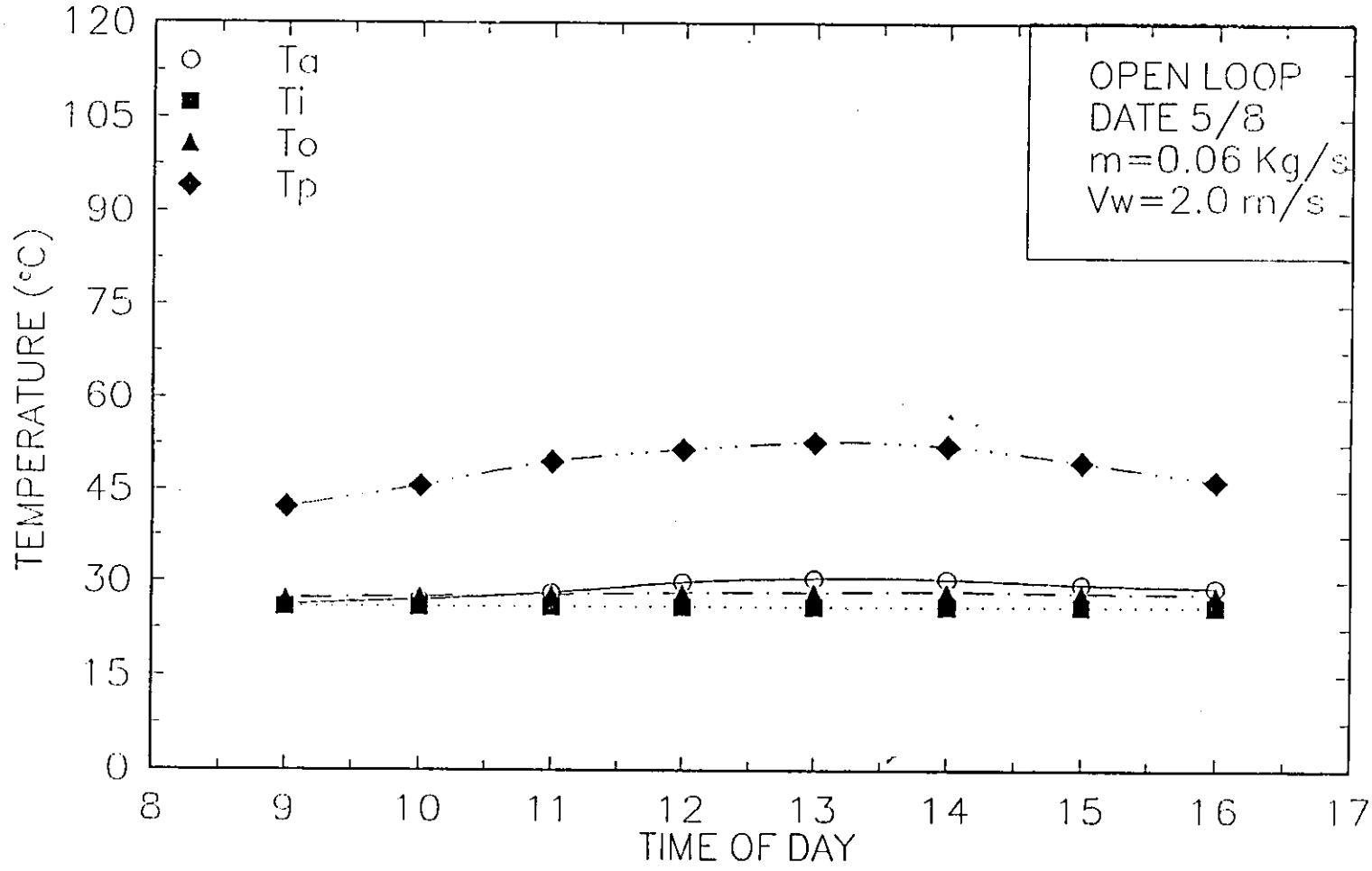

FIG (3.60). Variation of Inlet Temp., Outlet Temp., Amb. Temp. and the Plate Temp. with Time for the Serpentine Tube Flat (Non_Metallic) Plate Solar Collectors.

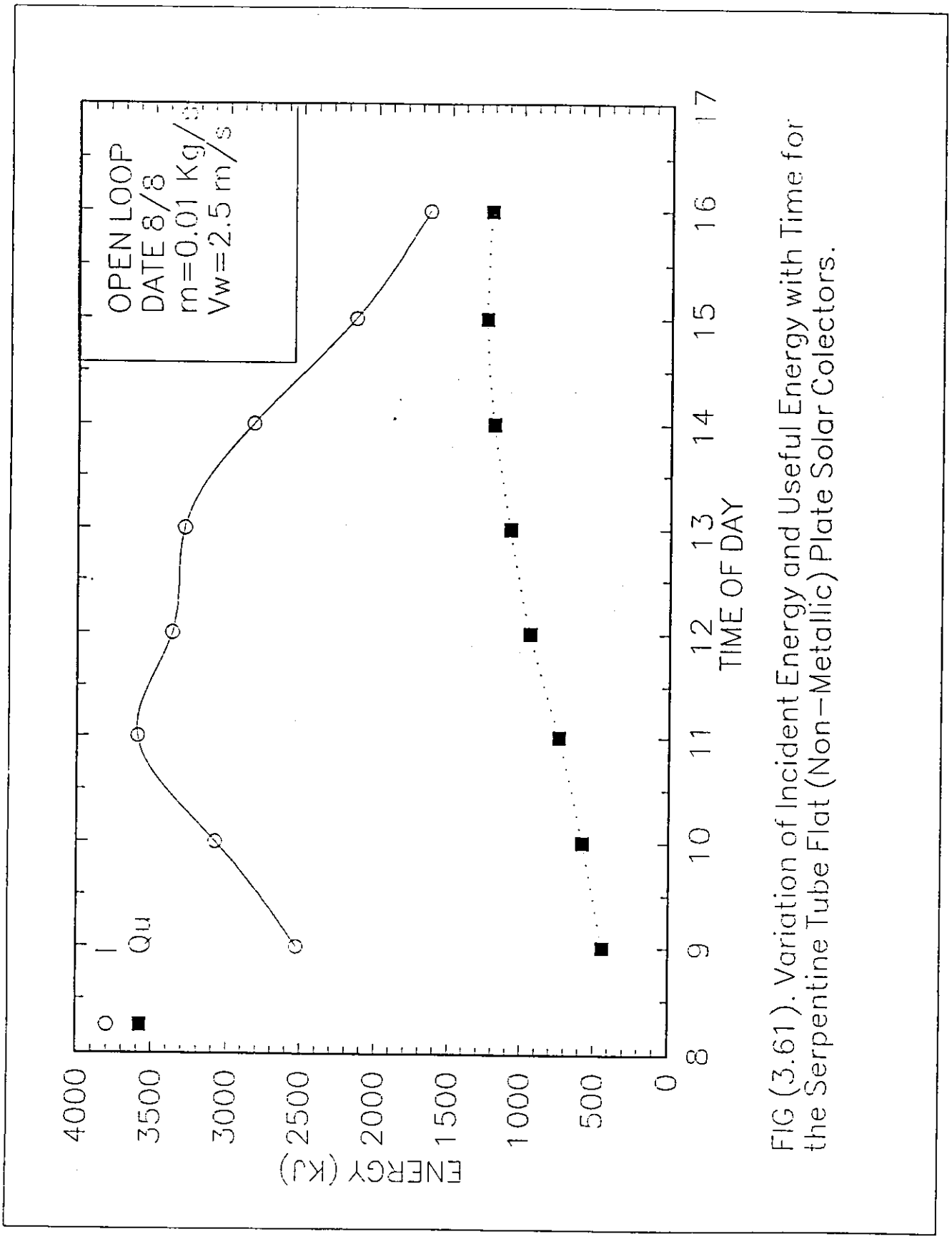

FIG (3.61). Variation of Incident Energy and Useful Energy with Time for the Serpentine Tube Flat (Non-Metallic) Plate Solar Colectors.

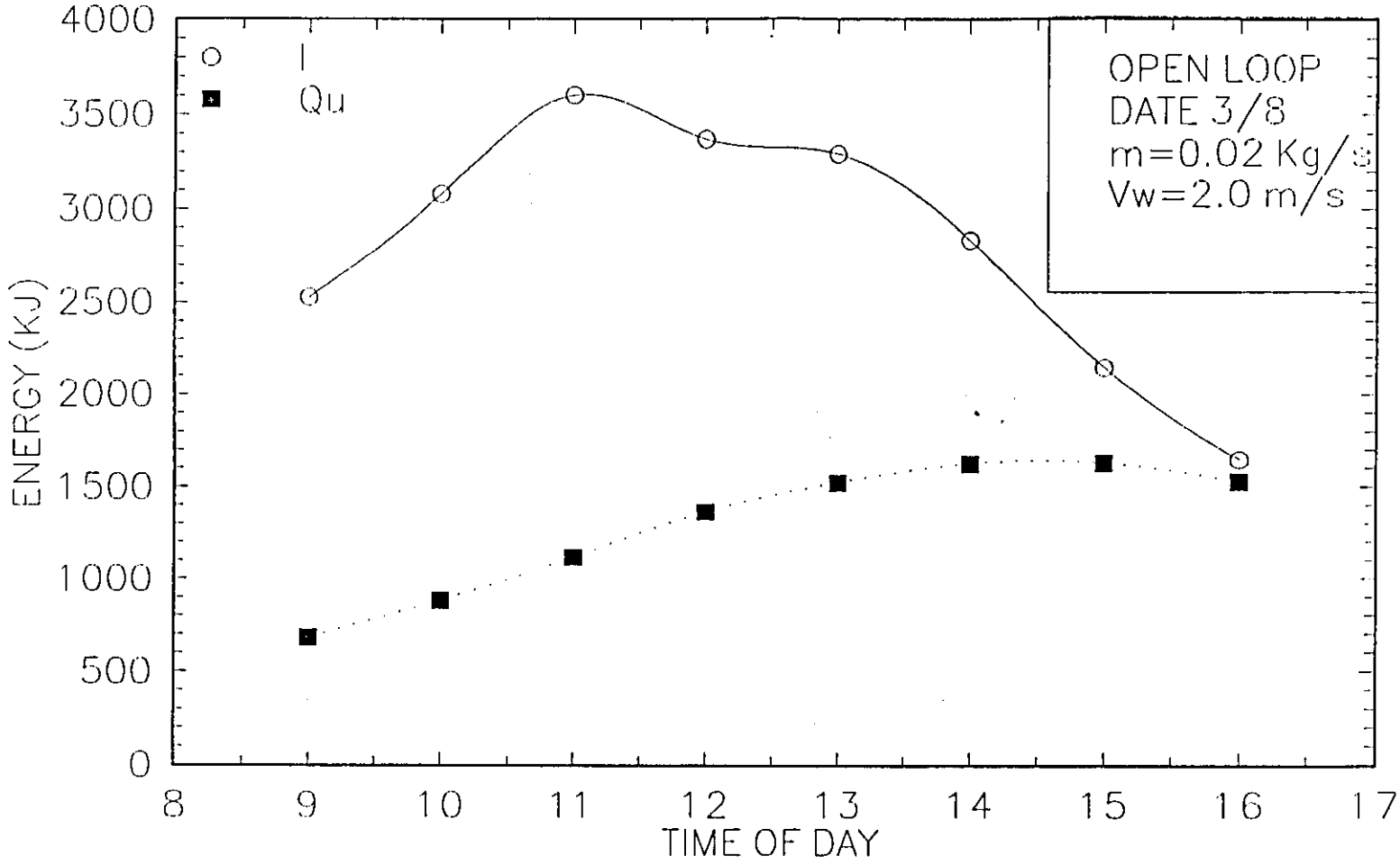

FIG (3.62). Variation of Incident Energy and Useful Energy with Time for the Serpentine Tube Flat (Non–Metallic) Plate Solar Colectors.

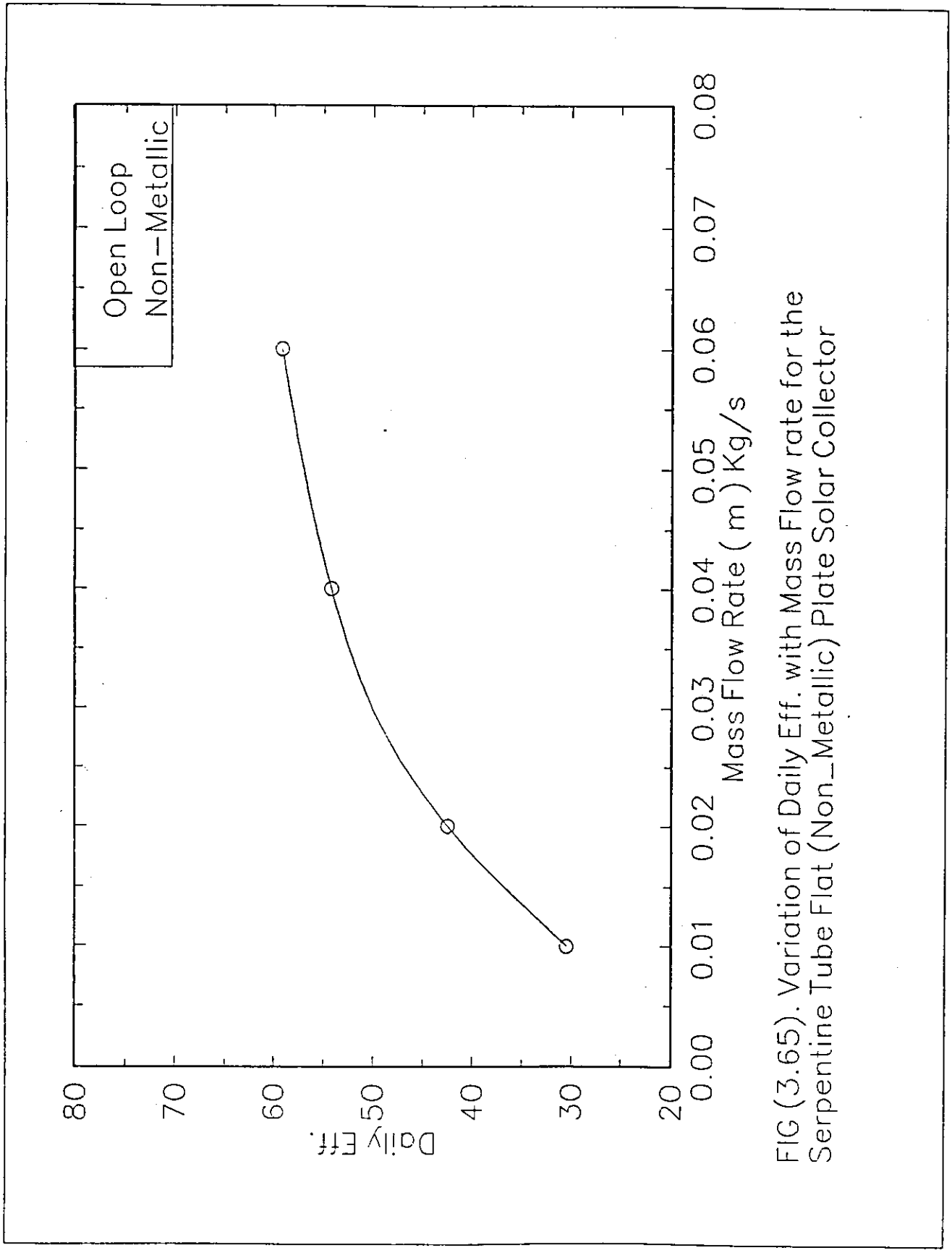

FIG (3.65). Variation of Daily Eff. with Mass Flow rate for the Serpentine Tube Flat (Non_Metallic) Plate Solar Collector

Chapter Four

COMPARISON BETWEEN THEORETICAL AND EXPERIMENTAL WORK.

The purpose of this chapter is to compare the theoretical performance of the present work for metallic and non-metallic serpentine collectors, with that of experimental work. The experimental parameters considered for comparison are obtained from [21], for metallic serpentine collector, [23] for non-metallic serpentine collector for the following test conditions.

4.1 Forced circulation test with no load conditions:

This test was performed by Abu- Yaha [21] and Adas [23]based on two different storage tank volumes, which are 150 Liter and 50 Liter.

One of the tanks of mixed type, and has a capacity of 150 Liter as shown in Figure (4.8a), while the other one has 50 Liter capacity and of stratified type as shown in Figure (4.8b) .

The experimental results for the metallic serpentine collector, for the 150 Liter tank, were obtained from [21]. These results were taken from four tests, performed on August , 3_{rd}, 4_{th}, 5_{th}, 10_{th}, with flow rates of 0.05, 0.03, 0.02 ,and 0.04 kg/s, respectively. The layout of this test is shown in Figure (4.7), while the calculated data of these tests are shown in Tables (A.1-A.4) of Appendix A.

For the 50 Liter storage tank, four tests were performed on September 2_{nd}, 3_{rd}, 4_{th}, and August 27_{th}, with flow rates of 0.03, 0.02, 0.05 and 0.07 kg/s respectively[21]. The calculated data of these tests are shown in Tables (A.5-A.8) of Appendix A.:

On the other hand, the experimental results for the non- metallic serpentine collector were obtained from [23]. When the 150 Liter storage tank was used, four tests were performed on August 20_{th}, 24_{th}, 25_{th}, and 26_{th}, with flow rates 0.03, 0.06, 0.02, and 0.04 kg/s, respectively. The calculated data of this test are shown in Tables (A.9-A.12) of Appendix A.

For the 50 Liter storage tank, four tests were performed on September 15, 16, 19, 20 with flow rates of 0.06, 0.02, 0.01 and 0.04 kg/s,

respectively. The calculated data of these tests are shown in Tables (A.13-A.16) of Appendix A

The values of the performance parameters obtained from the above tests are used to compare the present theoretical performance parameters such as the instantaneous efficiency, the heat removal factor and the overall heat transfer coefficient for different mass flow rates.

4.2 Forced circulation test with load conditions:

This test was performed by [21] and [23] for metallic and non-metallic collector, respectively. Aims of this test are to evaluate the daily efficiency for each collector model at different mass flow rates. For this case, no storage tanks are needed. Instead, a constant head tank of 1000 liter capacity is used to supply fresh water continuously at constant temperature to feed the collectors.

The outlet hot water from the collector is used as a hot water load as shown in Figure (4.6). For the metallic serpentine collector the experimental data are based on tests performed on September 12_{th}, and 14_{th}, with flow rates of 0.02, and 0.05 kg/s respectively. The calculated data of this test are shown in Tables (A.17-A.18) of Appendix A.

the weather conditions on that day. Note, that the ambient temperature model of this work is for general conditions, and not for a specific day of a specific year.

Figures (4.3 - 4.4), show the comparison for the Solar intensity for both the experimental and theoretical models. It can be seen that both curves have almost the same behavior. The useful energy also has the same behavior but, for the metallic case there was a somehow high error at the mid of the day. The theoretical model gave higher energy values than the measured data. But, for the non-metallic model the results were much closer, as can be shown in the same figures.

From Figure (4.5), the efficiency can be shown to be almost the same at the afternoon period but somehow it has different values at the morning hours. This is due to the difference in the starting conditions between the theoretical model and the experimental work. The present work model assumes that the solar collector works from sunrise to sunset. On the other hand, the experimental data of Ref. [23] assumes that the starting hour of operating the collector is at 8:00. Thus the heat gain from sunrise to this hour is not accounted for.

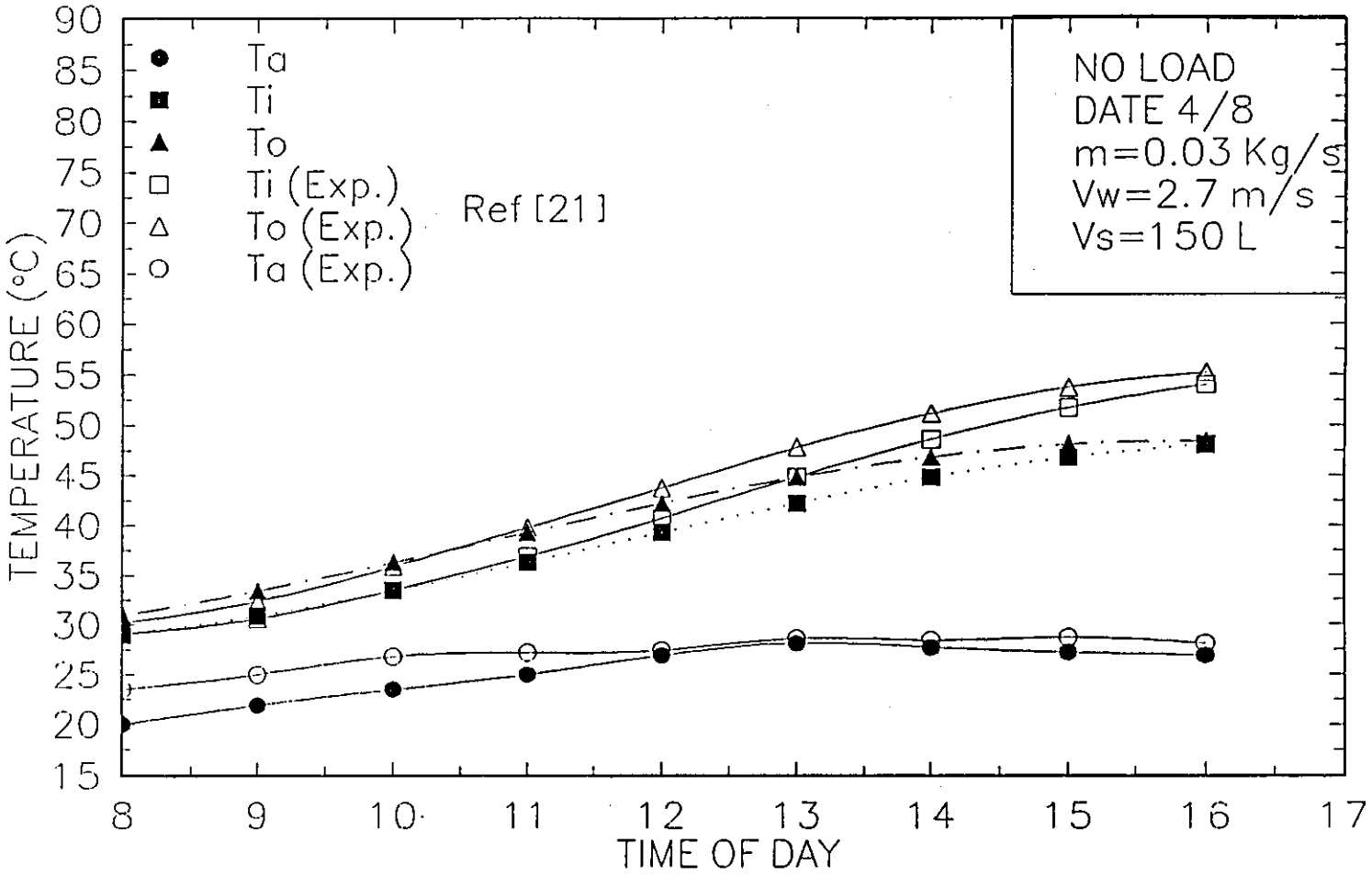

FIG (4.1). Variation of Inlet Temp. Outlet Temp. and the Amb. Temp. with Time for the Serpentine Tube Flat Metallic Plate Solar Colectors.

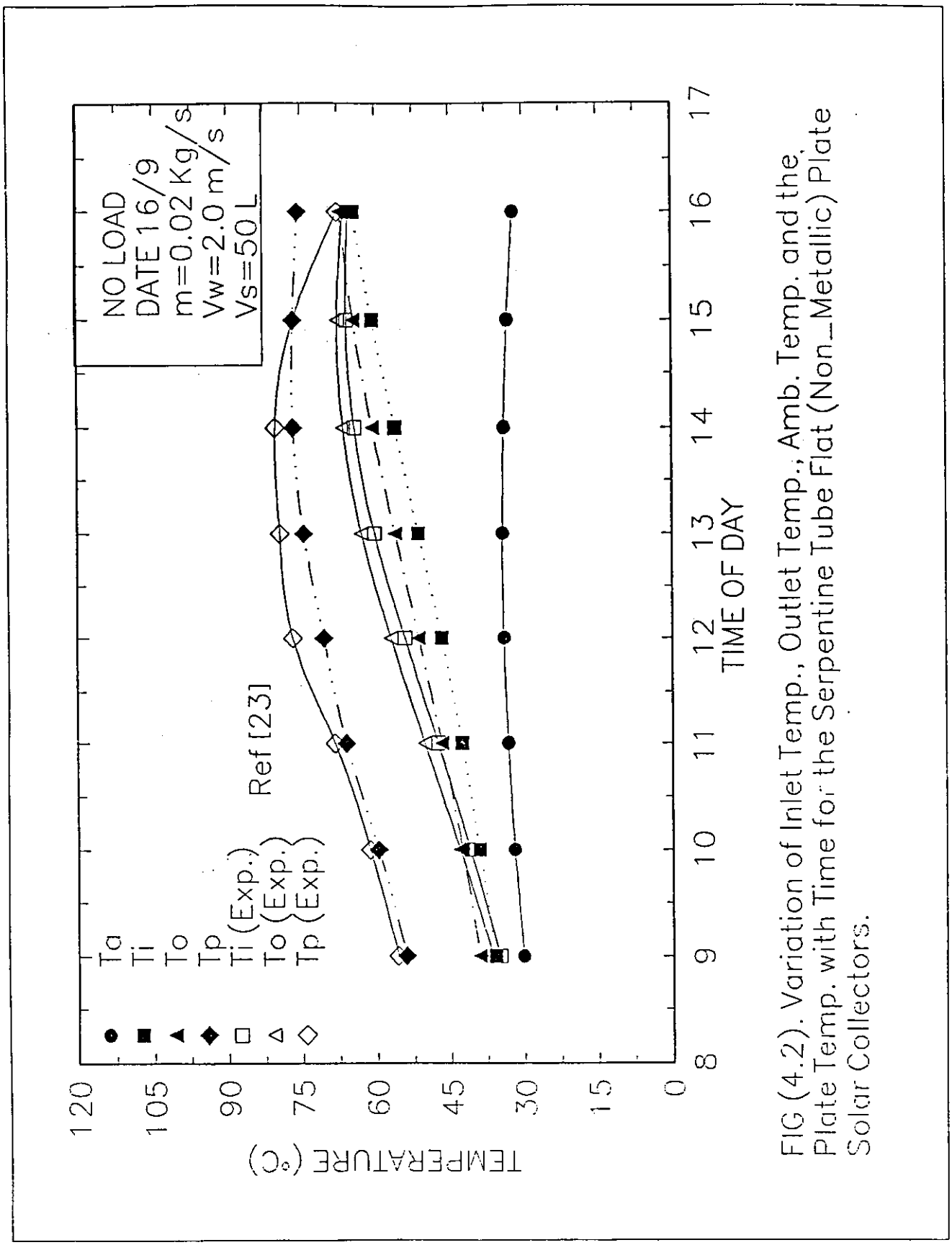

FIG (4.2). Variation of Inlet Temp., Outlet Temp., Amb. Temp. and the Plate Temp. with Time for the Serpentine Tube Flat (Non_Metallic) Plate Solar Collectors.

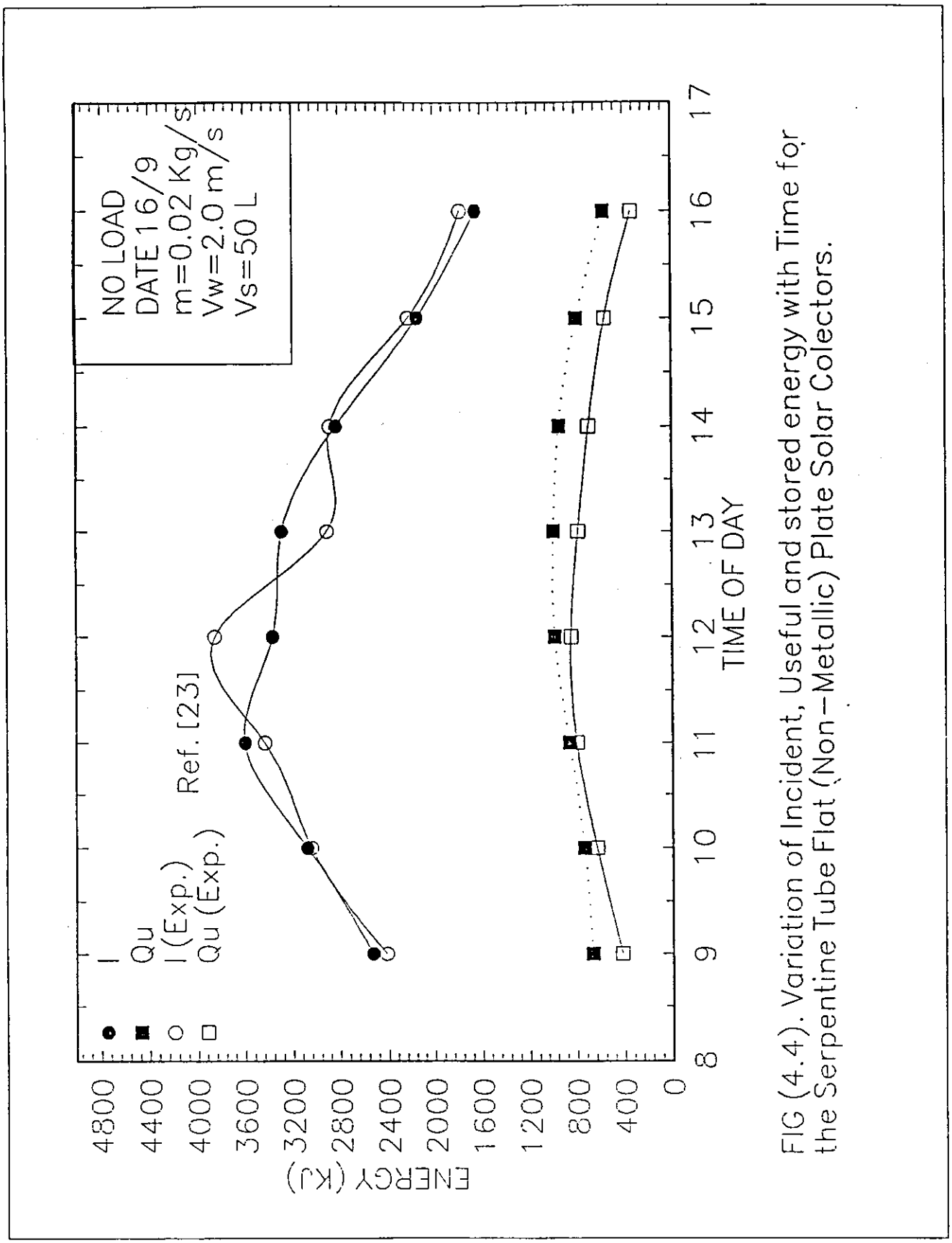

FIG (4.4). Variation of Incident, Useful and stored energy with Time for the Serpentine Tube Flat (Non-Metallic) Plate Solar Colectors.

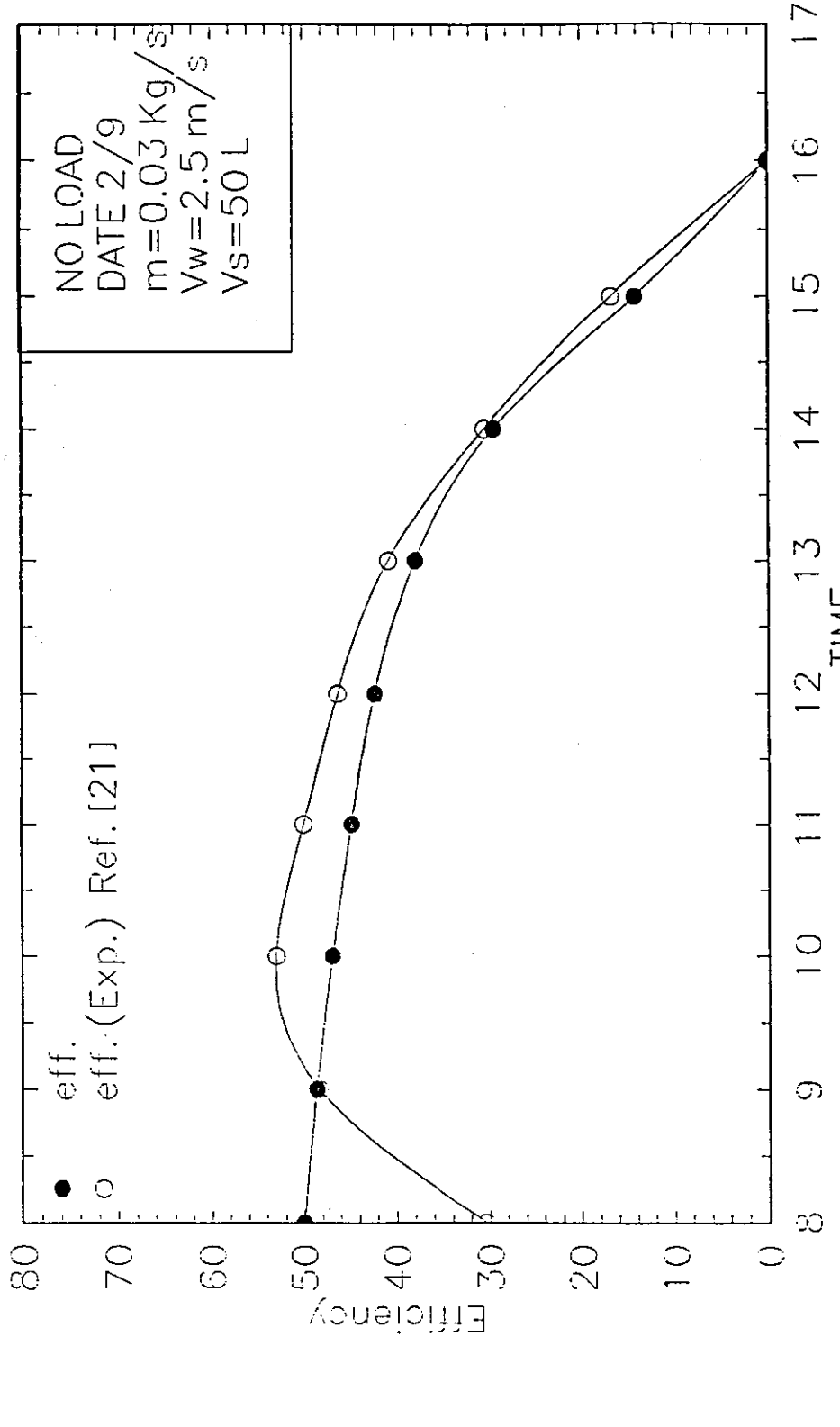

FIG (4.5). Variation of Instantaneous Efficiency against Time of Day for the Serpentine Tube Flat Metallic Plate Solar Colectors.

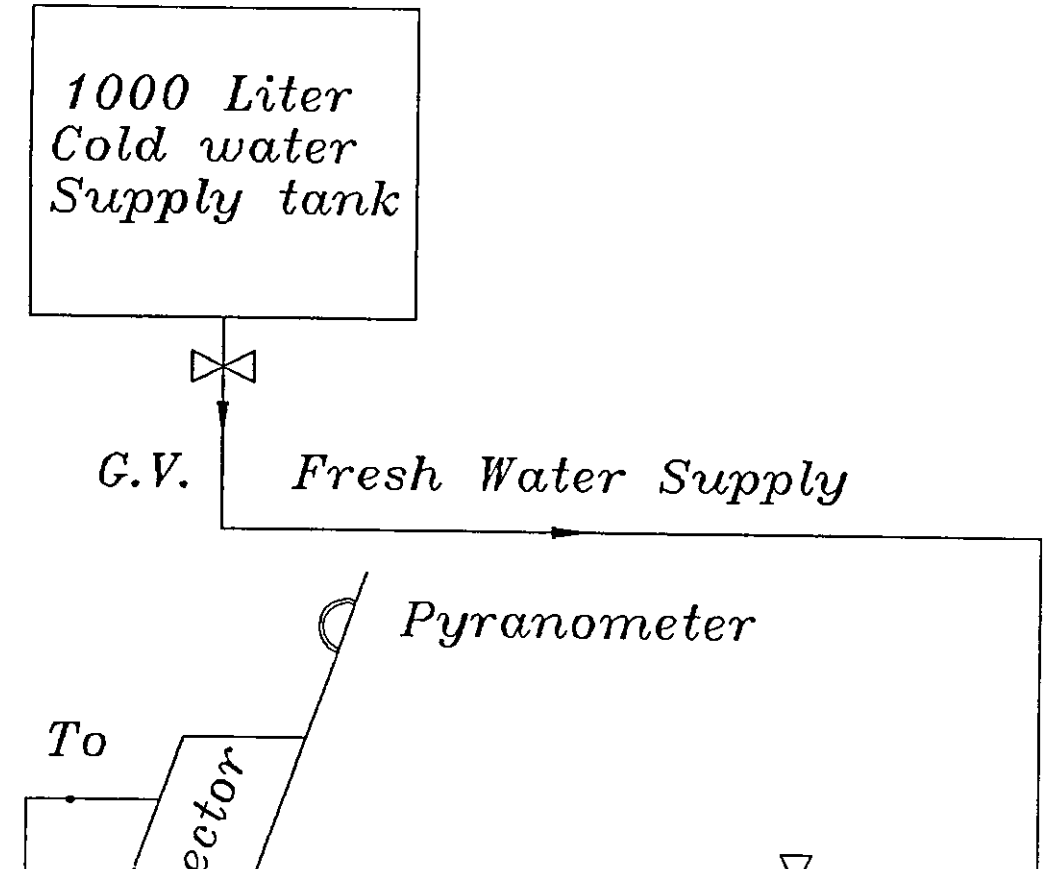

Fig (4.6) Open Loop setup for load test

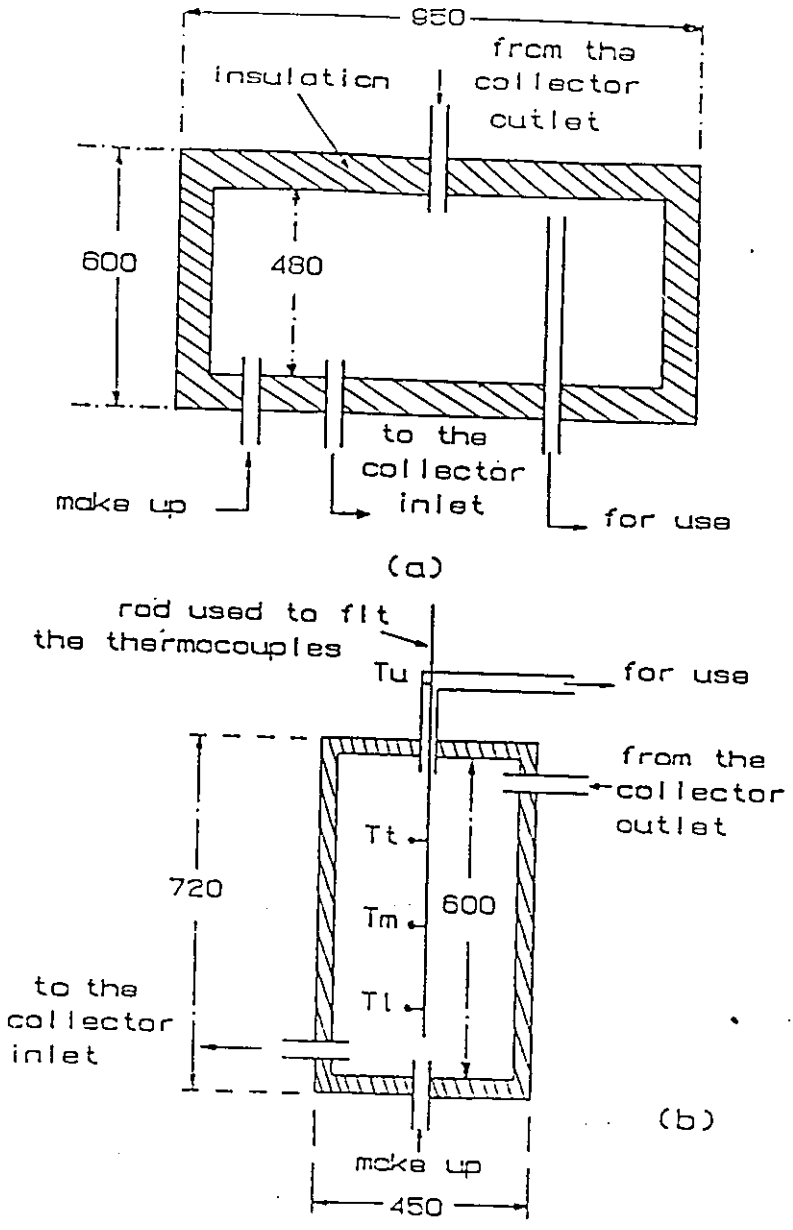

Fig.(4.8) Storage tanks:
(a) Well mixed storage tank of 150 liter.
(b) Stratified storage tank of 50 liter.

Chapter Five

CONCLUSIONS AND RECOMMENDATIONS

5.1 Conclusions

The following conclusions are obtained from the present study :

1- For both collectors, (metallic and non-metallic), the heat removal factor is more sensitive to the flow rate variations when small storage tanks are used.

2- Under no load conditions, as the storage tank capacity is decreased, the performance parameters of both collectors decreased.

3- The overall heat loss coefficients of both collectors show week dependence on the flow rate variations.

4- Under forced flow circulation, the non-metallic collector (concrete) with galvanized steel serpentine tubes has an inferior performance parameters when compared to the metallic serpentine collector with galvanized steel tubes.

5- Under forced flow open loop circulation, the daily efficiency of the metallic serpentine collector is higher than that of the non- metallic serpentine collector for all water mass flow rates investigated.

6- The stored energy in non-metallic serpentine collector model behaves as that of Ref. [23]. This energy constitutes a positive input for early morning where it reaches a maximum value around 11:00 am. The stored energy begins to constitute a negative input in the after noon hours.The stored energy constitutes a significant energy for the collector, even after the diminishing of the solar intensity.

7- As the solar intensity is increased, the ability of both, metallic and non-metallic serpentine collector, in converting the solar irradiance into useful heat gain becomes more significant.

8- comparison of performance parameters of the theoretical and experimental studies showed good agreements except at the early hours and late after noon.

REFERENCES

1. Duffie, J. A. and Bekman, W. A.: "Solar engineering of thermal processes", Wiley and Sons, New York, 1980.

2. Alsaad, M., Hijazi, M., Habali, S. and Rabadi, N.: "An Inexpensive and reliable solar water heater for Jordan", Dirasat, Vol. XII, No. 1, 1985, pp.111-128, University of Jordan.

3. Hottel, H. C. and Woertz, B. B.: "Performance of flat-plate solar heat collectors", Transaction of the American Society of Mechanical Engineers, 64, 91 (1942).

4. Moore, S. W., Balcomb, J. D. and Hedstorm, J. C.: "Design and testing of a structurlly integrated steel solar collector uint based on expanded flat metal plates", Ft. Collins ISES meeting, August 1974.

5. Spencer, D. L. and Strud, R. L.: "Integration of solar collector in fabricated roof/wall sections", Proc. ISES Sliver Jubilee Congress, Atalanta, CA, May. 1979, pp. 384-354.

6. Frank, C. and Mcgowan, G.: "Performance modeling of non-metallic flat plate solar collectors", Solar energy, Vol. 33, No. 3/4, 1984, pp. 305-319.

7. Turner, R. H.: "Concrete slabs as summer solar collectors", Proc. International heat transfer conference, San Francisco, CA, 1986, pp. 683-689.

8. Russel, L. D. and Guven, H. M.: "Modeling and analysis of an all plastics flat plate solar collectors", J. Solar Energy Eng., Vol. 104, 1982.

9. Madsen, P. and Gooss, K.: "Report on non-metallic solar collectors", Solar age, Vol.6, No.1, Jan. 1981, pp.28-32.

10. Wilhelm, W. G.:"Low-cost solar collectors using thin film plastics

absorbers and glassings", Proc. Annual metting of the American section of the International Solar Energy Society, Vol. 3, No. 1, 1980, pp. 456-460.

11. Currin, C. G.: "Sillicone-glass cloth for solar greenhouse", Proc. Living and growing conference, Plymouth, Mass, 1979.

12. Abu Faris, N.: "Development, modeling, manufacturing, and testing of non-metallic solar collectors under Jordanian climate", Msc Thesis, University of Jordan, Amman, Jordan, 1991.

13. ASHRAE Standerd 93-77. Methods of testing to determine the thermal performance of solar collectors, ASHRAE, NewWork, 1977.

14. Abdel-Khalik, S. T.: "Heat removal for a flat plate solar collector with serpentine tube", Solar Energy, Vol.18, No.1, 1976, pp.59-64.

15. Zhang, H. and Lavan, Z.: " Thermal performance of a serpentine absorber plate", Solar Energy, Vol.34, 1985, pp.175-177.

16. Akgun, M. A.: "Heat removal factor for a serpentine absorber plate", Solar Energy, Vol. 41, No.1, 1988, pp.109-111.

17. Borde, I., Yaron, I. and Jelinek, M.: " Comparative study of parallel tubes and serpentine type flat-plate solar collectors", Proc. Int. Solar Energy Soc. Sliver Jubilee, 1979, pp.277.

18. Chiou, J. P. and Perera, D. G.: "Performance analysis of a serpentine type flat-plate solar collectors", Proc. ASME-ASES Solar Energy Conference Konxville, March.1985.

19. Johnson, S.: "Standardized performance tests of collectors of solar thermal energy. A flat plate solar collector with a singel tube serpentine flow distribution", NASA Technical Memorandum, NASA TMX-73417, 1-2 Leewis Research Center, Cleveland, Ohio, April. 1976.

20. Hill, J. E., Jenkins, J. P. and Jones, D. E.: "Experimental verification of a standard test procedure for solar collectors", National Burean of Standards Building Soience Series 117, Washington D.C., 5-39. 1979.

21. Abu Yahia, F.: "Performance comparison of parallel tube and serpentine type solar collectors", MSC Thesis, University of Jordan, Amman, Jordan, 1992.

22. Zhang, H.: "Unified design method for a range of a solar collectors", Solar Engineering, Vol. , No. , 1990.

23. Adas, H. M.: "Design, Manufactoring and Performance of Non-Metallic Serpentine Type Solar Collector", M.Sc. Thesis, University of Jordan, Amman, 1994, 182 p.

24. Muhaddin, S. B. and Adam, S. K.: "Estimating Top Heat Losses From Flat-Plate Solar Collectors", Internatinal Renewable Energy Conference, Amman, Jordan, 1992, pp 22-26.

25. Audi, M. S.: "Estimation of solar energy flux in Jordan", Dirasat, Vol.6, No.2, 1979, pp. 121-134.

26. Alsaad, M. A.: "Improved correlations for predicting global radiation for different locations in Jordan", Int. J. Solar Energy, Vol.8, 1990, pp.97-107.

27. Alsaad, M. A.: "Characteristic distribution of global solar radiation for Jordan", Solar and Wind Technology, Vol.7, 1990, pp.261-266.

28. Alsaad, M. A. and Audi, M. S.: "Solar radiation models for Jordan", Internatinal Renewable Energy Conference, Amman, Jordan, 1992,pp 53-66.

29. Garnier, B. J. and Ohmura, A.: "The evaluation of surface variation in solar radiation income", Solar Energy, Vol.13, 1970, pp.21-34.

APPENDIX A

Appendix A Tables of Calculated Results

Table (A.1). Results for the forced circulation for metallic collector with no load conditions (m=.05 Kg/s and Vs=150 l). All temperature. in C° on the 3rd of August.

Time Int.	Ta	Ti	To	Tp	I W.h/m^2
8.0- 9.0	20.00	28.50	30.60	48.00	655.08
9.0-10.0	21.90	30.60	33.20	47.50	817.50
10.0-11.0	23.50	33.20	36.20	55.10	915.89
11.0-12.0	25.00	36.20	39.40	60.90	951.50
12.0-13.0	26.90	39.40	42.40	64.70	926.44
13.0-14.0	28.10	42.40	45.10	66.70	843.42
14.0-15.0	27.70	45.10	47.20	66.30	705.92
15.0-16.0	27.20	47.20	48.40	63.20	519.58
16.0-17.0	26.90	48.40	48.80	58.10	295.53

Table (A.2). Results for the forced circulation for metallic collector with no load conditions (m=.03 Kg/s and Vs=150 l). All temperature. in C° on the 4th of August.

time int.	Ta	Ti	To	Tp	I W.h/m^2
8.0- 9.0	20.00	29.00	30.90	45.00	654.08
9.0-10.0	21.90	30.90	33.40	50.60	816.28
10.0-11.0	23.50	33.40	36.30	59.00	914.50
11.0-12.0	25.00	36.30	39.30	65.20	950.00
12.0-13.0	26.90	39.30	42.20	69.20	924.92
13.0-14.0	28.10	42.20	44.80	70.90	841.97
14.0-15.0	27.70	44.80	46.80	70.00	704.61
15.0-16.0	27.20	46.80	48.10	66.00	518.47
16.0-17.0	26.90	48.10	48.40	59.70	294.64

Table (A.3). Results for the forced circulation for metallic collector with no load conditions (m=.02 Kg/s and Vs=150 l). All temperature. in C^0 on the 5th of August.

Time Int.	Ta	Ti	To	Tpm	I W.h/m^2
8.0- 9.0	20.00	28.00	29.80	40.00	653.06
9.0-10.0	21.90	29.80	32.20	52.80	815.00
10.0-11.0	23.50	32.20	34.90	62.00	913.03
11.0-12.0	25.00	34.90	37.70	68.70	948.44
12.0-13.0	26.90	37.70	40.50	72.80	923.36
13.0-14.0	28.10	40.50	43.00	74.30	840.44
14.0-15.0	27.70	43.00	45.00	72.70	703.25
15.0-16.0	27.20	45.00	46.20	67.70	517.33
16.0-17.0	26.90	46.20	46.60	60.30	293.75

Table (A.4). Results for the forced circulation for metallic collector with no load conditions (m=.04 Kg/s and Vs=150 l). All temperature. in C^0 on the 10th of August.

Time Int.	Ta	Ti	To	Tp	I W.h/m^2
8.0- 9.0	23.30	28.00	30.20	45.00	647.47
9.0-10.0	26.20	30.20	33.00	49.80	808.08
10.0-11.0	27.10	33.00	36.10	58.30	905.06
11.0-12.0	28.20	36.10	39.30	63.80	939.86
12.0-13.0	29.90	39.30	42.40	67.50	914.69
13.0-14.0	30.50	42.40	45.10	69.30	832.17
14.0-15.0	30.40	45.10	47.20	68.50	695.81
15.0-16.0	29.60	47.20	48.50	65.20	511.14
16.0-17.0	29.10	48.50	48.90	59.60	288.92

Table (A,5). Results for the forced circulation for metallic collector with no load conditions (m=.07 Kg/s and Vs=50 l). All temperature. in C^0 on the 27th of August.

Time Int.	Ta	Ti	To	Tp	I W.h/m^2
8.0- 9.0	20.00	24.00	30.60	40.00	623.19
9.0-10.0	21.90	30.60	38.60	47.40	777.42
10.0-11.0	23.50	38.60	47.10	58.30	869.36
11.0-12.0	25.00	47.10	55.40	67.50	901.25
12.0-13.0	26.90	55.40	62.80	74.80	875.42
13.0-14.0	28.10	62.80	68.80	80.00	794.58
14.0-15.0	27.70	68.80	72.40	82.30	662.31
15.0-16.0	27.20	72.40	73.40	80.70	483.78
16.0-17.0	26.90	73.40	71.50	75.60	268.64

Table (A.6). Results for the forced circulation for metallic collector with no load conditions (m=.03 Kg/s and Vs=50 l). All temperature. in C^0 on the 2nd September.

Time Int.	Ta	Ti	To	Tp	I W.h/m^2
8.0- 9.0	20.00	21.00	27.10	40.00	612.86
9.0-10.0	21.90	27.10	34.50	49.20	764.14
10.0-11.0	23.50	34.50	42.50	60.20	853.83
11.0-12.0	25.00	42.50	50.40	69.20	884.33
12.0-13.0	26.90	50.40	57.70	75.80	858.17
13.0-14.0	28.10	57.70	63.60	80.20	778.08
14.0-15.0	27.70	63.60	67.40	81.40	647.61
15.0-16.0	27.20	67.40	68.70	78.70	471.97
16.0-17.0	26.90	68.70	67.40	72.60	260.17

Table (A.7). Results for the forced circulation for metallic collector with no load conditions (m=.02 Kg/s and Vs=50 l). All temperature. in C° on the 3rd of September.

Time Int.	Ta	Ti	To	Tp	I W.h/m^2
8.0- 9.0	20.00	22.00	27.60	40.00	611.06
9.0-10.0	21.90	27.60	34.50	52.50	761.83
10.0-11.0	23.50	34.50	42.10	64.00	851.11
11.0-12.0	25.00	42.10	49.70	73.20	881.36
12.0-13.0	26.90	49.70	56.80	79.80	855.14
13.0-14.0	28.10	56.80	62.70	83.70	775.17
14.0-15.0	27.70	62.70	66.70	84.30	645.03
15.0-16.0	27.20	66.70	68.20	80.80	469.89
16.0-17.0	26.90	68.20	67.20	73.70	258.69

Table (A.8). Results for the forced circulation for metallic collector with no load conditions (m=.05 Kg/s and Vs=50 l). All temperature. in C° on the 4th of September.

Time Int.	Ta	Ti	To	Tp	I W.h/m^2
8.0- 9.0	20.00	21.00	27.50	40.00	609.25
9.0-10.0	21.90	27.50	35.30	46.20	759.47
10.0-11.0	23.50	35.30	43.50	56.80	848.33
11.0-12.0	25.00	43.50	51.50	65.60	878.36
12.0-13.0	26.90	51.50	58.70	72.30	852.06
13.0-14.0	28.10	58.70	64.40	76.90	772.22
14.0-15.0	27.70	64.40	67.90	78.60	642.42
15.0-16.0	27.20	67.90	68.90	76.60	467.78
16.0-17.0	26.90	68.90	67.20	71.30	257.22

Table (A.9). Results for the forced circulation for metallic collector with load conditions (m=.02 Kg/s). All temperature. in C^0 on the 12th of September.

Time Int.	Ta	Ti	To	Tp	I W.h/m^2
8.0- 9.0	20.00	24.00	27.60	35.00	594.00
9.0-10.0	21.90	24.00	28.70	47.00	739.67
10.0-11.0	23.50	24.00	29.50	54.00	825.03
11.0-12.0	25.00	24.00	29.80	58.60	852.92
12.0-13.0	26.90	24.00	29.80	60.80	826.03
13.0-14.0	28.10	24.00	29.30	60.70	747.28
14.0-15.0	27.70	24.00	28.40	57.90	620.25
15.0-16.0	27.20	24.00	27.20	52.20	450.06
16.0-17.0	26.90	24.00	25.80	44.60	244.81

Table (A.10). Results for the forced circulation for metallic collector with load conditions (m=.02 Kg/s). All temperature. in C^0 on 14th of September.

Time Int.	Ta	Ti	To	Tp	I W.h/m^2
8.0- 9.0	20.00	25.00	26.70	35.00	590.03
9.0-10.0	21.90	25.00	27.20	42.00	734.47
10.0-11.0	23.50	25.00	27.50	47.20	818.89
11.0-12.0	25.00	25.00	27.70	50.60	846.19
12.0-13.0	26.90	25.00	27.60	52.20	819.17
13.0-14.0	28.10	25.00	27.40	52.10	740.67
14.0-15.0	27.70	25.00	27.00	50.10	614.39
15.0-16.0	27.20	25.00	26.50	45.80	445.39
16.0-17.0	26.90	25.00	25.80	40.20	241.58

Table (A.11). Results for the forced circulation for metallic collector with load conditions (m=.03 Kg/s). All temperature. in C° on the 6th of September.

Time Int.	Ta	Ti	To	Tp	I W.h/m^2
8.0- 9.0	23.30	27.00	29.70	40.00	605.56
9.0-10.0	26.20	27.00	30.60	47.50	754.69
10.0-11.0	27.10	27.00	31.10	54.10	842.72
11.0-12.0	28.20	27.00	31.30	57.70	872.22
12.0-13.0	29.90	27.00	31.20	59.30	845.78
13.0-14.0	30.50	27.00	30.90	59.20	766.22
14.0-15.0	30.40	27.00	30.30	56.50	637.08
15.0-16.0	29.60	27.00	29.40	51.70	463.50
16.0-17.0	29.10	27.00	28.30	45.00	254.19

Table (A.12). Results for the forced circulation for metallic collector with load conditions (m=.04 Kg/s). All temperature. in C° on 20th of September.

Time Int.	Ta	Ti	To	Tp	I W.h/m^2
8.0- 9.0	23.30	30.00	31.90	45.00	577.83
9.0-10.0	26.20	30.00	32.60	46.60	718.39
10.0-11.0	27.10	30.00	32.90	52.50	799.86
11.0-12.0	28.20	30.00	33.10	55.50	825.36
12.0-13.0	29.90	30.00	33.00	56.80	797.78
13.0-14.0	30.50	30.00	32.80	56.70	720.14
14.0-15.0	30.40	30.00	32.30	54.30	596.17
15.0-16.0	29.60	30.00	31.60	50.10	430.89
16.0-17.0	29.10	30.00	30.90	44.30	231.64

Table (A.13). Results for the forced circulation nonmetallic collector with no load conditions (m=.03 Kg/s and Vs=150 l). All temperature in C° on the 20th of August.

Time Int.	Ta	Ti	To	Tp	I W.h/m^2
9.0-10.0	26.20	29.70	31.20	48.70	702.06
10.0-11.0	27.10	31.20	32.80	52.80	855.08
11.0-12.0	28.20	32.80	34.80	57.80	1000.08
12.0-13.0	29.90	34.80	37.00	61.00	936.11
13.0-14.0	30.50	37.00	39.30	63.50	914.11
14.0-15.0	30.40	39.30	41.60	64.20	786.14
15.0-16.0	29.60	41.60	43.70	62.90	595.17
16.0-17.0	29.10	43.70	45.50	60.80	457.17

Table (A.14). Results for the forced circulation nonmetallic collector with no load conditions (m=.06 Kg/s and Vs=150 l). All temperature in C° on the 24th of August.

Time Int.	Ta	Ti	To	Tp	I W.h/m^2
9.0-10.0	26.20	28.40	30.40	45.20	702.06
10.0-11.0	27.10	30.40	32.40	48.60	855.08
11.0-12.0	28.20	32.40	34.70	53.00	1000.08
12.0-13.0	29.90	34.70	37.20	55.90	936.11
13.0-14.0	30.50	37.20	39.80	58.20	914.11
14.0-15.0	30.40	39.80	42.30	58.90	786.14
15.0-16.0	29.60	42.30	44.40	58.00	595.17
16.0-17.0	29.10	44.40	46.10	56.50	457.17

Table (A.15). Results for the forced circulation nonmetallic collector with no load conditions (m=.02 Kg/s and Vs=150 l). All temperature in C° on 25th of August.

Time Int.	Ta	Ti	To	Tp	I W.h/m^2
9.0-10.0	26.20	27.40	28.80	49.80	702.06
10.0-11.0	27.10	28.80	30.20	54.30	855.08
11.0-12.0	28.20	30.20	32.00	59.80	1000.08
12.0-13.0	29.90	32.00	34.00	63.50	936.11
13.0-14.0	30.50	34.00	36.10	66.20	914.11
14.0-15.0	30.40	36.10	38.30	67.00	786.14
15.0-16.0	29.60	38.30	40.50	65.50	595.17
16.0-17.0	29.10	40.50	42.30	63.10	457.17

Table (A.16). Results for the forced circulation nonmetallic collector with no load conditions (m=.04 Kg/s and Vs=150 l). All temperature. in C° on the 26th of August.

Time Int.	Ta	Ti	To	Tp	I W.h/m^2
9.0-10.0	26.20	32.00	33.80	49.70	702.06
10.0-11.0	27.10	33.80	35.60	53.30	855.08
11.0-12.0	28.20	35.60	37.60	57.80	1000.08
12.0-13.0	29.90	37.60	39.90	60.70	936.11
13.0-14.0	30.50	39.90	42.30	63.00	914.11
14.0-15.0	30.40	42.30	44.70	63.70	786.14
15.0-16.0	29.60	44.70	46.70	62.50	595.17
16.0-17.0	29.10	46.70	48.40	60.60	457.17

Table (A.17). Results for the forced circulation nonmetallic collector with no load conditions (m=.06 Kg/s and Vs=50 l). All temperature in C° on the 15th of September.

Time Int.	Ta	Ti	To	Tp	I W.h/m^2
9.0-10.0	30.20	37.00	42.10	51.30	702.06
10.0-11.0	32.00	42.10	46.60	56.10	855.08
11.0-12.0	33.20	46.60	51.40	62.00	1000.08
12.0-13.0	34.00	51.40	56.50	66.40	936.11
13.0-14.0	34.20	56.50	61.20	70.40	914.11
14.0-15.0	33.90	61.20	65.30	73.00	786.14
15.0-16.0	33.20	65.30	68.30	73.80	595.17
16.0-17.0	32.00	68.30	70.10	73.70	457.17

Table (A.18). Results for the forced circulation nonmetallic collector with no load conditions (m=.02 Kg/s and Vs=150 l). All temperature in C° on the 16th of September.

Time Int.	Ta	Ti	To	Tp	I W.h/m^2
9.0-10.0	30.20	35.90	39.10	54.10	702.06
10.0-11.0	32.00	39.10	42.60	59.60	855.08
11.0-12.0	33.20	42.60	46.70	66.00	1000.08
12.0-13.0	34.00	46.70	51.40	70.60	936.11
13.0-14.0	34.20	51.40	56.10	74.50	914.11
14.0-15.0	33.90	56.10	60.60	76.60	786.14
15.0-16.0	33.20	60.60	64.40	76.60	595.17
16.0-17.0	32.00	64.40	67.10	75.60	457.17

Table (A.19). Results for the forced circulation nonmetallic collector with no load conditions (m=.01 Kg/s and Vs=50 l). All temperature in C° on the 19th of September.

Time Int.	Ta	Ti	To	Tp	I W.h/m^2
9.0-10.0	30.20	32.60	34.90	56.10	702.06
10.0-11.0	32.00	34.90	37.60	62.30	855.08
11.0-12.0	33.20	37.60	40.80	69.50	1000.08
12.0-13.0	34.00	40.80	44.70	74.70	936.11
13.0-14.0	34.20	44.70	48.90	78.90	914.11
14.0-15.0	33.90	48.90	53.30	80.90	786.14
15.0-16.0	33.20	53.30	57.40	80.50	595.17
16.0-17.0	32.00	57.40	60.80	78.70	457.17

Table (A.20). Results for the forced circulation nonmetallic collector with no load conditions (m=.04 Kg/s and Vs=50 l). All temperature in C° on the 20th of September.

Time Int.	Ta	Ti	To	Tp	I W.h/m^2
9.0-10.0	30.20	36.30	40.50	51.50	702.06
10.0-11.0	32.00	40.50	44.70	56.60	855.08
11.0-12.0	33.20	44.70	49.40	62.60	1000.08
12.0-13.0	34.00	49.40	54.50	67.00	936.11
13.0-14.0	34.20	54.50	59.30	71.00	914.11
14.0-15.0	33.90	59.30	63.60	73.40	786.14
15.0-16.0	33.20	63.60	66.90	74.00	595.17
16.0-17.0	32.00	66.90	68.90	73.70	457.17

Table (A.21). Results for the forced circulation nonmetallic collector with load conditions (m=.02 Kg/s). All temperature in C° on the 3rd of August.

Time Int.	Ta	Ti	To	Tp	I W.h/m^2
9.0-10.0	26.20	27.00	29.30	46.60	702.06
10.0-11.0	27.10	27.00	29.90	51.80	855.08
11.0-12.0	28.20	27.00	30.70	57.50	1000.08
12.0-13.0	29.90	27.00	31.50	61.20	936.11
13.0-14.0	30.50	27.00	32.00	63.70	914.11
14.0-15.0	30.40	27.00	32.40	64.00	786.14
15.0-16.0	29.60	27.00	32.40	61.80	595.17
16.0-17.0	29.10	27.00	32.10	58.50	457.17

Table (A.22). Results for the forced circulation nonmetallic collector with load conditions (m=.04 Kg/s). All temperature in C° on 4th of August.

Time Int.	Ta	Ti	To	Tp	I W.h/m^2
9.0-10.0	26.20	26.00	27.60	43.50	702.06
10.0-11.0	27.10	26.00	28.00	47.50	855.08
11.0-12.0	28.20	26.00	28.50	52.00	1000.08
12.0-13.0	29.90	26.00	28.90	54.60	936.11
13.0-14.0	30.50	26.00	29.20	56.20	914.11
14.0-15.0	30.40	26.00	29.30	55.80	786.14
15.0-16.0	29.60	26.00	29.20	53.30	595.17
16.0-17.0	29.10	26.00	28.90	50.00	457.17

Table (A.23). Results for the forced circulation nonmetallic collector with load conditions (m=.06 Kg/s). All temperature in C° on the 5th of August.

Time Int.	Ta	Ti	To	Tp	I W.h/m^2
9.0-10.0	26.20	26.00	27.30	42.20	702.06
10.0-11.0	27.10	26.00	27.60	45.70	855.08
11.0-12.0	28.20	26.00	27.90	49.60	1000.08
12.0-13.0	29.90	26.00	28.20	51.60	936.11
13.0-14.0	30.50	26.00	28.30	52.80	914.11
14.0-15.0	30.40	26.00	28.40	52.20	786.14
15.0-16.0	29.60	26.00	28.20	49.60	595.17
16.0-17.0	29.10	26.00	28.00	46.50	457.17

Table (A.24). Results for the forced circulation nonmetallic collector with load conditions (m=.01 Kg/s). All temperature in C° on the 8th of August.

Time Int.	Ta	Ti	To	Tp	I W.h/m^2
9.0-10.0	26.20	28.00	30.90	50.90	702.06
10.0-11.0	27.10	28.00	31.80	57.10	855.08
11.0-12.0	28.20	28.00	32.90	63.90	1000.08
12.0-13.0	29.90	28.00	34.30	68.80	936.11
13.0-14.0	30.50	28.00	35.20	72.50	914.11
14.0-15.0	30.40	28.00	36.00	73.80	786.14
15.0-16.0	29.60	28.00	36.30	72.30	595.17
16.0-17.0	29.10	28.00	36.10	69.20	457.17

Table (A.25). Calculated parameters for the forced circulation for metallic collector with no load conditions (m=.05 Kg/s and Vs=150 l) on the 3rd of August.

Time Int.	I (kJ)	Qu (kJ)	η%	(Ti-Ta)/I%
8.0- 9.0	2358.30	1289.50	47.10	1.30
9.0-10.0	2943.00	1674.90	49.00	1.06
10.0-11.0	3297.20	1900.20	49.60	1.06
11.0-12.0	3425.40	1973.90	49.60	1.18
12.0-13.0	3335.20	1910.10	49.30	1.35
13.0-14.0	3036.30	1687.30	47.90	1.70
14.0-15.0	2541.30	1292.50	43.80	2.47
15.0-16.0	1870.50	785.80	36.20	3.85
16.0-17.0	1063.90	212.70	17.20	7.29

Table (A.26). Calculated parameters for the forced circulation for metallic collector with no load conditions (m=.03 Kg/s and Vs=150 l) on the 4th of August.

Time Int.	I (kJ)	Qu (kJ)	η%	(Ti-Ta)/I%
8.0- 9.0	2354.70	1205.00	44.10	1.37
9.0-10.0	2938.60	1577.40	46.20	1.11
10.0-11.0	3292.20	1804.60	47.20	1.09
11.0-12.0	3420.00	1887.90	47.50	1.19
12.0-13.0	3329.70	1837.10	47.50	1.34
13.0-14.0	3031.10	1631.80	46.40	1.68
14.0-15.0	2536.60	1259.60	42.80	2.43
15.0-16.0	1866.50	776.20	35.80	3.79
16.0-17.0	1060.70	226.80	18.40	7.19

Table (A.27). Calculated parameters for the forced circulation for metallic collector with no load conditions (m=.02 Kg/s and Vs=150 l) on the 5th of August.

Time Int.	I (kJ)	Qu (kJ)	η%	(Ti-Ta)/I%
8.0- 9.0	2351.00	1130.70	41.40	1.22
9.0-10.0	2934.00	1483.50	43.60	0.97
10.0-11.0	3286.90	1705.30	44.70	0.95
11.0-12.0	3414.40	1793.50	45.20	1.04
12.0-13.0	3324.10	1754.20	45.50	1.18
13.0-14.0	3025.60	1567.20	44.60	1.48
14.0-15.0	2531.70	1220.90	41.50	2.18
15.0-16.0	1862.40	767.40	35.50	3.44
16.0-17.0	1057.50	251.20	20.50	6.57

Table (A.28). Calculated parameters for the forced circulation for metallic collector with no load conditions (m=.04 Kg/s and Vs=150 l) on the 10th of August.

Time Int.	I (kJ)	Qu (kJ)	η%	(Ti-Ta)/I%
8.0- 9.0	2330.90	1352.70	50.00	0.72
9.0-10.0	2909.10	1756.50	52.00	0.49
10.0-11.0	3258.20	1951.00	51.60	0.65
11.0-12.0	3383.50	2010.80	51.20	0.83
12.0-13.0	3292.90	1943.60	50.80	1.02
13.0-14.0	2995.80	1709.00	49.10	1.42
14.0-15.0	2504.90	1330.80	45.80	2.11
15.0-16.0	1840.10	828.90	38.80	3.44
16.0-17.0	1040.10	259.00	21.40	6.73

Table (A.29). Calculated parameters for the forced circulation for metallic collector with no load conditions (m=.07 Kg/s and Vs=50 l) on the 27th of August.

Time Int.	I (kJ)	Qu (kJ)	η%	(Ti-Ta)/I%
8.0- 9.0	2243.50	1391.00	53.40	0.64
9.0-10.0	2798.70	1670.90	51.40	1.13
10.0-11.0	3129.70	1777.40	48.90	1.74
11.0-12.0	3244.50	1732.50	46.00	2.45
12.0-13.0	3151.50	1558.00	42.60	3.26
13.0-14.0	2860.50	1238.00	37.30	4.38
14.0-15.0	2384.30	765.10	27.60	6.20
15.0-16.0	1741.60	206.00	10.20	9.35
16.0-17.0	967.10	-389.40	****	17.31

Table (A.30). Calculated parameters for the forced circulation for metallic collector with no load conditions (m=.03 Kg/s and Vs=50 l) on the 2nd of September.

Time Int.	I (kJ)	Qu (kJ)	η%	(Ti-Ta)/I%
8.0- 9.0	2206.30	1281.80	50.00	0.16
9.0-10.0	2750.90	1550.90	48.60	0.69
10.0-11.0	3073.80	1673.60	46.90	1.30
11.0-12.0	3183.60	1657.50	44.80	1.98
12.0-13.0	3089.40	1516.10	42.30	2.75
13.0-14.0	2801.10	1232.60	37.90	3.81
14.0-15.0	2331.40	799.80	29.50	5.54
15.0-16.0	1699.10	280.10	14.20	8.52
16.0-17.0	936.60	-277.10	****	16.09

Table (A.31). Calculated parameters for the forced circulation for metallic collector with no load conditions (m=.02 Kg/s and Vs=50 l) on the 3rd of September.

Time Int.	I (kJ)	Qu (kJ)	η%	(Ti-Ta)/I%
8.0- 9.0	2199.80	1168.60	45.80	0.33
9.0-10.0	2742.60	1442.90	45.30	0.75
10.0-11.0	3064.00	1587.70	44.60	1.29
11.0-12.0	3172.90	1600.80	43.50	1.93
12.0-13.0	3078.50	1488.90	41.70	2.67
13.0-14.0	2790.60	1233.90	38.10	3.71
14.0-15.0	2322.10	827.70	30.70	5.43
15.0-16.0	1691.60	327.00	16.70	8.41
16.0-17.0	931.30	-216.90	****	15.98

Table (A,.32). Calculated parameters for the forced circulation for metallic collector with no load conditions (m=.05 Kg/s and Vs=50 l) on the 4th of September.

Time Int.	I (kJ)	Qu (kJ)	η%	(Ti-Ta)/I%
8.0- 9.0	2193.30	1363.70	53.60	0.16
9.0-10.0	2734.10	1625.20	51.20	0.74
10.0-11.0	3054.00	1720.80	48.50	1.39
11.0-12.0	3162.10	1672.90	45.60	2.10
12.0-13.0	3067.40	1502.60	42.20	2.89
13.0-14.0	2780.00	1193.50	37.00	3.96
14.0-15.0	2312.70	738.80	27.50	5.71
15.0-16.0	1684.00	207.10	10.60	8.71
16.0-17.0	926.00	-353.80	****	16.33

Table (A.33). Calculated parameters for the forced circulation for metallic collector with load conditions (m=.02 Kg/s) on the 12th of September.

Time Int.	I (kJ)	Qu (kJ)
8.0- 9.0	2138.40	1096.10
9.0-10.0	2662.80	1428.70
10.0-11.0	2970.10	1645.60
11.0-12.0	3070.50	1745.50
12.0-13.0	2973.70	1738.40
13.0-14.0	2690.20	1605.70
14.0-15.0	2232.90	1336.00
15.0-16.0	1620.20	976.50
16.0-17.0	881.30	554.60

Table (A.34). Calculated parameters for the forced circulation for metallic collector with load conditions (m=.05 Kg/s) on the 14th of September.

Time Int.	I (kJ)	Qu(kJ)
8.0- 9.0	2124.10	1257.00
9.0-10.0	2644.10	1644.20
10.0-11.0	2948.00	1888.30
11.0-12.0	3046.30	1997.50
12.0-13.0	2949.00	1985.30
13.0-14.0	2666.40	1830.70
14.0-15.0	2211.80	1520.80
15.0-16.0	1603.40	1107.50
16.0-17.0	869.70	618.80

Table (A.35). Calculated parameters for the forced circulation for metallic collector with load conditions (m=.03 Kg/s) on the 6th of September.

Time Int.	I (kJ)	Qu(kJ)
8.0- 9.0	2180.00	1229.90
9.0-10.0	2716.90	1625.50
10.0-11.0	3033.80	1837.30
11.0-12.0	3140.00	1933.10
12.0-13.0	3044.80	1919.90
13.0-14.0	2758.40	1759.10
14.0-15.0	2293.50	1472.10
15.0-16.0	1668.60	1073.40
16.0-17.0	915.10	603.30

Table (A.36). Calculated parameters for the forced circulation for metallic collector with load conditions (m=.04 Kg/s) on the 20th of September.

Time Int.	I (kJ)	Qu(kJ)
8.0- 9.0	2080.20	1156.10
9.0-10.0	2586.20	1557.60
10.0-11.0	2879.50	1763.70
11.0-12.0	2971.30	1853.90
12.0-13.0	2872.00	1836.90
13.0-14.0	2592.50	1673.00
14.0-15.0	2146.20	1384.80
15.0-16.0	1551.20	986.80
16.0-17.0	833.90	517.50

Table (A.37). Calculated parameters for the forced circulation non_metallic collector with no load conditions (m=.03 Kg/s and Vs=150 L) on the 20th of August.

Time Int.	I (kJ)	Qu(kJ)	Qs(kJ)	η%	(Tin-Ta)/I%
9.0-10.0	2527.40	942.50	681.97	46.50	0.49
10.0-11.0	3078.30	1045.30	975.68	44.90	0.48
11.0-12.0	3600.30	1210.10	1173.33	45.00	0.46
12.0-13.0	3370.00	1383.50	774.89	48.70	0.51
13.0-14.0	3290.80	1454.30	589.36	49.50	0.71
14.0-15.0	2830.10	1456.80	163.48	50.70	1.13
15.0-16.0	2142.60	1340.10	-313.50	51.30	2.01
16.0-17.0	1645.80	1119.50	-498.66	49.50	3.21

Table (A.38). Calculated parameters for the forced circulation non_metallic collector with no load conditions (m=.06 Kg/s and Vs=150 l) on the 24th of August.

Time Int.	I (kJ)	Qu(kJ)	Qs(kJ)	η%	(Ti-Ta)/I%
9.0-10.0	2527.40	1238.70	464.67	55.20	0.31
10.0-11.0	3078.30	1292.20	815.54	52.00	0.39
11.0-12.0	3600.30	1445.60	1031.41	51.10	0.42
12.0-13.0	3370.00	1582.50	680.89	53.90	0.51
13.0-14.0	3290.80	1608.30	543.49	53.90	0.74
14.0-15.0	2830.10	1548.30	181.38	54.30	1.20
15.0-16.0	2142.60	1352.70	-220.48	53.70	2.12
16.0-17.0	1645.80	1067.60	-352.63	50.40	3.36

Table (A.39). Calculated parameters for the forced circulation non_metallic collector with no load conditions (m=.02 Kg/s and Vs=150 l)on the 25th of August.

Time Int.	I (kJ)	Qu(kJ)	Qs(kJ)	η%	(Ti-Ta)/I%
9.0-10.0	2527.40	830.90	792.20	43.30	0.17
10.0-11.0	3078.30	930.90	1083.51	42.00	0.20
11.0-12.0	3600.30	1081.90	1288.43	42.00	0.20
12.0-13.0	3370.00	1261.00	869.94	46.00	0.22
13.0-14.0	3290.80	1352.20	656.37	47.10	0.38
14.0-15.0	2830.10	1392.30	185.49	48.90	0.73
15.0-16.0	2142.60	1331.20	-350.46	50.30	1.46
16.0-17.0	1645.80	1164.90	-585.23	49.60	2.49

Table (A.40). Calculated parameters for the forced circulation non_metallic collector with no load conditions (m=.04 Kg/s and Vs=150 L) on the 26th of August.

Time Int.	I (kJ)	Qu(kJ)	Qs(kJ)	η%	(Ti-Ta)/I%
9.0-10.0	2527.40	1080.30	499.70	48.90	0.83
10.0-11.0	3078.30	1144.90	842.19	46.60	0.78
11.0-12.0	3600.30	1295.10	1063.54	46.30	0.74
12.0-13.0	3370.00	1446.50	698.46	49.60	0.82
13.0-14.0	3290.80	1492.50	543.13	50.00	1.03
14.0-15.0	2830.10	1462.80	153.37	50.80	1.52
15.0-16.0	2142.60	1306.40	-283.29	50.60	2.52
16.0-17.0	1645.80	1052.80	-439.69	47.70	3.86

Table (A.41). Calculated parameters for the forced circulation non_metallic collector with no load conditions (m=.06 Kg/s and Vs=50 L) on the 15th of September.

Time Int.	I (kJ)	Qu(kJ)	Qs(kJ)	η%	(Ti-Ta)/I%
9.0-10.0	2527.40	1058.60	616.73	50.60	0.98
10.0-11.0	3078.30	939.10	1132.81	43.30	1.18
11.0-12.0	3600.30	1017.60	1387.49	41.10	1.33
12.0-13.0	3370.00	1060.30	1050.50	41.40	1.87
13.0-14.0	3290.80	989.20	950.09	38.40	2.44
14.0-15.0	2830.10	857.80	604.44	35.30	3.48
15.0-16.0	2142.60	626.20	190.56	29.70	5.40
16.0-17.0	1645.80	364.20	-23.33	20.40	7.94

Table (A.42). Calculated parameters for the forced circulation non_metallic collector with no load conditions (m=.02 Kg/s and Vs=150 L) on the 16th of September.

Time Int.	I (kJ)	Qu(kJ)	Qs(kJ)	η%	(Ti-Ta)/I%
9.0-10.0	2527.40	672.20	968.39	38.60	0.82
10.0-11.0	3078.30	736.80	1303.26	36.90	0.83
11.0-12.0	3600.30	857.10	1516.41	36.50	0.94
12.0-13.0	3370.00	979.70	1092.40	38.80	1.36
13.0-14.0	3290.80	989.00	917.46	37.90	1.88
14.0-15.0	2830.10	940.10	494.40	37.00	2.82
15.0-16.0	2142.60	791.50	5.70	34.50	4.61
16.0-17.0	1645.80	564.50	-230.75	28.30	7.08

Table (A.43). Calculated parameters for the forced circulation non_metallic collector with no load conditions (m=.01 Kg/s and Vs=50 L) on the 19th of September.

Time Int.	I (kJ)	Qu(kJ)	Qs(kJ)	η%	(Tin-Ta)/I%
9.0-10.0	2527.40	488.10	1159.46	31.50	0.34
10.0-11.0	3078.30	563.10	1480.17	30.90	0.34
11.0-12.0	3600.30	673.80	1697.69	31.10	0.44
12.0-13.0	3370.00	818.30	1231.00	34.30	0.73
13.0-14.0	3290.80	881.90	994.64	34.80	1.15
14.0-15.0	2830.10	910.10	486.57	35.70	1.91
15.0-16.0	2142.60	860.30	-103.87	35.80	3.38
16.0-17.0	1645.80	718.30	-415.82	32.90	5.55

Table (A.44). Calculated parameters for the forced circulation non_metallic collector with no load conditions (m=.04 Kg/s and Vs=50 L) on the 20th of September.

Time Int.	I (kJ)	Qu(kJ)	Qs(kJ)	η%	(Tin-Ta)/I%
9.0-10.0	2527.40	891.90	789.10	46.40	0.87
10.0-11.0	3078.30	882.00	1196.82	41.90	1.00
11.0-12.0	3600.30	984.30	1427.24	40.40	1.15
12.0-13.0	3370.00	1057.50	1057.87	41.40	1.65
13.0-14.0	3290.80	1009.30	936.24	38.90	2.22
14.0-15.0	2830.10	898.80	570.90	36.50	3.23
15.0-16.0	2142.60	686.90	139.31	31.80	5.11
16.0-17.0	1645.80	428.10	-75.27	23.30	7.63

Table (A.45). Calculted parameters for the forced circulation non_metallic collector with load conditions (m=.02 Kg/s) on 3rd of August.

Time Int.	I	Qu
9.0-10.0	2527.40	681.50
10.0-11.0	3078.30	883.10
11.0-12.0	3600.30	1116.40
12.0-13.0	3370.00	1363.00
13.0-14.0	3290.80	1520.80
14.0-15.0	2830.10	1624.10
15.0-16.0	2142.60	1628.70
16.0-17.0	1645.80	1528.70

Table (A.46). Calculated parameters for the forced circulation non_metallic collector with load conditions (m=.04 Kg/s) on the 4th of August.

Time Int.	I	Qu
9.0-10.0	2527.40	993.30
10.0-11.0	3078.30	1233.40
11.0-12.0	3600.30	1513.00
12.0-13.0	3370.00	1771.80
13.0-14.0	3290.80	1920.60
14.0-15.0	2830.10	1985.90
15.0-16.0	2142.60	1920.20
16.0-17.0	1645.80	1740.40

Table (A.47). Calculated parameters for the forced circulation non_metallic collector with load conditions (m=.06 Kg/s) on the 5th of August.

Time Int.	I	Qu
9.0-10.0	2527.40	1158.30
10.0-11.0	3078.30	1407.40
11.0-12.0	3600.30	1703.20
12.0-13.0	3370.00	1957.10
13.0-14.0	3290.80	2093.10
14.0-15.0	2830.10	2130.90
15.0-16.0	2142.60	2022.20
16.0-17.0	1645.80	1798.90

Table (A.48). Calculated parameters for the forced circulation non_metallic collector with load conditions (m=.01 Kg/s) on the 8th of August.

Time Int.	I	Qu
9.0-10.0	2527.40	442.90
10.0-11.0	3078.30	578.70
11.0-12.0	3600.30	742.00
12.0-13.0	3370.00	943.00
13.0-14.0	3290.80	1083.00
14.0-15.0	2830.10	1198.60
15.0-16.0	2142.60	1251.50
16.0-17.0	1645.80	1220.10

APPENDIX B

Appendix B Computer Programs

```
C  PROGRAM 1
C  THIS PROGRAM IS DESIGNED TO OBTAINING THE
THIRETICAL RESULTS
C  OF METALIC SERPENTINE SOLAR COLLECTOR.

      IMPLICIT REAL*8 (A-Z)
      DIMENSION I0(20),IH(20),IB(20),ID(20),IT(20),MO(12)
     = ,W1(20),W2(20),WW(20),H(20),RB(20),KT(20),UL(20),FR(20)
     = ,QU(20),EFF(20),IBN(20),CCOS(20),DBF(20),QUU(20),IT1(20)
     = ,QU1(20),CSIN(20)
      CHARACTER*5 QASSIM(18)
      OPEN(1,FILE='50L.OUT',STATUS='NEW')
      OPEN(2,FILE='RESS.DAT',STATUS='OLD')
C  CP:SPESIFIC HEAT OF WATER (KJ/KG.C).
C  M:MASS FLOW RATE OF WATER (KG/S).
C  TAF:EFFECTIVE TRANSMITIVE-ABSORBTANCE PRODUCT.
C  T:THICKNESS OF ABSORBER PLATE (M).
C  KN:THERMAL CONDUCTIVITY OF INSULATION MATERIAL.
C  LN:THICKNESS OF INSULATION MATERIAL(M).
C  AC:COLLECTOR AREA (M).
C  EG:TRANSPARANT COVER EMISSIVITY .
C  EP:ABSORBER PLATE  EMISSIVITY.
```

```
C  VW:WIND VELOCITY.
C  TG:GLASS COVER TEMPERATURE (C).
C  BC: STEFAN BOLTZMAN CONSTANT.
C  HW:WIND CONVECTIVE HEAT TRANSFER COEFFICIENT.
C  GAMA:SURFACE AZMITH ANGLE.
C  GCS:SOLAR CONSTANT.
C  ROG:REFLECTANCE SOLAR OF THE GROUND.
C  N:THE DAY NUMBER OF YEAR.
C  B:TILT ANGLE OF THE MODEL.
C  FI:LATITUDE, THE ANGULAR LOCATION NORTH OR SOUTH
OF THE EQUATOR.

      READ(2,*)L,EP,NG,BC,EG,LN,KN,K,W,DOT,T,MU
      =,DIN,AC,NS,CP,KW,LY,LCP,CONS,TAF,AA
      B=22
      FI=32
      ROG=.25
      GSC=1367

      MO(1)=0
      MO(2)=31
```

```
MO(3)=59
MO(4)=90
MO(5)=120
MO(6)=151
MO(7)=181
MO(8)=212
MO(9)=243
MO(10)=273
MO(11)=304
MO(12)=334
WRITE(*,*)'MONTH='
READ(*,*)MON
WRITE(*,*)'DAY='
READ(*,*) DAY
N=(MO(MON)+DAY)
WRITE(*,*)'N=',N
WRITE(*,*)'TIN='
READ(*,*)TIN
WRITE(*,*)'TPM='
READ(*,*)TPM
WRITE(*,*)'M='
```

```
      READ(*,*)M
      GA=0.00
      WRITE(1,*)M
      WRITE(*,*)'SG='
      READ(*,*)SG
      WRITE(*,*)'V='
      READ(*,*)V
      WRITE(1,*)'DATE : ',DAY,'/',MON
       H(1)=3
       W1(1)=-60
       W2(1)=-45
      ZO=3.14159/180
      FDE=(360*(284+N))/365
      DELTA=23.45*SIN(ZO*FDE)
      WRITE(1,*)'TIME INT.| TA  | TIN | TOUT| TPM  | IT  |  QU  | EFF
      + |  UL | FR | (TIN-TA/I)'
      WRITE(1,*)'##############################################
#########
      +#####################################'
      OO=8.
      OP=9.
```

```
C#####################################################
      DO 10 IP=1,9
C#####################################################
      X=7+IP
      T1=15.0045+0.24348*X+0.00609613*X**2-0.00123364*X**3
      A0=1.45449
      A1=13.32247
      A2=0.880859
      T2=A0*EXP(-0.5*((X-A1)/A2)**2)
      A0=13.6507
      A1=15.8189
      A2=6.24817
      T3=A0*EXP(-0.5*((X-A1)/A2)**2)
      A0=1.64694
      A1=11.642
      A2=.763324
      T4=A0*EXP(-0.5*((X-A1)/A2)**2)
      A0=2.06127
      A1=9.29022
      A2=.6993
      T5=A0*EXP(-0.5*((X-A1)/A2)**2)
```

```
      TA=T1+T2+T3+T4+T5
C     TA=-5.19651+4.29576*(IP+7)-0.143173*(IP+7)**2+
C     = 1.86203*10**(-5)*(IP+7)**3+1.63731*EXP(-0.5*(((IP+7)-
12.8344)/
C     = .980885)**2)
C     TA=7.17872-.388107*(IP+7)+0.316504*(IP+7)**2
C     = -.0136785*(IP+7)**3
      IF(IP.GT.1)THEN
      TIN=EXCH1
      TPM=TIN+(QU(IP-1)/AA/FR(IP-1)/UL(IP-1))*(1-FR(IP-1))
      WRITE(*,*)TPM
       W1(IP)=W1(IP-1)+15
       W2(IP)=W2(IP-1)+15
       H(IP)=H(IP-1)+1
      ENDIF
C#############################################################
C     INCIDENT SOLAR RADIATION
C#############################################################
      I0(IP)=12*GSC/3.14159*(1+0.033*COS(0.986*N*ZO))*
      = (COS(FI*ZO)*COS(DELTA*ZO)*(SIN(W2(IP)*ZO)-
SIN(W1(IP)*ZO))+
```

```
= 3.14159*(W2(IP)-W1(IP))*(SIN(FI*ZO)*SIN(DELTA*ZO))/180)
AH=191.3343*(-1)+322.8383*H(IP)-32.8510*(H(IP))**2+0.6137
= *(H(IP))**3
BH=142.1121+31.9338*H(IP)+0.4338*(H(IP))**2-0.2908*
= (H(IP))**3
FH=75.1929+2.1360*H(IP)+0.0779*(H(IP))**2-0.0194
= *(H(IP))**3
IH(IP)=AH+BH*SIN((360*N/365-FH)*ZO)
KT(IP)=IH(IP)/I0(IP)
IF(KT(IP).GE.0.0.AND.KT(IP).LT.0.137)THEN
ID(IP)=IH(IP)*(0.344+1.45*KT(IP))
ENDIF
IF(KT(IP).GE.0.137.AND.KT(IP).LT.0.785)THEN
ID(IP)=IH(IP)*(0.636-0.670*KT(IP))
ENDIF
IF(KT(IP).GE.0.785)THEN
ID(IP)=0.11*IH(IP)
ENDIF
WW(IP)=(W1(IP)+W2(IP))/2
CCOS(IP)=COS(FI*ZO)*COS(DELTA*ZO)*COS(WW(IP)*ZO)+
= SIN(FI*ZO)*SIN(DELTA*ZO)
```

```
      IB(IP)=IH(IP)*(0.145+1.032*KT(IP))
      IBN(IP)=(IH(IP)-ID(IP))/CCOS(IP)
      DBF(IP)=COS(B*ZO)*(SIN(FI*ZO)*SIN(DELTA*ZO)+COS(FI*Z
O)
     +   *COS(DELTA*ZO)*COS(WW(IP)*ZO))
     +   +SIN(B*ZO)*(COS(GA*ZO)*(TAN(FI*ZO)*(SIN(FI*ZO)
     +
*SIN(DELTA*ZO)+COS(FI*ZO)*COS(DELTA*ZO)*COS(WW(IP)*ZO))
     +   -SIN(DELTA*ZO)*1/(COS(FI*ZO)))
     +   +SIN(GA*ZO)*COS(DELTA*ZO)*SIN(WW(IP)*ZO))
      IT1(IP)=IBN(IP)*DBF(IP)+(COS(.5*B*ZO))**2.*ID(IP)
     + +(SIN(.5*B*ZO))**2.*IH(IP)*ROG
      IT(IP)=IT1(IP)*3.6
C ************************************************
C  OVER ALL HEAT COEFF.
      HW=8.6*(V)**.6/(L)**0.4
      TSE=0.0552*TA**(1.5)
      C=1-EXP(-0.01*(TPM-TA))/(TA-TSE+1)
      TG=(C*HW**0.38/430)*(240*EP-170+TPM)*(TPM-TA)+TA
      UT1=12.75*((TPM-
TG)*COS(B*ZO))**(0.264)/((TPM+TG)**(0.46)
```

```
      = *LCP**(0.21))
      UT2=BC*(TPM**2+TG**2)*(TPM+TG)/(1/EP+1/EG-1)
      UT3=(HW+(EG*(TG**4-TSE**4)/(TG-TA)))**(-1)
      UT=((UT1+UT2)**(-1)+UT3)**(-1)
      UB=KN/LN
      UL(IP)=(UT+UB+0.1)*3.6

   C##########################################################
####
   C  HEAT REMOVAL FACTOR
      N2=((W-DOT)**2*(UL(IP)/K/T))**0.5
      K1=K*T*N2/(W-DOT)/SINH(N2)
   C##########################################################
####
   C  HEAT TRANSFER COEFF. INSIDE TUBES
      RE=4*M/3.14159/DOT/MU
      F22=(0.79*LOG(RE)-1.64)**(-2)
      PR=12.48-0.27955*TIN+0.00252*TIN**2-0.00001*TIN**3
      NU=(F22/8)*RE*PR/(1.07+12.7*(F22/8)**.5*(PR**2/3-1))
      HI=NU*KW/DOT
      R=1/3.14159/DIN/HI
```

```
      GAMA=COSH(N2)*(-2)-DOT*UL(IP)/K1
      C=(K1*R*(1+GAMA)-1)**2-(K1*R)**2
      F2=1/(K1*R*(1+GAMA)**2-1-GAMA-K1*R)
      F1=NS*K1*LY/F2/AC/UL(IP)/C
      B1=M*CP/F1/AC/UL(IP)
      FR(IP)=F1*B1*(1-EXP((F2-1)/B1))
      QU(IP)=AA*FR(IP)*(IT1(IP)*TAF*3.6-UL(IP)*(TIN-TA))
      QU(IP)=AA*FR(IP)*(IT1(IP)*TAF*3.6-UL(IP)*(TIN-TA))/
     + (1.+(FR(IP)*UL(IP)/SG/4.186/2.))
      TOUT=TIN+QU(IP)/SG/4.186
      EXCH1=TOUT
      EFF(IP)=QU(IP)/IT(IP)/AA*100
      PER=(TIN-TA)/IT1(IP)*100
      WRITE(1,23)OO,OP,TA,TIN,TOUT,TPM,IT(IP),QU(IP),EFF(IP),U
L(IP)
     +,FR(IP),PER
   23 FORMAT(F4.1,'-',F4.1,' |',F4.1,' |',F4.1,' |',F4.1,' |',F4.1,
     +' |',F6.1,' |',F6.1,' |',F4.1,' |',F4.1,' |',F4.3,' |',F5.2)
      OO=OO+1
      OP=OP+1
      ITOT=ITOT+IT(IP)
```

```
      QUTOT=QUTOT+QU(IP)
   C#############################################################
########
   10 CONTINUE
      DEFF=QUTOT/ITOT
      WRITE(1,*)'TOTAL I=',ITOT
      WRITE(1,*)'TOTAL QU=',QUTOT
      WRITE(1,*)'DAYLY EFF.=',DEFF
   C#############################################################
   C#############################################################
      STOP
      END
```

```
C     TG:GLASS COVER TEMPERATURE (C).
C     BC: STEFAN BOLTZMAN CONSTANT.
C     HW:WIND CONVECTIVE HEAT TRANSFER COEFFICIENT.
C     GAMA:SURFACE AZMITH ANGLE.
C     GCS:SOLAR CONSTANT.
C     ROG:REFLECTANCE SOLAR OF THE GROUND.
C     N:THE DAY NUMBER OF YEAR.
C     B:TILT ANGLE OF THE MODEL.
C     FI:LATITUDE, THE ANGULAR LOCATION NORTH OR SOUTH
OF THE EQUATOR.

      READ(2,*)L,EP,NG,BC,EG,LN,KN,K,W,DOT,T,MU
      =,DIN,AC,NS,CP,KW,LY,LCP,CONS,TAF,AA
      B=30
      FI=32
      ROG=.25
      GSC=1367
      GA=0.00
      MO(1)=0
      MO(2)=31
      MO(3)=59
      MO(4)=90
      MO(5)=120
      MO(6)=151
```

```
MO(7)=181
MO(8)=212
MO(9)=243
MO(10)=273
MO(11)=304
MO(12)=334
WRITE(*,*)'MONTH='
READ(*,*)MON
WRITE(*,*)'DAY='
READ(*,*) DAY
N=(MO(MON)+DAY)
WRITE(*,*)'N=',N
WRITE(*,*)'TIN='
READ(*,*)TIN
WRITE(*,*)'TPM='
READ(*,*)TPM
TP(0)=TPM
WRITE(*,*)'M='
READ(*,*)M
GA=0.00
WRITE(1,*)M
WRITE(*,*)'SG='
READ(*,*)SG
WRITE(1,*)'SG=',SG
WRITE(*,*)'V='
READ(*,*)V
(1,*)'DATE : ',DAY,'/',MON
```

```
      T3=A0*EXP(-0.5*((X-A1)/A2)**2)
      A0=1.64694
      A1=11.642
      A2=.763324
      T4=A0*EXP(-0.5*((X-A1)/A2)**2)
      A0=2.06127
      A1=9.29022
      A2=.6993
      T5=A0*EXP(-0.5*((X-A1)/A2)**2)
      TA=T1+T2+T3+T4+T5
C     AMBIANT TEMPERATURE AT SEPTEMBER
C     TA=-15.10131+8.28251*X-.397318*X**2+.0039851*X**3
      W1(IP+1)=W1(IP)+15
      W2(IP+1)=W2(IP)+15
      H(IP+1)=H(IP)+1
C#####################################################
C INCIDENT SOLAR RADIATION
C#####################################################
      I0(IP)=12*GSC/3.14159*(1+0.033*COS(0.986*N*ZO))*
     = (COS(FI*ZO)*COS(DELTA*ZO)*(SIN(W2(IP)*ZO)-
SIN(W1(IP)*ZO))+
     = 3.14159*(W2(IP)-W1(IP))*(SIN(FI*ZO)*SIN(DELTA*ZO))/180)
      AH=191.3343*(-1)+322.8383*H(IP)-32.8510*(H(IP))**2+0.6137
     = *(H(IP))**3
      BH=142.1121+31.9338*H(IP)+0.4338*(H(IP))**2-0.2908*
     = (H(IP))**3
      FH=75.1929+2.1360*H(IP)+0.0779*(H(IP))**2-0.0194
     = *(H(IP))**3
```

```
      IH(IP)=AH+BH*SIN((360*N/365-FH)*ZO)
      KT(IP)=IH(IP)/I0(IP)
      IF(KT(IP).GE.0.0.AND.KT(IP).LT.0.137)THEN
      ID(IP)=IH(IP)*(0.344+1.45*KT(IP))
      ENDIF
      IF(KT(IP).GE.0.137.AND.KT(IP).LT.0.785)THEN
      ID(IP)=IH(IP)*(0.636-0.670*KT(IP))
      ENDIF
      IF(KT(IP).GE.0.785)THEN
      ID(IP)=0.11*IH(IP)
      ENDIF
C     ID(IP)=IH(IP)*(1.189-3.05*KT(IP)+3.875*KT(IP)**2
C     =  -2.386*KT(IP)**3)
      WW(IP)=(W1(IP)+W2(IP))/2
      CCOS(IP)=COS(FI*ZO)*COS(DELTA*ZO)*COS(WW(IP)*ZO)+
      = SIN(FI*ZO)*SIN(DELTA*ZO)
      IB(IP)=IH(IP)*(0.145+1.032*KT(IP))
      IBN(IP)=(IH(IP)-ID(IP))/CCOS(IP)
      DBF(IP)=COS(B*ZO)*(SIN(FI*ZO)*SIN(DELTA*ZO)+COS(FI*ZO)
      +   *COS(DELTA*ZO)*COS(WW(IP)*ZO))
      ++SIN(B*ZO)*(COS(GA*ZO)*(TAN(FI*ZO)*(SIN(FI*ZO)
      +*SIN(DELTA*ZO)+COS(FI*ZO)*COS(DELTA*ZO)*COS(WW(IP)
*ZO))
      +-SIN(DELTA*ZO)*(1/(COS(FI*ZO))))
      ++SIN(GA*ZO)*COS(DELTA*ZO)*SIN(WW(IP)*ZO))
C     WRITE(*,*)CCOS(IP),DBF(IP),IBN( IP)
      IT1(IP)=IBN(IP)*DBF(IP)+(COS(.5*B*ZO))**2.*ID(IP)
      ++(SIN(.5*B*ZO))**2.*IH(IP)*ROG
```

```
      IT(IP)=IT1(IP)*3.6
      IPT=IP+7
      IT1(IP)=-7968.7+1972.69*IPT-140.12*IPT**2+3.10874*IPT**3
      IT1(IP)=IT1(IP)+128.665*EXP(-0.5*((IPT-11.3222)/.356403)**2)
      IT1(IP)=IT1(IP)+101.061*EXP(-0.5*((IPT-13.3796)/.728347)**2)
      IT(IP)=IT1(IP)*3.6
C     CALCULATION OF OVER ALL HEAT COEFF.
      HW=8.6*(V)**.6/(L)**0.4
      TSE=0.0552*TA**(1.5)
      C=1-EXP(-0.01*(TPM-TA))/(TA-TSE+1)
      TG=(C*HW**0.38/430)*(240*EP-170+TPM)*(TPM-TA)+TA
      UT1=12.75*((TPM-TG)*COS(B*ZO))**(0.264)/((TPM+TG)**(0.46)
     =  *LCP**(0.21))
      UT2=BC*(TPM**2+TG**2)*(TPM+TG)/(1/EP+1/EG-1)
      UT3=(HW+(EG*(TG**4-TSE**4)/(TG-TA)))**(-1)
      UT=((UT1+UT2)**(-1)+UT3)**(-1)
      UB=KN/LN
      UL(IP)=(UT+UB+0.1)*3.6
C#####################################################

C     HEAT REMOVAL FACTOR
      N2=((W-DOT)**2*(UL(IP)/K/T))**0.5
      K1=K*T*N2/(W-DOT)/SINH(N2)
C     HEAT TRANSFER COEFF. INSIDE TUBES
      RE=4*M/3.14159/DOT/MU
      F22=(0.79*LOG(RE)-1.64)**(-2)
      PR=12.48-0.27955*TIN+0.00252*TIN**2-0.00001*TIN**3
      NU=(F22/8)*RE*PR/(1.07+12.7*(F22/8)**.5*(PR**2/3-1))
```

ملخص

محاكاة أداء المجمعات الشمسية المعدنية و غير المعدنية, ذات الأنبوب المتصل.

إعداد

أبو القاسم علي محمد الصغير

إشراف

أ.د. محمد أحمد السعد

تتعرض هذه الرسالة لدراسة نظرية لنموذجين مختلفين للمجمعات الشمسية ؛ المعدنية و غير المعدنية. و ذلك لتعين معاملات الأداء لهذه المجمعات مثل معامل فقد الحرارة , عوامل فقد الحرارة الكلية, الكسب الحراري, الكفاءة اليومية, و اللحظية.

و قد أظهرت هذه الدراسة أن المجمعات المعدنية الشمسية متفوقة من حيث معاملات الأداء على المجمعات الشمسية غير المعدنية, تحت ظروف الجريان القسري. و قد دلت هذه الدارسة أيضا على أن عوامل فقد الحرارة الكلية لكلا النموذجين تظهر تغيرا طفيفا عند التغير في معدلات التدفق. كذلك فإن معامل الفقد الحراري يعتمد بصورة كبيرة على معدل التدفق لكلا لنموذجين, عند استخدام خزانات ذات سعة صغيرة. كما تبين أيضا أن الطاقة المختزنة, في المجمعات غير المعدنية, يمكن أن يستفاد منها كطاقة حرارية مفيدة حتى بعد غياب أشعة الشمس.

و قد قورنت نتائج هذه الدراسة النظرية بنتائج لدرسات عملية سابقة, و وجد أن هنالك تطابقا جيدا بينهما, ما عدا تلك النتائج التي تم الحصول عليها في ساعات الصباح الباكر وساعات المساء.